

REGULATOR INFORMATION DISTRIBUTION SYSTEM (RIDS)

ACCESSION NBR: 8404050185 DOC. DATE: 84/03/30 NOTARIZED: NO DOCKET #
 FACIL: 50-315 Donald C, Cook Nuclear Power Plant, Unit 1, Indiana & 05000315
 50-316 Donald C, Cook Nuclear Power Plant, Unit 2, Indiana & 05000316
 AUTH. NAME AUTHOR AFFILIATION
 ALEXICH, M. P. Indiana & Michigan Electric Co.
 RECIP. NAME RECIPIENT AFFILIATION
 DENTON, H. R. Office of Nuclear Reactor Regulation, Director

SUBJECT: Forwards addl response to 820730, 0916 & 830810 requests for
 info on hydrogen combustion & control. Info covers capability
 of air return/hydrogen skimmer sys fan & ice condenser doors
 to survive differential pressure loadings

DISTRIBUTION CODE: A001S COPIES RECEIVED: LTR 1 ENCL 1 SIZE: 106
 TITLE: OR Submittal: General Distribution

NOTES: See "84 Reports"

RECIPIENT ID CODE/NAME		COPIES LTTR ENCL		RECIPIENT ID CODE/NAME		COPIES LTTR ENCL	
NRR ORB1 BC	01	7	7				
INTERNAL: ELD/HDS3		1	0	NRR/DE/MTEB		1	1
NRR/DL DIR		1	1	NRR/DL/ORAB		1	0
NRR/DSI/METB		1	1	NRR/DSI/RAB		1	1
<u>REG FILE</u>	04	1	1	RGN3		1	1
EXTERNAL: ACRS	09	6	6	LPDR	03	2	2
NRC PDR	02	1	1	NSIC	05	1	1
NTIS		1	1				

1. The first step in the process of the development of a new product is the identification of a market need. This is often done through market research, which can be conducted in a variety of ways, including surveys, focus groups, and interviews. The goal of market research is to gather information about the needs and preferences of potential customers.

2. Once a market need has been identified, the next step is to develop a concept for a new product that meets that need. This involves brainstorming ideas and creating a prototype. The prototype is a preliminary version of the product that is used to test the concept and gather feedback from potential customers.

3. After the concept has been developed, the next step is to conduct a feasibility study. This study is designed to determine whether the product is technically feasible, financially viable, and commercially viable. It involves a detailed analysis of the costs and benefits of the product, as well as an assessment of the competitive landscape.

4. If the feasibility study is positive, the next step is to develop a business plan. This plan outlines the strategy for the product, including the marketing and sales approach, the distribution channels, and the financial projections. The business plan is a key document that is used to secure funding for the product.

5. Once the business plan has been developed, the next step is to secure funding for the product. This can be done through a variety of sources, including venture capitalists, angel investors, and crowdfunding. The goal is to raise the capital needed to develop and launch the product.

6. After funding has been secured, the next step is to develop the product. This involves hiring a team of engineers and designers to create the product, as well as manufacturing the product. The product is then launched into the market, and the company begins to sell it.

7. The final step in the process is to monitor the product's performance in the market. This involves tracking sales, customer feedback, and other key metrics. The goal is to identify any areas for improvement and make adjustments to the product and the marketing strategy as needed.

የሚከተሉት ስራዎች በሚከተለው ደረጃ ይከተላሉ፡

THE UNIVERSITY OF CHICAGO

50 41

[illegible]

INDIANA & MICHIGAN ELECTRIC COMPANY

P.O. BOX 16631
COLUMBUS, OHIO 43216

March 30, 1984
AEP:NRC:0500M

Donald C. Cook Nuclear Plant Unit Nos. 1 and 2
Docket Nos. 50-315 and 50-316
License Nos. DPR-58 and DPR-74
ADDITIONAL RESPONSES TO REQUESTS FOR INFORMATION ON
HYDROGEN COMBUSTION AND CONTROL

Mr. Harold R. Denton, Director
Office of Nuclear Reactor Regulation
U. S. Nuclear Regulatory Commission
Washington, D. C. 20555

Dear Mr. Denton:

This letter and its Attachments provide additional information on hydrogen combustion and control during degraded core accidents for the Donald C. Cook Nuclear Plant Unit Nos. 1 and 2. More specifically, the information contained herein is being provided as a partial response to three (3) Requests For Information transmitted to Mr. John E. Dolan of the Indiana & Michigan Electric Company (IMECO) by Mr. S. A. Varga of the NRC. These Requests For Information are dated July 30, 1982, September 16, 1982, and August 10, 1983. The enclosed information, which is also being provided in partial fulfillment of commitments made to NRC staff at a meeting held in Bethesda, Maryland, on September 13, 1983, is as follows:

- Attachment 1 to this letter provides responses to all three (3) questions contained in the August 10, 1983, Request For Information. This material includes information on the capability of the air return/hydrogen skimmer system fan and ice condenser doors to survive various differential pressure loadings. The results of a new CLASIX analysis utilizing a modified heat transfer correlation is also presented in response to this Request For Information. This new analysis represents what we believe to be a reasonable basis for assessment of the consequences of hydrogen combustion within containment. Additionally, this analysis is intended to provide an analytical framework for what we believe to be an effective program for evaluating the effectiveness of controls to mitigate the consequences of such events.

8404050185 840330
PDR ADDCK 05000315
P PDR

Appl
1/1

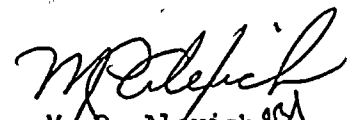
- Attachment 2 to this letter responds to Questions 6, 12, 13, 14(d), and 14(e) of the September 16, 1982, Request For Information. These responses provide additional information on the CLASIX spray model and the applicability of CLASIX analyses performed by Duke Power Company with regard to igniter effectiveness.
- Attachment 3 to this letter provides responses to Questions 2, 4(f), 5, 8, 10(a), and 11 of the July 30, 1982, Request For Information. This material includes information on compressible flows within containment resulting from hydrogen deflagrations and the CLASIX ice bed heat transfer model.

In addition to the above, we have contracted with Westinghouse Electric Corporation/Offshore Power Systems (W/OPS) to assist American Electric Power Service Corporation (AEPSC) in the preparation of responses to Questions 7 and 8 of the September 16, 1982, Request For Information. It is presently expected that responses to these questions will be submitted to NRC staff on or before April 30, 1984, thereby completing IMECO's responses to the three (3) Requests For Information cited above (previous responses were contained in IMECO letter Nos. AEP:NRC:0500J, AEP:NRC:0500K, and AEP:NRC:0500L, dated October 15, 1982, October 10, 1983, and December 17, 1982, respectively).

Furthermore, it is noted that we are continuing to evaluate the information on the air return/hydrogen skimmer system fans presented in Attachment 1 to this letter. The results of this evaluation are expected to be submitted to NRC staff along with the responses to Questions 7 and 8 of the September 16, 1982, Request For Information.

This document has been prepared following Corporate Procedures which incorporate a reasonable set of controls to ensure its accuracy and completeness prior to signature by the undersigned.

Very truly yours,


M. P. Alexich
Vice President 3/30/84

MPA/dam
Attachments

cc: (attached)

cc: John E. Dolan
W. G. Smith, Jr. - Bridgman
R. C. Callen
G. Charnoff
E. R. Swanson - NRC Resident Inspector, Bridgman
A. Sudduth - Duke Power Company, Charlotte, NC
D. Renfro - Tennessee Valley Authority, Knoxville, TN

Figure 1. The effect of the concentration of the H_2O_2 solution on the amount of the released H_2O from the H_2O_2 -loaded hydrogel. The amount of the released H_2O was measured by the weight difference of the hydrogel before and after the release. The concentration of the H_2O_2 solution was 0.1, 0.2, 0.3, 0.4, 0.5, 0.6, 0.7, 0.8, 0.9, and 1.0 wt. %.

Atcl #8404050185

ATTACHMENT 1 TO AEP:NRC:0500M
RESPONSES TO QUESTIONS ON HYDROGEN CONTROL
CONTAINED IN MR. S. A. VARGA'S LETTER DATED AUGUST 10, 1983
DONALD C. COOK NUCLEAR PLANT UNIT NOS. 1 AND 2

Question 1:

With regard to the CLASIX code, the staff has previously requested clarification of the structural heat sink heat transfer models. The following pertinent points have been derived from the responses:

- i) Heat transfer is based on a temperature difference determined by $(T_{\text{bulk}} - T_{\text{wall}})$.
- ii) Heat transfer coefficients for degraded core accident analysis are determined from a natural convection (stagnant) correlation applicable to condensation heat transfer.
- iii) CLASIX does not explicitly model mass removal due to condensation heat transfer.

Based on the description of the CLASIX structural heat sink model, it appears that the CLASIX model differs dramatically from generally accepted approaches and is not, as is claimed, consistent with standard methods such as those used in CONTEMPT. The differences are related to the treatment of the three items cited above. By comparison, previously accepted approaches are characterized by the following:

- i) Heat transfer is based on $(T_{\text{sat}} - T_{\text{wall}})$, when the surface temperature of the heat sink is less than T_{sat} ; i.e., $T_{\text{wall}} < T_{\text{sat}}$.
- ii) Heat transfer coefficients are based on condensation only when $T_{\text{wall}} < T_{\text{sat}}$.
- iii) Condensed mass removal is based on condensation heat transfer with provisions for revaporizing a small fraction of the condensate.

A more detailed description of accepted practice is contained in NUREG-0588 and NUREG/CR-0255.

The effect of the CLASIX models would appear to be the de-superheating of the atmosphere too rapidly thus reducing gas temperatures and possibly altering the combustion characteristics.

Based on the above discussion, provide justification for the models incorporated in CLASIX or provide the results of analyses with acceptable models as outlined above. The analyses should encompass selected sensitivity studies to assure that the effects of the changes are determined for both containment integrity and equipment survivability considerations.

Response to Question 1:

To provide a structural heat sink heat transfer model more acceptable to the NRC, a new heat transfer correlation has been added to CLASIX. The heat transfer model represented by this option is based on

a combination of those presented in NUREG-0588, Branch Technical Position CSB 6-1, and the CONTEMPT program description document. This model was developed in consultation with the NRC staff in an effort to minimize the potential for future modifications. The condensing heat transfer coefficient is based on the Uchida correlation, and that is how this option is referred to within this text.

To evaluate the use of the Uchida correlation in the CLASIX computer code, two complete cases were performed. First, a case utilizing the new Uchida heat transfer correlation was performed; this will be referred to as the base case. Second, a case was performed utilizing the Tagami correlation as in previous Donald C. Cook Nuclear Plant hydrogen analyses (References (1-1) and (1-2)). The Tagami case serves as a comparison in evaluating the effect of the Uchida correlation on the hydrogen combustion transient.

A schematic diagram of the CLASIX containment model for the Donald C. Cook Nuclear Plant is given in Figure 1-1. Each case was performed using the same input parameters as used for CLASIX Case "C" of Reference (1-2), except for the time step and passive heat sink nodalization. The time step was increased from 0.01 to 0.1 second to reduce computer run time. Due to this time step change, the number of nodes in appropriate wall layers were reduced to maintain stability. Passive heat sink data are given in Tables 1-1 through 1-8 and reflect the noding changes. Also, due to the slightly different pressure response obtained by using the Uchida correlation, the fan and spray initiation time increased since the 3.0 psig set point was reached later in the transient. The spray initiation time increased from 141 to 190 seconds, while the air return fan/hydrogen skimmer system initiation time increased from 711 to 760 seconds.

The results of the Uchida base case analysis are summarized in Table 1-9. Plots of the compartment temperatures, pressures, oxygen volume fractions, and hydrogen volume fractions are given in Figures 1-2 through 1-25. During the transient, there were twelve burns in the ice condenser upper plenum, five burns in the ice condenser lower plenum, and eight burns in the lower compartment. No burns occurred in the upper compartment, the dead ended region, or the fan/accumulator rooms. Maximum hydrogen concentrations in these areas were 6.83, 6.54, and 6.73 volume percent, respectively.

At approximately 1630 seconds, a pressure rise of about 4 psi is seen throughout the containment. This is due to the fan flow from the dead ended region being initiated and forcing the hotter steam from the lower compartment through the dead ended region into the fan/accumulator rooms, resulting in a temperature and pressure rise throughout containment. This effect is due to the modeling of the air return fan system. As indicated in Figure 1, the air return fan/hydrogen skimmer system takes suction from different compartments. Fan flow between compartments will be initiated for each flow path, depending on transient pressure differentials.

The first burns occurred in the ice condenser upper plenum and lower plenum at 4574 seconds into the base case. These near simultaneous burns resulted in a relatively large upper plenum pressure rise of approximately 12.4 psi. Between about 4574 and 5730 seconds in the transient, lower compartment burns were intermixed with upper plenum burns at various intervals. From about 5730 seconds to the end of the transient, burns occurred in the upper plenum and lower plenum at various intervals, and one burn occurred in the lower compartment. A total of 1097 pounds of hydrogen burned. At the end of the transient, 441 pounds of hydrogen remained distributed throughout the containment.

The peak calculated pressure and temperature were 19.5 psig and 1067°F, respectively, both occurring in the upper plenum. The peak pressure occurred at 5730 seconds as a result of near simultaneous burns in both the upper plenum and lower plenum. In general, each burn resulted in a rapid pressure and temperature rise and an almost equally rapid return to approximately the pre-burn condition.

The various peak pressure differentials between compartments are summarized in Table 1-10. The largest pressure differentials occur between the upper plenum and adjoining compartments due to the large burn at 5730 seconds. Plots of pressure differentials for the upper compartment/fan accumulator rooms, lower compartment/lower plenum, lower plenum/upper plenum, and upper plenum/upper compartment are given in Figures 1-26 through 1-29, respectively (some peak differential pressures may not appear on these plots if the peaks occur between the one second plot intervals). These figures indicate differential pressures across the air return fans, inlet doors of the ice condenser, intermediate deck doors, and top deck doors, respectively. The maximum pressure differential indicated for the air return fan in the positive flow direction is 6.6 psi.

The Tagami case was performed to determine, by comparison, the effect of the Uchida heat transfer correlation. Input was similar to the Uchida base case analysis except for the spray and fan initiation time explained above. The results of the Tagami case analysis are summarized in Tables 1-11 and 1-12. Plots of compartment temperatures, pressures, oxygen volume fractions, hydrogen volume fractions, and selected differential pressures are given in Figures 1-30 through 1-57. Pressure and temperature profiles are very similar to those of the base case. The pressure rise indicated in the Uchida base case at 1630 seconds is absent due to modeling of the air return fan/hydrogen skimmer system characteristics and flow initiation timing.

The peak calculated pressure and temperature was 16.1 psig and 1038°F, respectively, which occurred in the ice condenser upper plenum. Peak pressures in other regions of the containment were higher by about 0.1 to 1.9 psi for the Tagami case, while peak temperatures were typically lower by about 2°F to 114°F. Generally, the Uchida base case and the Tagami case show similar response characteristics and result in similar conclusions about containment integrity.

Question 2:

Provide a complete evaluation of fan (both air return and hydrogen skimmer as applicable) operability and survivability for degraded core accidents. In this regard discuss the following items:

- a. The identification of conditions which will cause fan overspeed, in terms of differential pressure and duration, and hydrogen combustion events.
- b. The consequences of fan operation at overspeed conditions. The response should include a discussion of thermal and overcurrent breakers in the power supply to the fans, the setpoints and physical locations of these devices, and the fan loading conditions required to trip the breakers.
- c. Indication to the operator of fan inoperability, corrective actions which may be possible, and the times required for operators to complete these actions.
- d. The capability of fan system components to withstand differential pressure transients (e.g., ducts, blades, thrust bearings, housing), in terms of limiting conditions and components.

Response to Question 2(a):

The fan will start to overspeed whenever the suction pressure (i.e., the upper compartment pressure) is more than a few inches of water above the discharge pressure (i.e., the pressure in the fan/accumulator rooms). Hydrogen burns in the upper compartment and/or upper plenum could cause such pressure differentials to occur. See Figure 1-26 for a plot of this differential pressure for the new Uchida base case. Such pressure excursions last only a few seconds, which does not provide sufficient time for overspeed design limits to be exceeded.

Response to Question 2(b):

The maximum overspeed revolutions per minute (RPM) for the fan drive motor is 1125 RPM. The rated speed is 900 RPM. At a speed greater than 1125 RPM, the physical design limits of the motor will be exceeded.

In the overspeed condition, the motor will function as a generator, but will not disconnect itself from its power supply. The fan drive motors are connected to 600 V, Bus 1B, Motor Control Center (MCC) EZC-B Engineered Safeguards Systems (ESS) and Bus 1C, MCC EZC-C (ESS) for trains A and B, respectively. Each motor is protected by a 150 amperes circuit breaker for overload protection. At a speed of 1125 RPM, reverse current will be in the range of 70 to 90 amperes, well within the 150 ampere rated circuit breaker. Therefore, the circuit breaker will not disconnect the overspeeding motor from the power source.

Failure of the fan due to overspeed is not governing since it will occur at RPM levels above that of motor failure.

Response to Question 2(c):

The control room operator has an on/off indication of air return fan operability. Indication of fan failure is considered below:

- If the fan motor overspeeds to a point above the design limit of 1125 RPM, the motor will physically fail and result in a short. This will trip the circuit breaker and the control room operator will receive indication of fan inoperability.
- If fan failure results in a locked rotor, the circuit breaker will trip due to overcurrent and the control room operator will receive indication of fan inoperability.
- If the loading on the fan results in slight or intermittent interference, but no catastrophic failure or locked rotor, the motor may or may not trip due to overcurrent depending on the degree of interference. If it does trip, the control room operator will receive an indication of fan inoperability as noted above. If it does not trip, the fan will be performing at least a portion of its function.
- If the shaft connecting the motor to the fan should fail prior to tripping of the motor, and if there is not significant interference between the two broken ends of the shaft, the motor could continue to run. In this event, the operator would continue to receive a faulty indication that the fan was running. If there is significant interference between the broken ends of the shaft, the motor will trip due to overcurrent or due to some mode of motor failure. In this case, the operator would receive indication of fan failure due to motor trip.

Corrective actions to address air return fan and/or motor failure are not considered feasible during accident conditions. Therefore, in our judgement, control room indication of fan failure is not a particularly important consideration.

Response to Question 2(d):

All of the following references to differential pressure refer to situations in which the external pressure is greater than the internal pressure. Also, the material yield stress is used to define the capability limit of air return fan components. Although disabling failure is not likely to occur at this point, continued effective operation is difficult to ensure for these components beyond the material yield stress.



- Duct System. The duct system is made up of 14", 12", 8", 6", and 4" schedule 40 A-106 Grade B pipe. A 150 psi design cast steel butterfly wafer valve is used.

All valves (except for two 14" valves) and connecting flanges and fittings are 150 psi cast steel and will withstand a differential pressure of at least 50 psi. The 14" diameter valves will withstand a differential pressure of 12 psi. The remaining ductwork, fittings, and valves are capable of withstanding a differential pressure of at least 50 psi.

- Fan Drive Motor Bearings. The ball bearings in the fan drive motor (and fan) are capable of withstanding a differential pressure transient of 5 psi for a thrust load in either direction.
- Fan Drive Motor. The fan drive motor housing is capable of withstanding a differential pressure transient of at least 10 psi.
- Fan. The two fans in each containment are similar except for their direction of rotation. Both clockwise and counterclockwise rotation were considered. The fan wheel (blade) stress is not sensitive to increases in differential pressure since the centrifugal stresses dominate, provided the excursion is not of sufficient duration to result in overspeeding of the fan wheel.
- Fan Housing. The primary braces of the fan housing reach a material yield point at a differential pressure of 2.1 psi. Furthermore, the nominal clearance between the backplate and housing disappears at approximately 3.1 psi. Structural yielding of the inlet box will occur at 2.9 psi.

The critical components for the fan where structural capability is exceeded by predicted differential pressures, considering all failure modes, is the fan housing and associated components and the fan drive motor bearings. These items have failure modes at differential pressures less than the predicted peak differential pressures between the upper compartment and the fan/accumulator rooms presented in Tables 1-10 and 1-12.

In order to evaluate the significance of these fan failures, an initial scoping study has been performed with CLASIX in which the air return/hydrogen skimmer system fans were assumed to fail at the first hydrogen burn. During the resultant transient, there were ten burns in the lower compartment, six burns in the lower plenum, and three burns each in the upper plenum, dead ended region, and fan/accumulator rooms. No burns occurred in the upper compartment where the maximum hydrogen concentration reached 6.1 volume percent. Relatively high hydrogen concentrations at the time of some lower compartment burns were due to inadequate mixing as a result of fan failure (i.e., insufficient oxygen concentration).

The peak calculated pressure and temperature for this fan failure case was 37.6 psig and 1388⁰ F, respectively, and occurred in the dead ended region within containment. This peak pressure is well below the best estimate median limiting pressure capacity of the Donald C. Cook Nuclear Plant containment building (i.e., 57.8 psig, as identified in Reference (1-3)), and therefore it is believed that, except under the most pessimistic set of assumptions, containment failure will not occur.

Question 3:

Provide an evaluation of the ultimate capability of ice condenser doors to withstand reverse differential pressures.

Response to Question 3:

The material yield stress was used to define the capability limit of ice condenser door components. Although disabling failure is not likely to occur at this point, continued effective operation is difficult to ensure for these components beyond the material yield stress. The maximum reverse differential pressure capabilities of critical structural elements of the ice condenser doors and frames are given below:

<u>Ice Condenser Component</u>	<u>Structural Element</u>	<u>Maximum Reverse Pressure Capability (psi)</u>
Lower Inlet Doors	Center Door Beam	7.7
Intermediate Deck Doors and Frames	Outer Angle	7.2
	Door Panel	2.8
	Center Angle	5.5
Top Deck	Radial Beams	3.7
	Grating	3.2
Personnel Access Door	Frame Angle	20.9

Comparison of these values with the peak differential pressures presented in Tables 1-10 and 1-12 indicates that yielding of the lower inlet doors and the top deck grating and radial beams should not occur. The intermediate deck doors, however, have a maximum reverse pressure capability less than the differential pressures presented in Tables 1-10 and 1-12 for the CLASIX upper plenum to lower plenum flow path. Other factors which should be taken into account, however, include the following:

- CLASIX calculated pressures in the upper plenum, and CLASIX calculated differential pressures along the upper plenum to lower plenum flow path, are conservatively high. This conservatism is due to the simplistic CLASIX assumption that hydrogen burns in the upper plenum region will occur as

deflagrations engulfing the entire annular area. In reality, smaller localized "puff burns" would be expected. Additionally, it is noted that a steady flame front within the ice condenser has been postulated to occur under steady hydrogen supply conditions during the Duke Power Company McGuire Nuclear Plant hearings. In such an event, pressure differentials along the flow path of concern would be very small.

- Even if the intermediate deck doors were assumed to fail upon reaching the material yield point, a small bypass flow area is present around the intermediate deck to permit some flow through the ice condenser. Furthermore, door failure due to deformation would probably also allow for deck leakage. This leakage around the deformed intermediate deck doors would supplement bypass flow.

Based on the above, it is believed that ice condenser door survivability during postulated degraded core accidents is not a major concern for the Donald C. Cook Nuclear Plant.

References, Attachment 1

- (1-1) Letter No. AEP:NRC:0500E, dated July 2, 1981, Mr. R. S. Hunter (IMECo) to Mr. H. R. Denton (NRC), Hydrogen Mitigation and Control Studies for the Donald C. Cook Nuclear Plant Unit Nos. 1 and 2.
- (1-2) Letter No. AEP:NRC:0500H, dated September 30, 1982, Mr. R. S. Hunter (IMECo) to Mr. H. R. Denton (NRC), Hydrogen Mitigation and Control Studies for the Donald C. Cook Nuclear Plant Unit Nos. 1 and 2.
- (1-3) Letter No. AEP:NRC:0500I, dated March 1, 1984, Mr. M. P. Alexich (IMECo) to Mr. H. R. Denton (NRC), Status Summary Report on the Adequacy of the Distributed Ignition System for the Donald C. Cook Nuclear Plant.

Table 1-1

Cook CLASIX Input

Compartment Dependent Passive Heat Sink Parameters

<u>Parameter</u>	<u>Compartment</u>	<u>Value</u>
Temperature	Lower Compartment	110 F
	Ice Condenser Lower Plenum	*
	Ice Condenser Upper Plenum	15 F
	Upper Compartment	75 F
	Dead Ended Region	98 F
	Fan/Accumulator Rooms	110 F
Radiant Heat Transfer Beam Length	Lower Compartment	25.0 ft
	Ice Condenser Lower Plenum	8.5 ft
	Ice Condenser Upper Plenum	8.5 ft
	Upper Compartment	59.0 ft
	Dead Ended Region	8.5 ft
	Fan/Accumulator Rooms	8.5 ft

* See Table 1-5.



Table 1-2

Cook CLASIX Input

Material Dependent Passive Heat Sink Parameters

<u>Parameter</u>	<u>Material</u>	<u>Value</u>
Emmissivity*	Concrete	0.9
	Carbon Steel	0.9
	Paint	0.9
	Stainless Steel	0.4
Thermal Conductivity* (Btu/hr ft F)	Paint on Steel (UC)	0.21
	Paint on Steel (LC, DE, F/A, UP)	0.22
	Paint on Concrete	0.087
	Concrete	0.84
	Carbon Steel	27.3
	Stainless Steel	9.87
Volumetric Heat Capacity* (Btu/ft ³ F)	Paint on Steel (UC)	29.8
	Paint on Steel (LC, DE, F/A, UP)	14.7
	Paint on Concrete	29.8
	Concrete	30.2
	Carbon Steel	59.2
	Stainless Steel	59.2
Exit Heat Transfer Coefficient* (Btu/hr ft ² F)	Paint to Steel or Concrete	10 ⁴
	Concrete to Concrete	10 ⁸
	Concrete to Steel	10
	Steel to Concrete	10
	Steel to Steel	10 ⁸
	Last Layer Adiabatic Wall	0

* See individual lower plenum wall data in Table 1-5.

Table 1-3

Cook CLASIX Input

Upper Compartment Passive Heat Sinks

CLASIX Wall Number	Initial Wall Temperature (F)	Surface ₂ Area (ft ²)	Layer Number	Number of Nodes	Layer Material	Layer Thickness (ft)
1	75	26086	1	2	Paint	0.001
			2	3	Carbon steel	0.03
			3	12	Concrete	1.0
			4	10	Concrete	1.89
2	75	310	1	2	Paint	0.001
			2	3	Carbon steel	0.03
3	75	5284	1	2	Paint	0.001
			2	5	Carbon steel	0.05
			3	12	Concrete	1.0
			4	6	Concrete	1.0
			5	3	Concrete	1.5
4	75	595	1	2	Paint	0.001
			2	6	Carbon steel	0.06
			3	10	Concrete	0.83
5	75	350	1	3	Concrete	0.15
			2	3	Carbon steel	0.03
			3	8	Concrete	0.63
6	75	25433	1	12	Concrete	1.0
			2	3	Concrete	0.3
7	75	4381	1	12	Concrete	1.0
			2	8	Concrete	1.53

Table 1-4

Cook CLASIX Input

Lower Compartment Passive Heat Sinks

CLASIX Wall Number	Initial Wall Temperature (F)	Surface Area (ft ²)	Layer Number	Number of Nodes	Layer Material	Layer Thickness (ft)
8	110	540	1	2	Paint	0.001
			2	5	S. steel	0.03
9	110	595	1	2	Paint	0.001
			2	10	S. steel	0.06
			3	10	Concrete	0.83
10	110	3224	1	2	Paint	0.001
			2	5	S. steel	0.03
			3	12	Concrete	1.0
			4	6	Concrete	1.0
			5	4	Concrete	2.05
11	110	29306	1	2	Paint	0.001
			2	12	Concrete	1.0
			3	3	Concrete	0.49
12	110	9275	1	2	Paint	0.001
			2	12	Concrete	1.0
			3	6	Concrete	1.0
			4	3	Concrete	1.61

Table 1-5

Cook CLASIX Input

Ice Condenser Lower Plenum Passive Heat Sinks

CLASIX Wall Number	Initial Wall Temperature (F)	Surface Area (ft ²)	Layer Number	Number of Nodes	Layer Material	Layer Thickness (ft)	Layer Conductivity (Btu/hr ft F)	Layer Heat Capacity (Btu/ft ³ F)	Layer Heat Transfer (Btu/hr ft ² F)
13	80	19100	1	5	Insulation	1.0	0.15	2.75	0.7
			2	6	Steel	0.0625	26.0	56.4	0.0
14	80	13055	1	5	Insulation	1.0	0.2	3.663	0.7
			2	12	Concrete	1.0	0.8	28.8	0.0
15	15	3336	1	2	Paint	.000833	0.0833	28.4	10 ⁶
			2	4	Concrete	.33	0.8	28.8	0.0

Table 1-6

Cook CLASIX Input

Ice Condenser Upper Plenum Passive Heat Sinks

CLASIX Wall Number	Initial Wall Temperature (F)	Surface Area (ft ²)	Layer Number	Number of Nodes	Layer Material	Layer Thickness (ft)
16	15	9453	1	2	Paint	0.001
			2	3	Carbon steel	0.021
			3	8	Carbon steel	0.083
			4	10	Carbon steel	0.606

Table 1-7

Cook CLASIX Input

Dead Ended Region Passive Heat Sinks

CLASIX Wall Number	Initial Wall Temperature (F)	Surface Area (ft ²)	Layer Number	Number of Nodes	Layer Material	Layer Thickness (ft)
17	98	6590	1	2	Paint	0.001
			2	5	Carbon steel	0.05
			3	12	Concrete	1.0
			4	6	Concrete	1.0
			5	3	Concrete	1.5
18	98	16789	1	2	Paint	0.001
			2	12	Concrete	1.0
			3	3	Concrete	0.43

Table 1-8

Cook CLASIX Input

Fan/Accumulator Rooms Passive Heat Sinks

CLASIX Wall Number	Initial Wall Temperature (F)	Surface Area (ft ²)	Layer Number	Number of Nodes	Layer Material	Layer Thickness (ft)
19	110	5640	1	2	Paint	0.001
			2	5	Carbon steel	0.05
			3	12	Concrete	1.0
			4	6	Concrete	1.0
			5	3	Concrete	1.5
20	110	10134	1	2	Paint	0.001
			2	12	Concrete	1.0
			3	3	Concrete	0.54

Table 1-9

Cook CLASIX Results Summary

<u>Base Case</u>		
Number of burns	LC	8
	LP	5
	UP	12
Magnitude of burns (lbm)	LC	64-70
	LP	42-50
	UP	20-40
Total H ₂ burned (lbm)		1097
H ₂ remaining (lbm)		441
Peak temperature (F)	LC	915
	LP	588
	UP	1067
	UC	185
	DE	222*
	F/A	191*
Peak pressure (psig)	LC	10.6
	LP	9.4*
	UP	19.5
	UC	10.6
	DE	9.9
	F/A	9.8
Ice remaining (lbm)		1.5×10^6

*Occurs before the burn period.

Table 1-10

Cook CLASIX Results

Peak Differential Pressures Between Compartments *

From\To	<u>Base Case</u>					
	LC	LP	UP	UC	DE	F/A
LC	—	4.4	4.6	5.0	5.0	3.0
LP	3.6	—	0.6	1.4	3.6	3.6
UP	12.6	12.6	—	12.5	12.6	12.5
UC	6.6	6.5	0.4	—	6.2	6.6
DE	1.3	2.5	2.3	2.8	—	1.3
F/A	1.3	3.5	3.6	4.4	4.5	—

*Some differential pressures listed in this Table are not physically realistic. As an example, there is no junction between the ice condenser upper plenum and the dead ended regions within containment; therefore, that differential pressure listed above (i.e., 12.6 psi) cannot occur.

Table 1-11

Cook CLASIX Results Summary

Tagami Case

Number of burns	LC	9
	LP	3
	UP	11
Magnitude of burns (lbm)	LC	60-74
	LP	51-56
	UP	18-40
Total H ₂ burned (lbm)		1083
H ₂ remaining (lbm)		455
Peak temperature (F)	LC	826
	LP	474
	UP	1038
	UC	174
	DE	221
	F/A	194
Peak pressure (psig)	LC	12.5
	LP	11.0
	UP	16.1
	UC	10.7
	DE	10.9
	F/A	11.0
Ice remaining (lbm)		1.03 x 10 ⁶



Table 1-12

Cook CLASIX Results

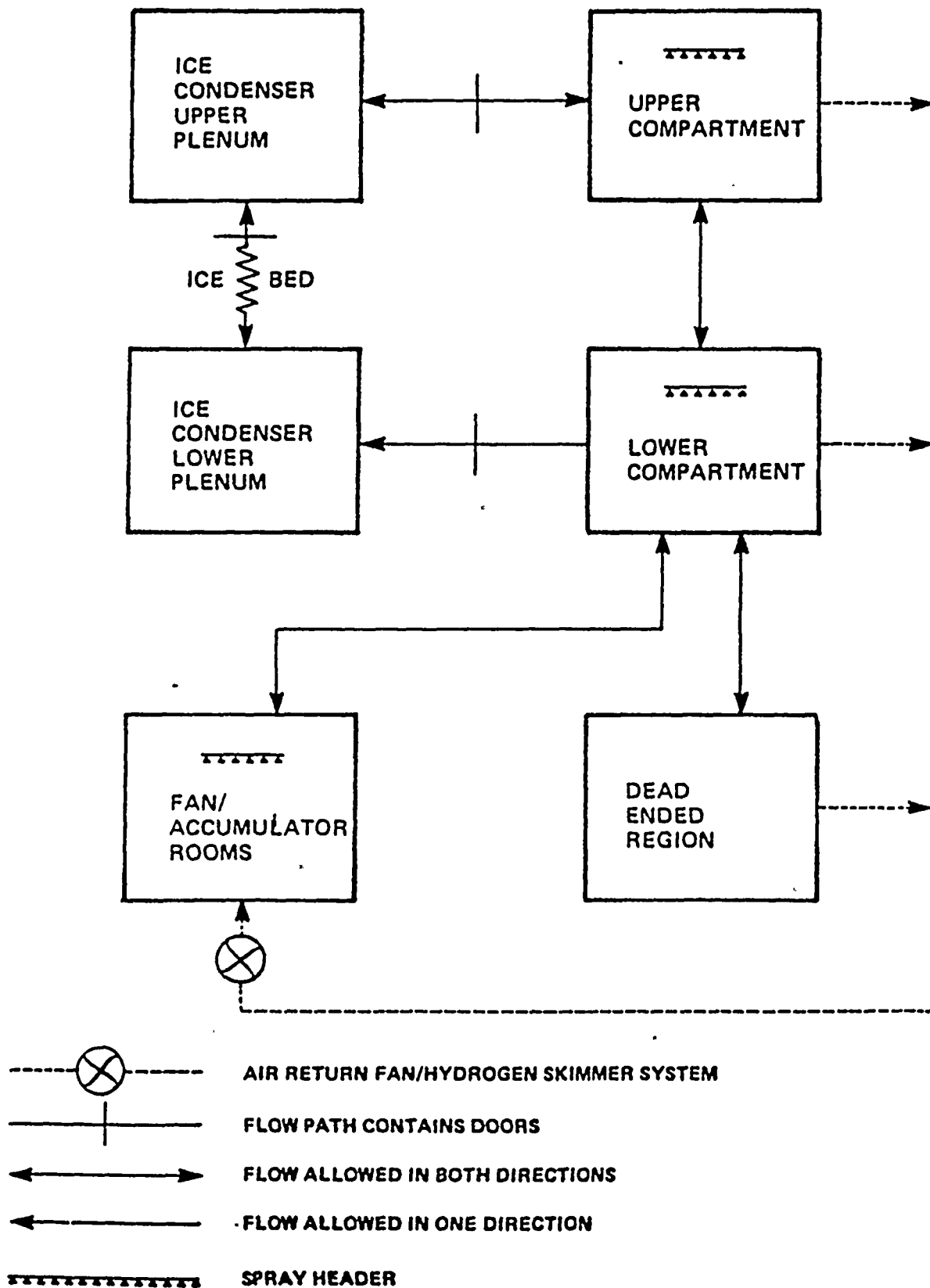
Peak Differential Pressures Between Compartments*

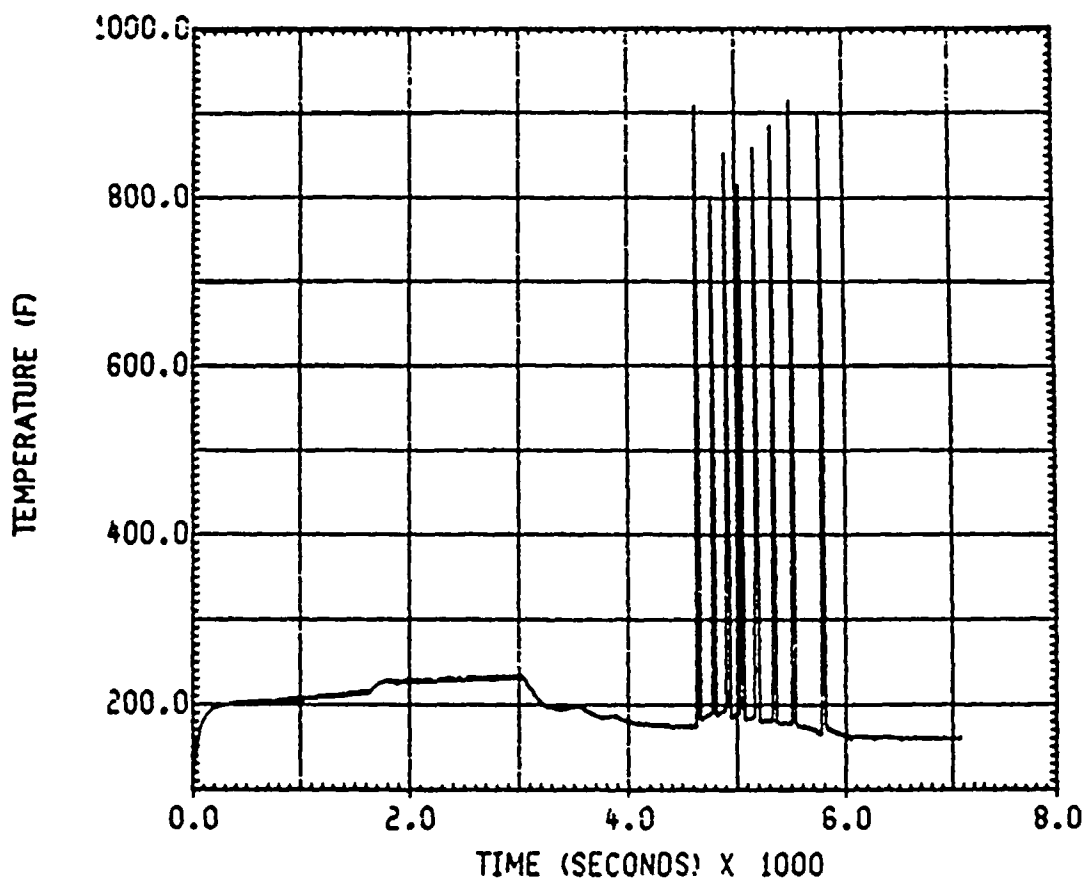
Tagami Case

From \ To	LC	LP	UP	UC	DE	F/A
LC	—	4.7	4.8	5.1	4.9	3.5
LP	3.2	—	0.4	3.7	3.3	3.2
UP	8.2	8.3	—	8.8	8.3	8.2
UC	6.5	6.0	0.6	—	6.5	6.5
DE	1.9	2.1	1.6	1.9	—	1.4
F/A	1.7	3.2	3.3	4.0	3.4	—

*Some differential pressures listed in this Table are not physically realistic. As an example, there is no junction between the ice condenser upper plenum and the dead ended regions within containment; therefore, that differential pressure listed above (i.e., 8.3 psi) cannot occur.

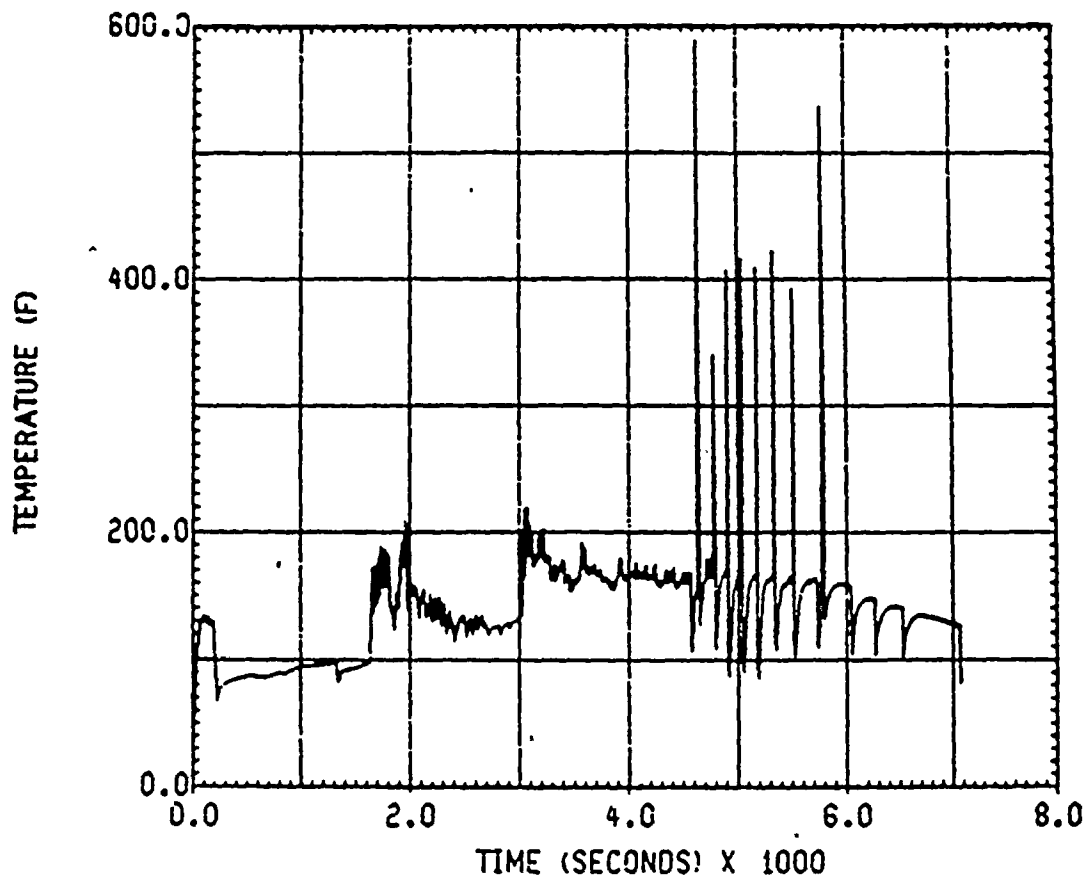
Figure 1-1
D.C. COOK CLASIX MODEL





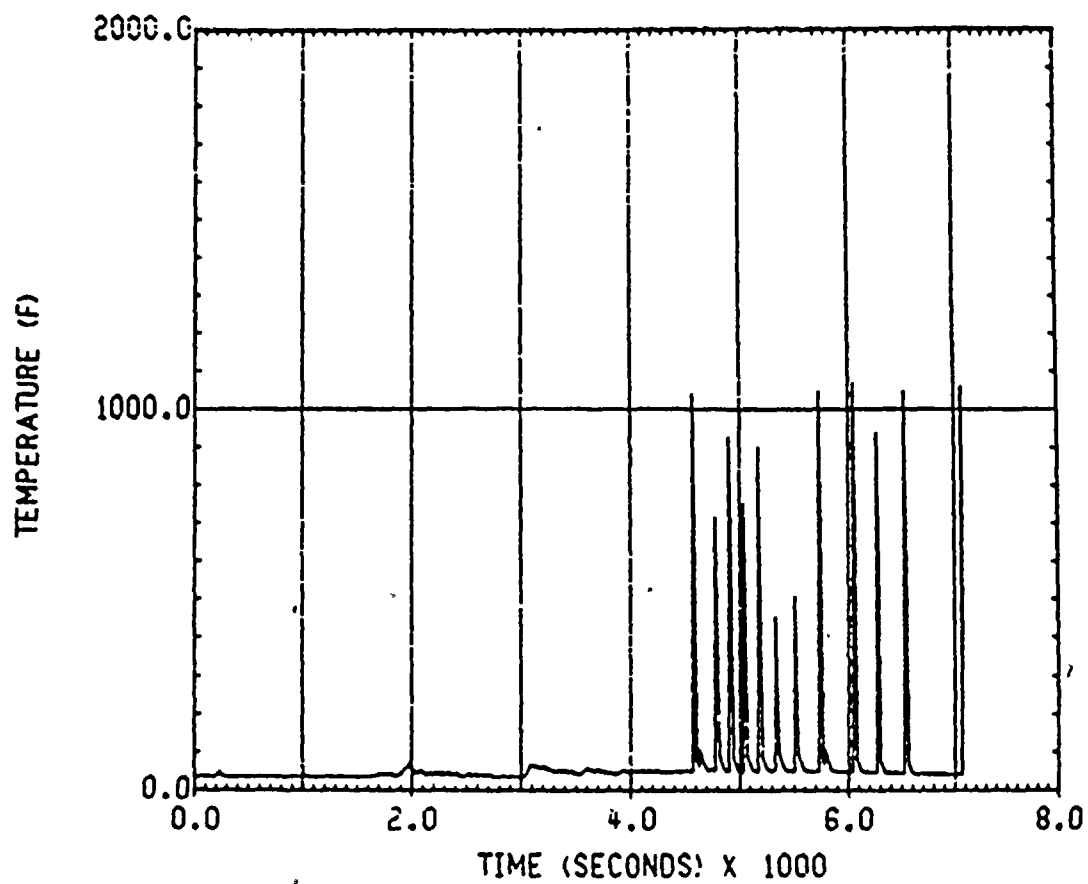
AEP D.C. COOK S2D BASE CASE
UCHIDA HTC 6328 GPM SPR 2FAN 85PCT 8V/0
LOWER COM TEMPERATURE

Figure 1-2



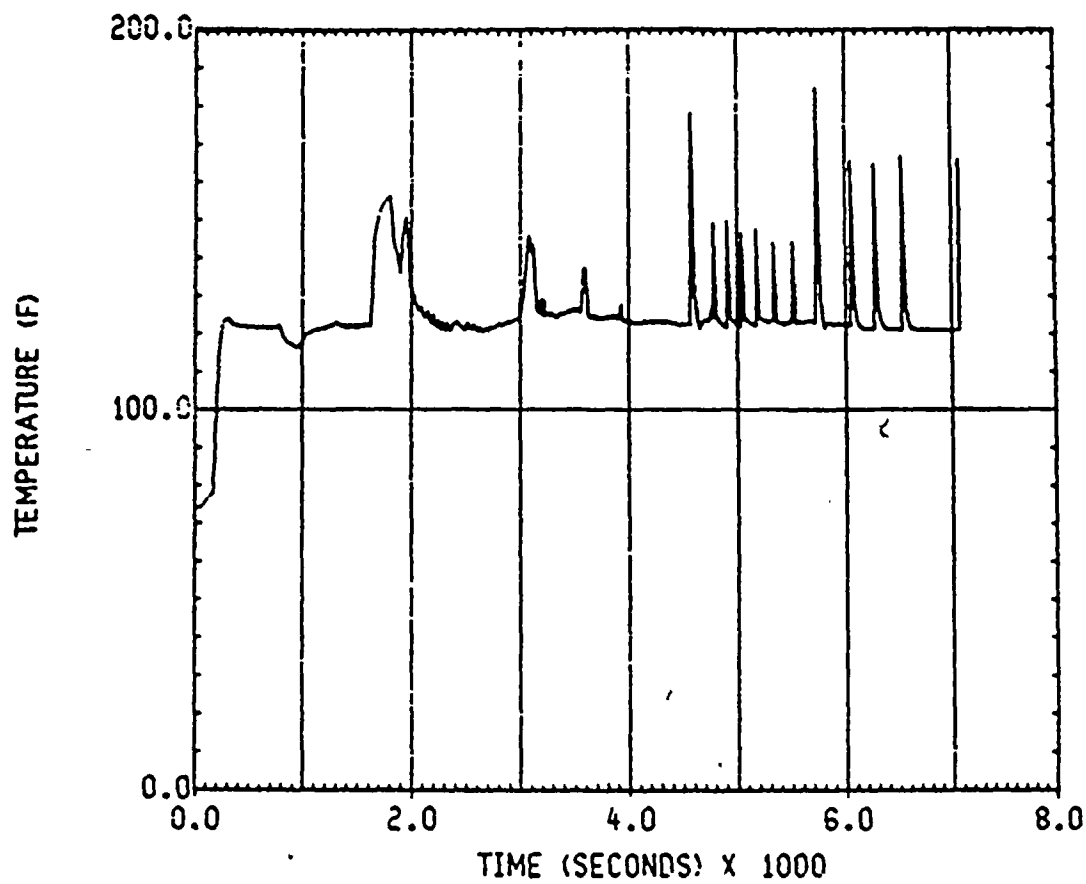
AEP D.C. COOK S20 BASE CASE
UCHIDA HTC 6328 GPM SPR 2FAN 85PCT 8V/0
LOWER PLN TEMPERATURE

Figure 1-3



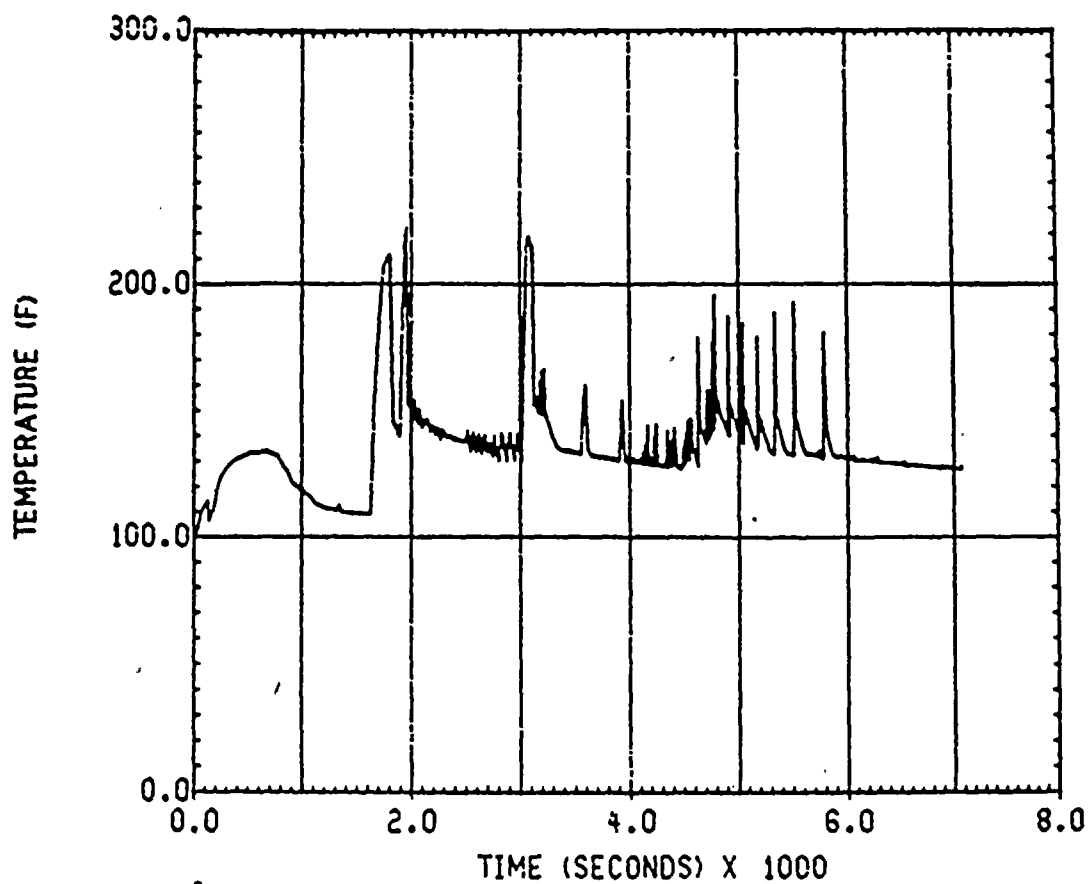
AEP D.C. COOK S2D BASE CASE
UCHIDA HTC 6328 GPM SPR 2FAN 85PCT 8V/0
UPPER PLN TEMPERATURE

Figure 1-4



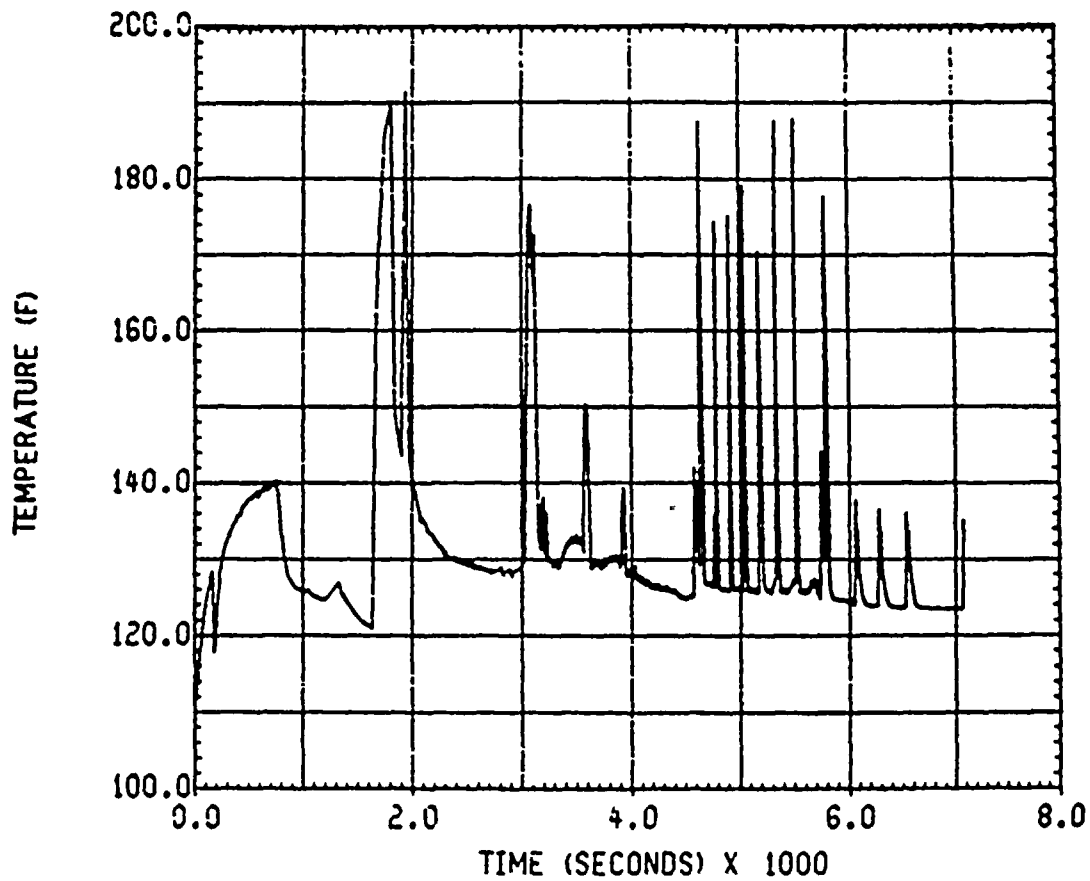
AEP D.C. COOK S2D BASE CASE
UCHIDA HTC 6328 GPM SPR 2FAN 85PCT 8V/O
UPPER COM TEMPERATURE

Figure 1-5



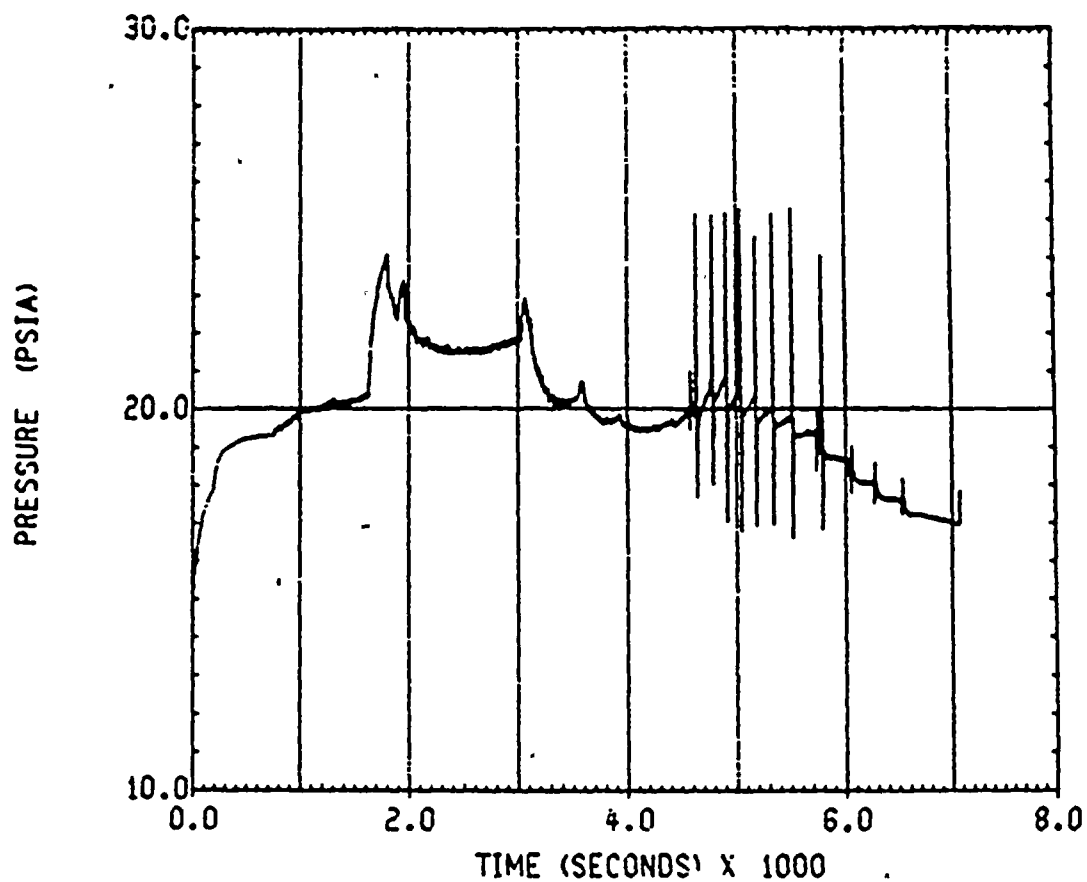
AEP D.C. COOK S20 BASE CASE
UCHIDA HTC 6328 GPM SPR 2FAN 85PCT 8V/O
DEAD-END TEMPERATURE

Figure 1-6



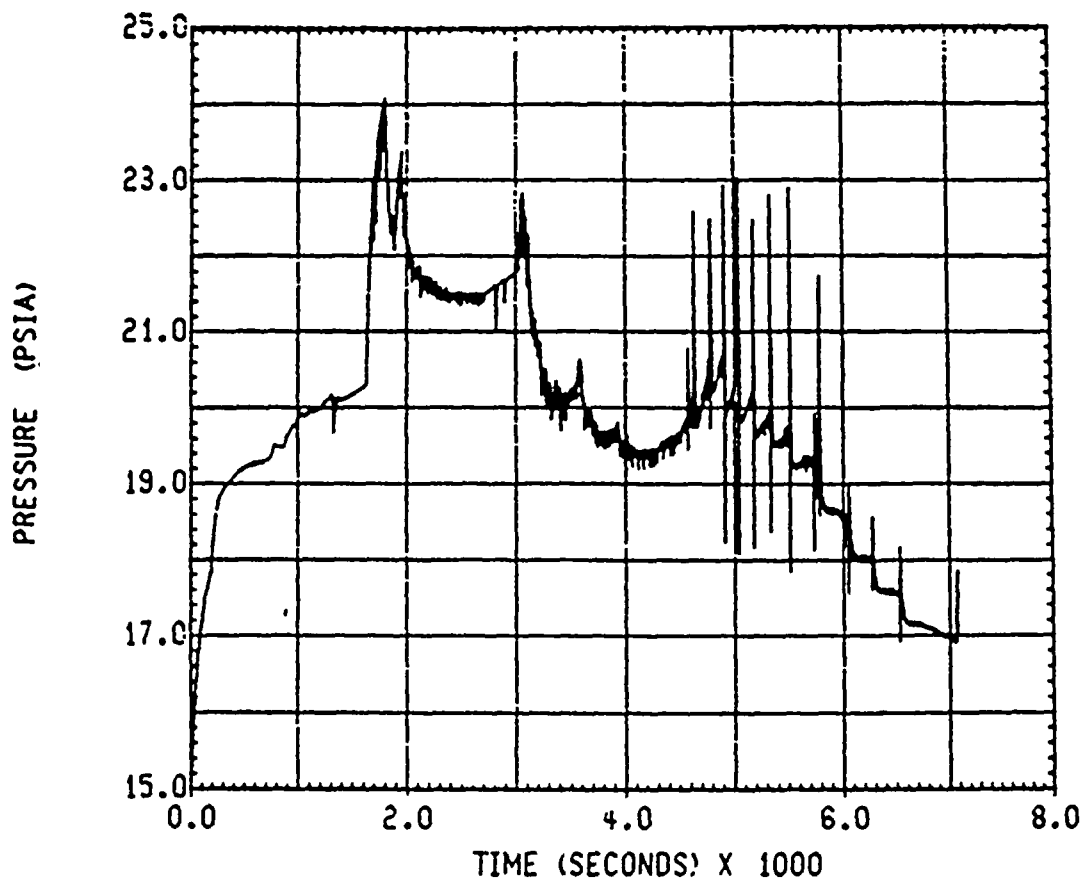
AEP D.C. COOK S2D BASE CASE
UCHIDA HTC 6328 GPM SPR 2FAN 85PCT 8V/0
FAN/AC RM TEMPERATURE

Figure 1-7



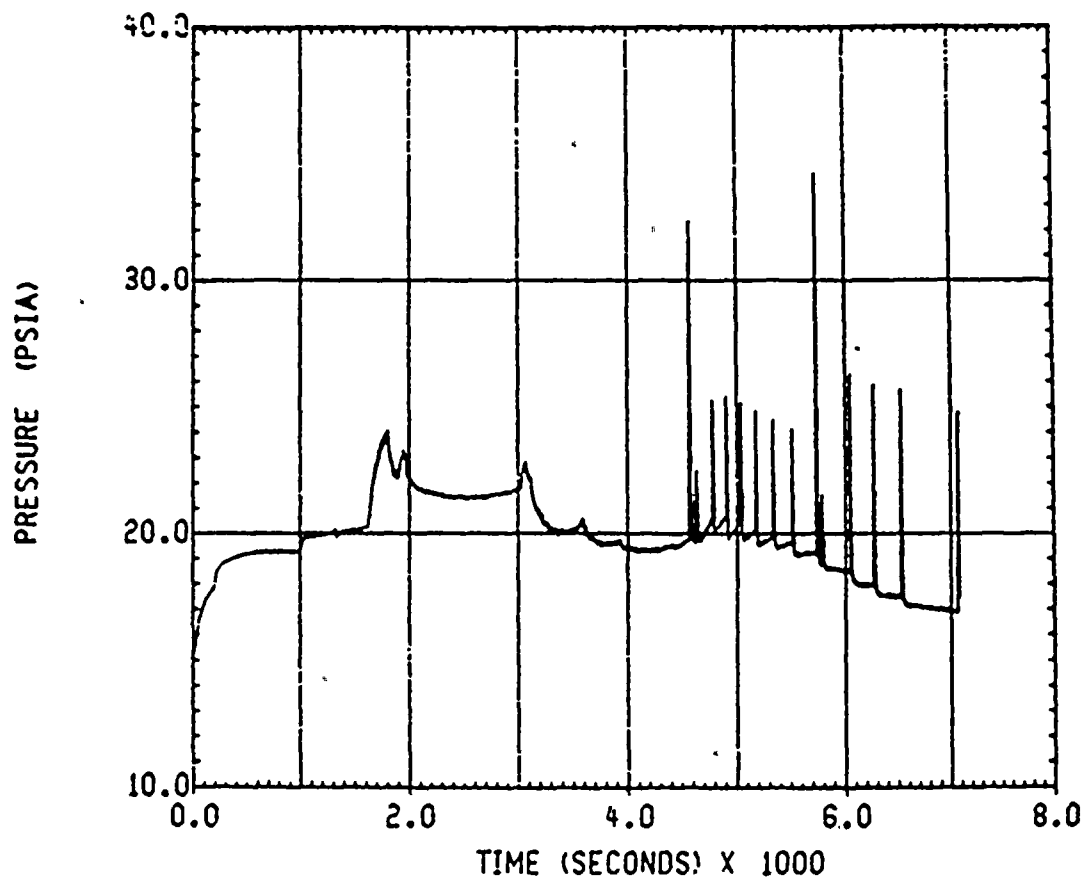
AEP D.C. COOK S2D BASE CASE
UCHIDA HTC 6328 GPM SPR 2FAN 85PCT 8V/O
LOWER COM PRESSURE

Figure 1-8



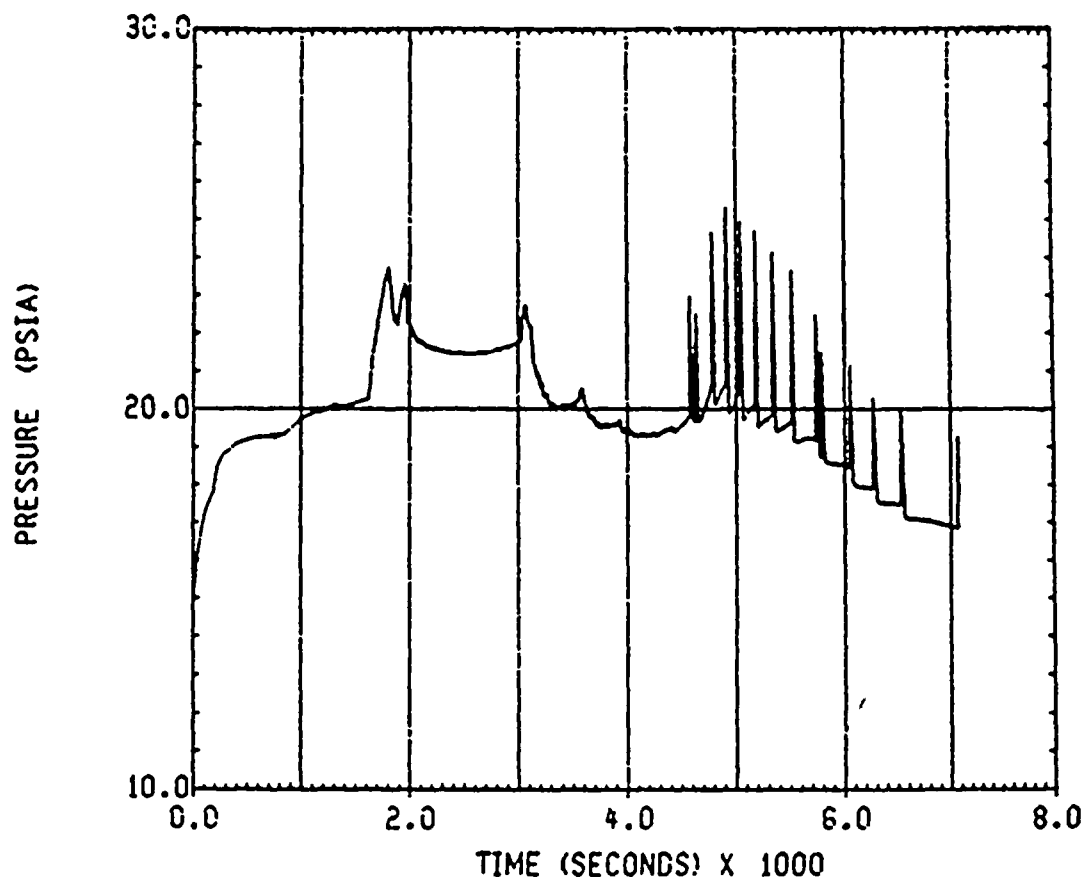
AEP D.C. COOK S2D BASE CASE
UCHIDA HTC 6328 GPM SPR 2FAN 85PCT 8V/0
LOWER PLN PRESSURE

Figure 1-9



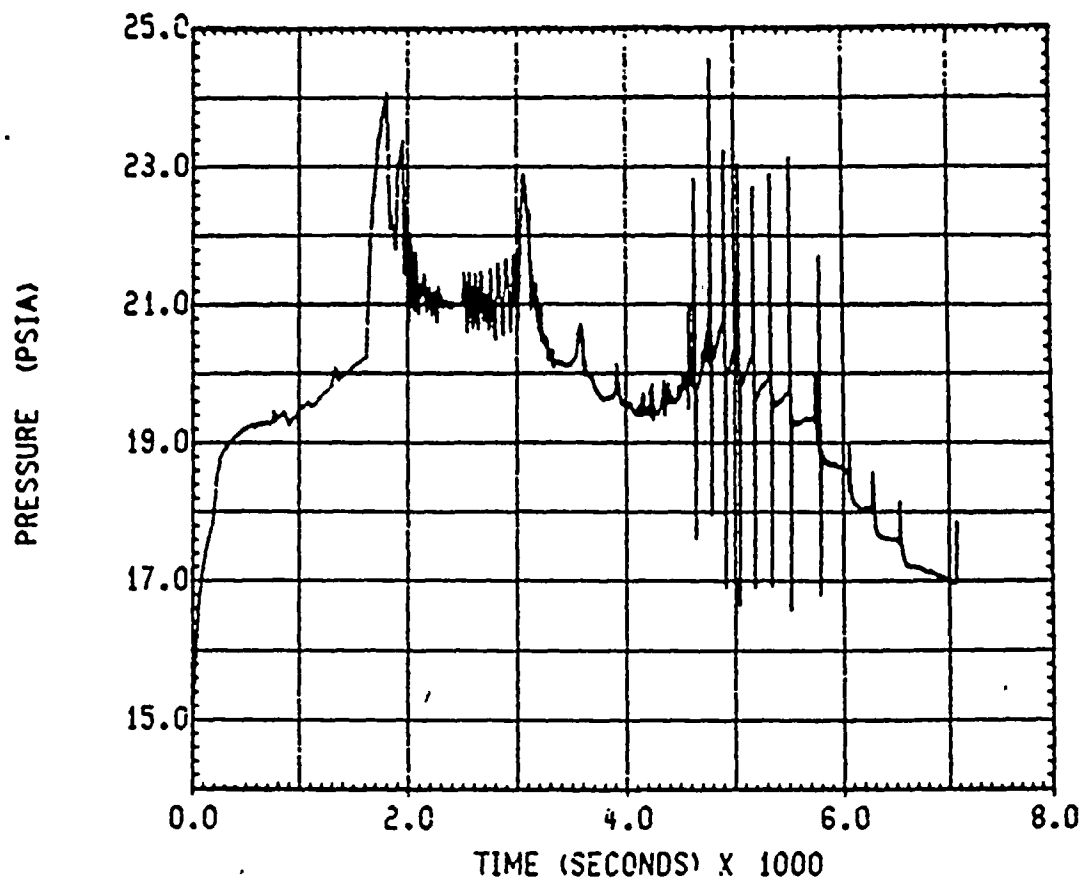
AEP D.C. COOK S2D BASE CASE
UCHIDA HTC 6328 GPM SPR 2FAN 85PCT 8V/O
UPPER PLN PRESSURE

Figure 1-10



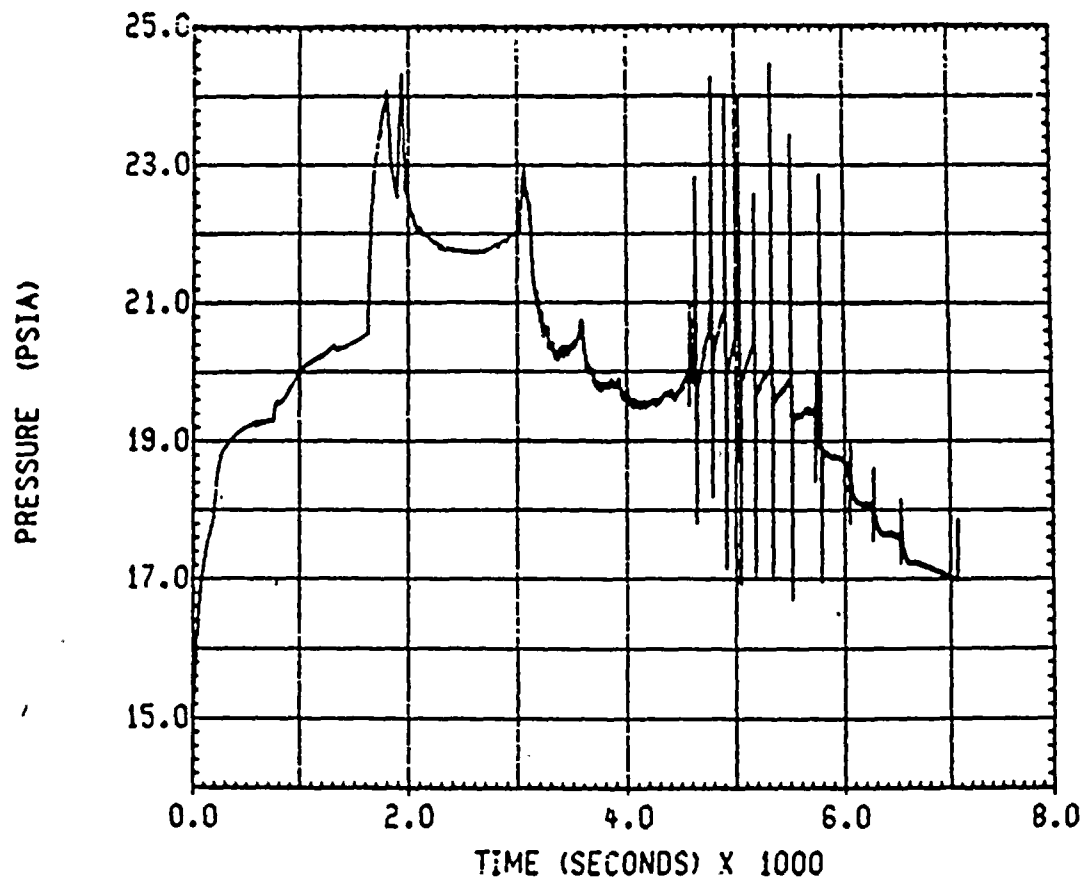
AEP D.C. COOK S2D BASE CASE
UCHIDA HTC 6328 GPM SPR 2FAN 85PCT 8V/0
UPPER COM PRESSURE

Figure 1-11



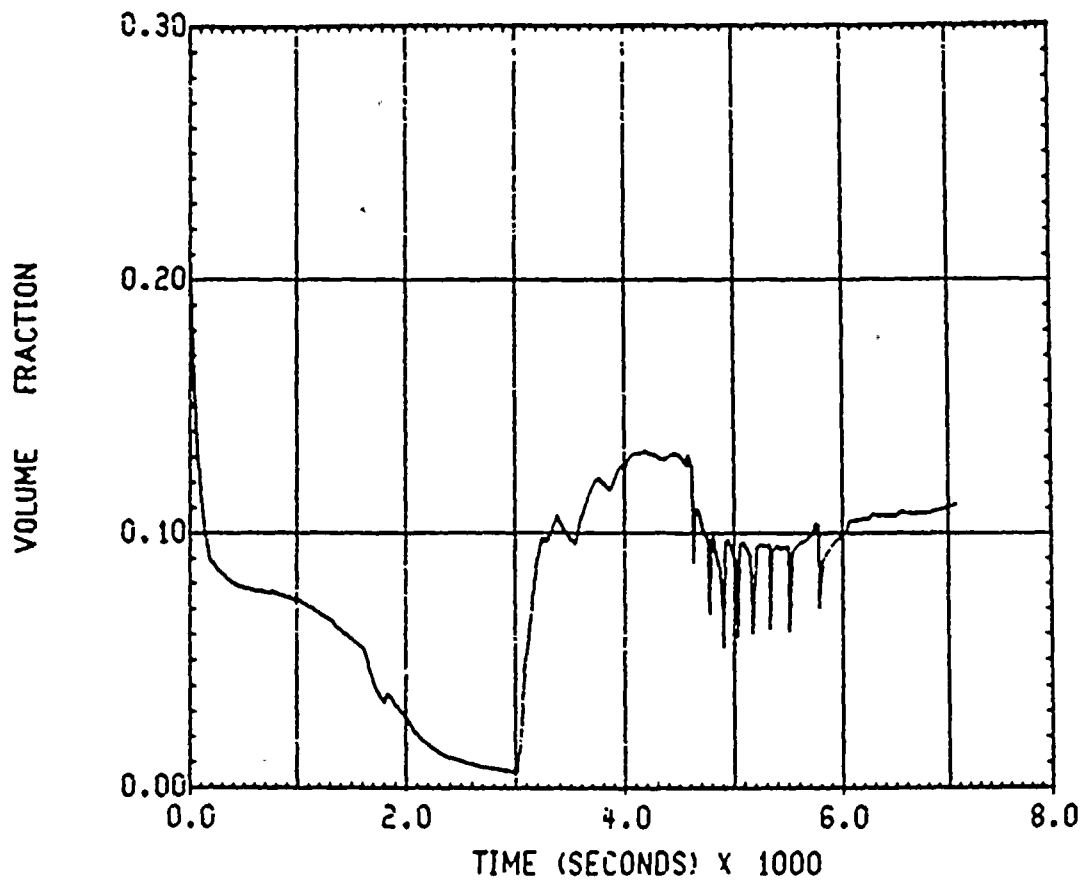
AEP D.C. COOK S2D BASE CASE
UCHIDA HTC 6328 GPM SPR 2FAN 85PCT 8V/O
DEAD-END PRESSURE

Figure 1-12



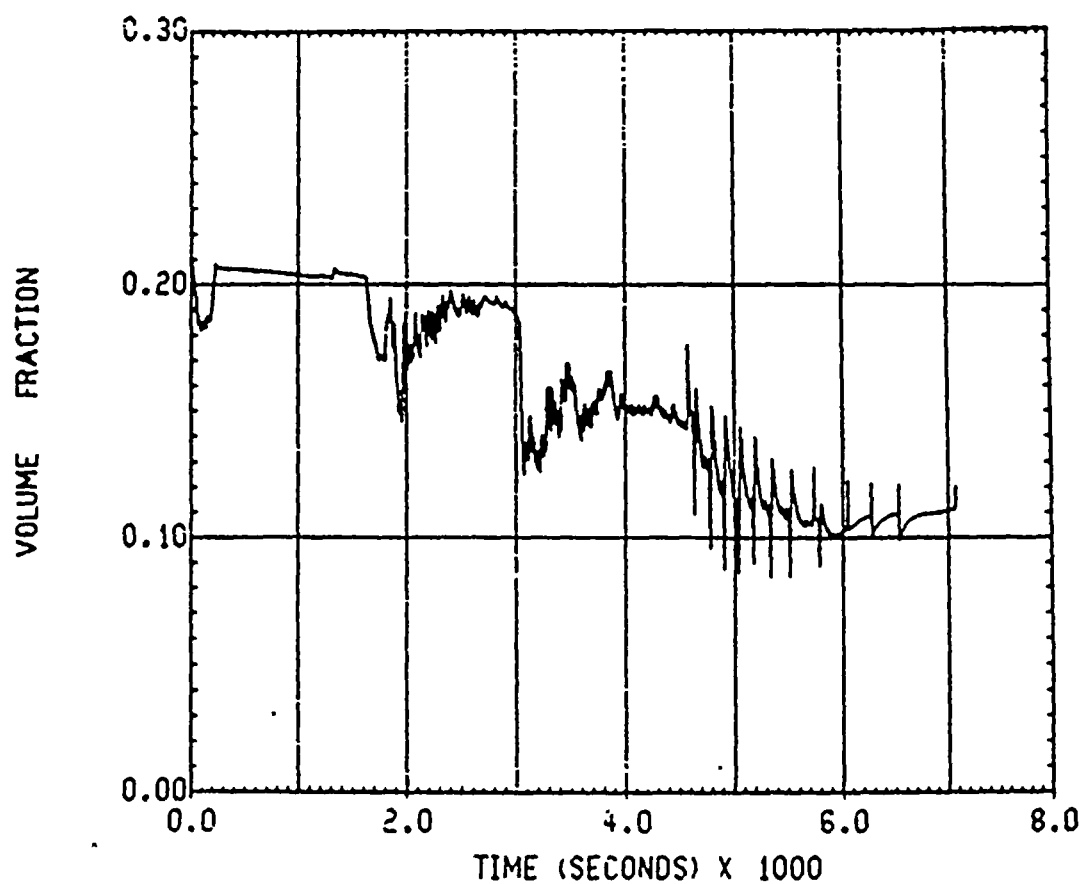
AEP D.C. COOK S2D BASE CASE
UCHIDA HTC 6328 GPM SPR 2FAN 85PCT 8V/O
FAN/AC RM PRESSURE

Figure 1-13



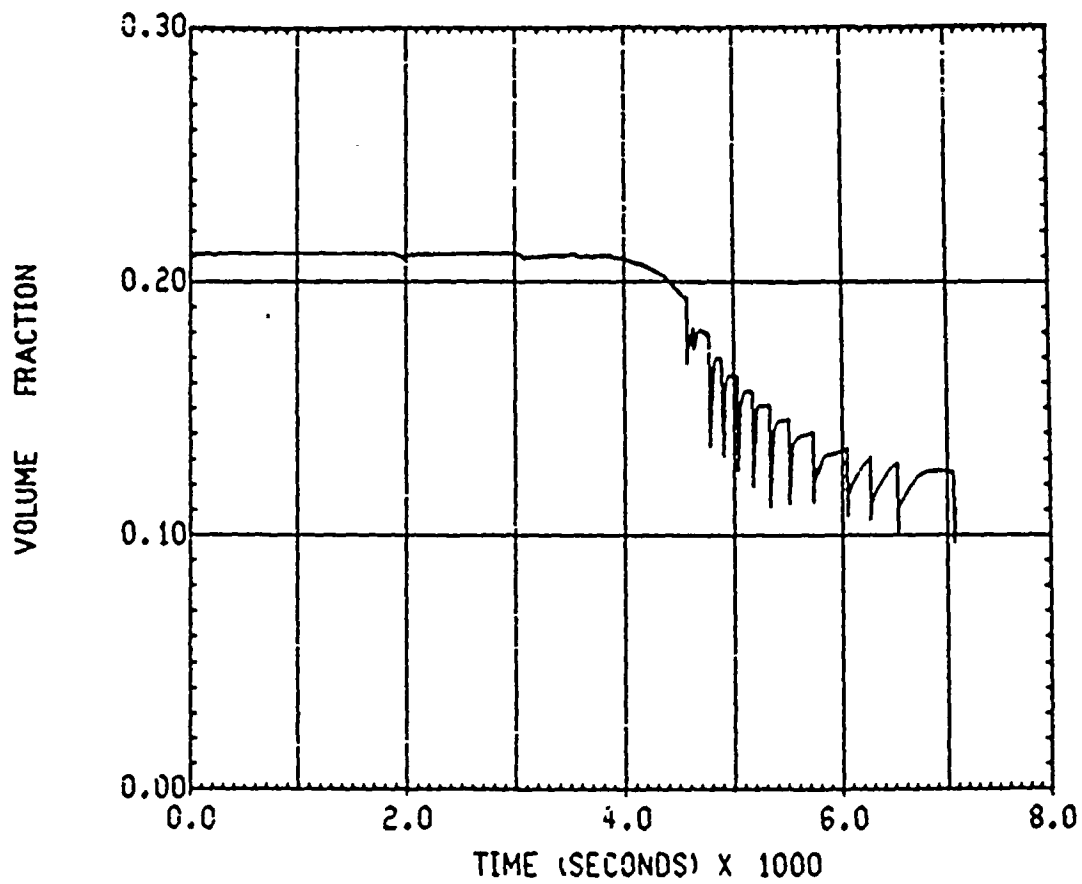
AEP D.C. COOK S2D BASE CASE
UCHIDA HTC 6328 GPM SPR 2FAN 85PCT 8V/O
LOWER COM 02 GAS CONCENTRATION

Figure 1-14



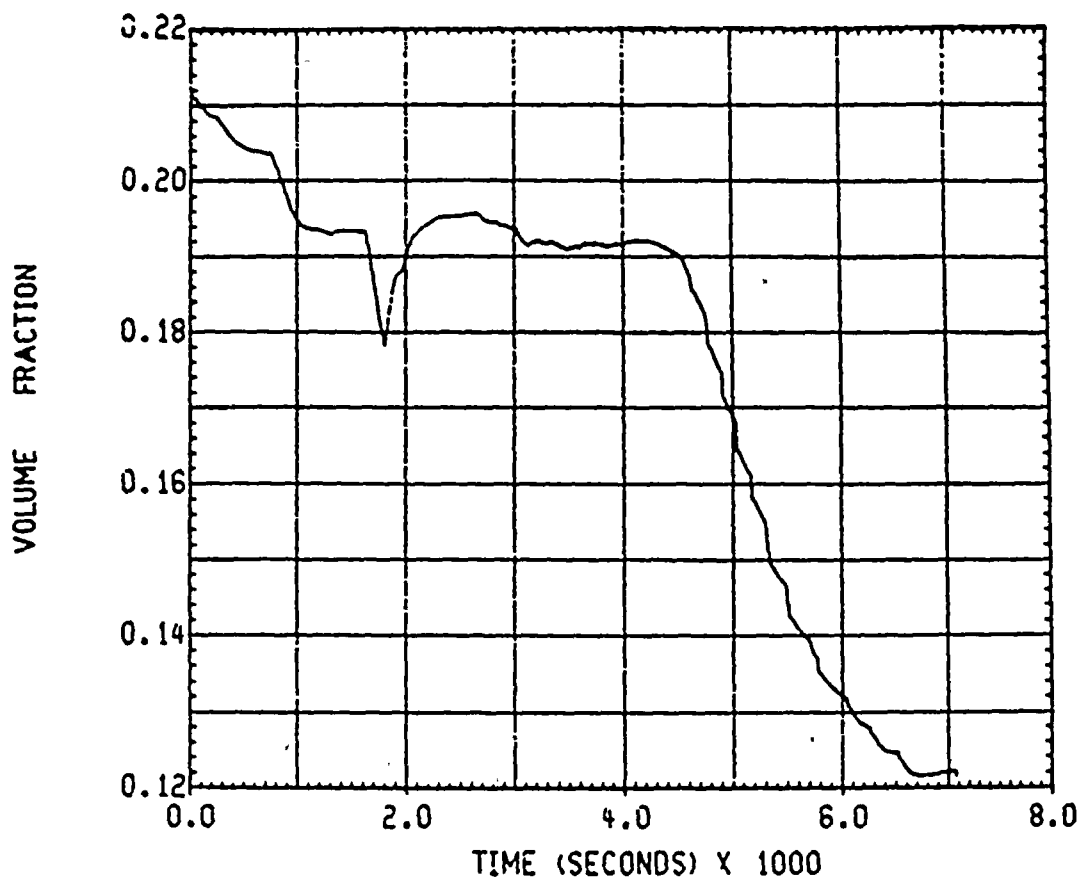
AEP D.C. COOK S2D BASE CASE
UCHIDA HTC 6328 GPM SPR 2FAN 85PCT 8V/0
LOWER PLN 02 GAS CONCENTRATION

Figure 1-15



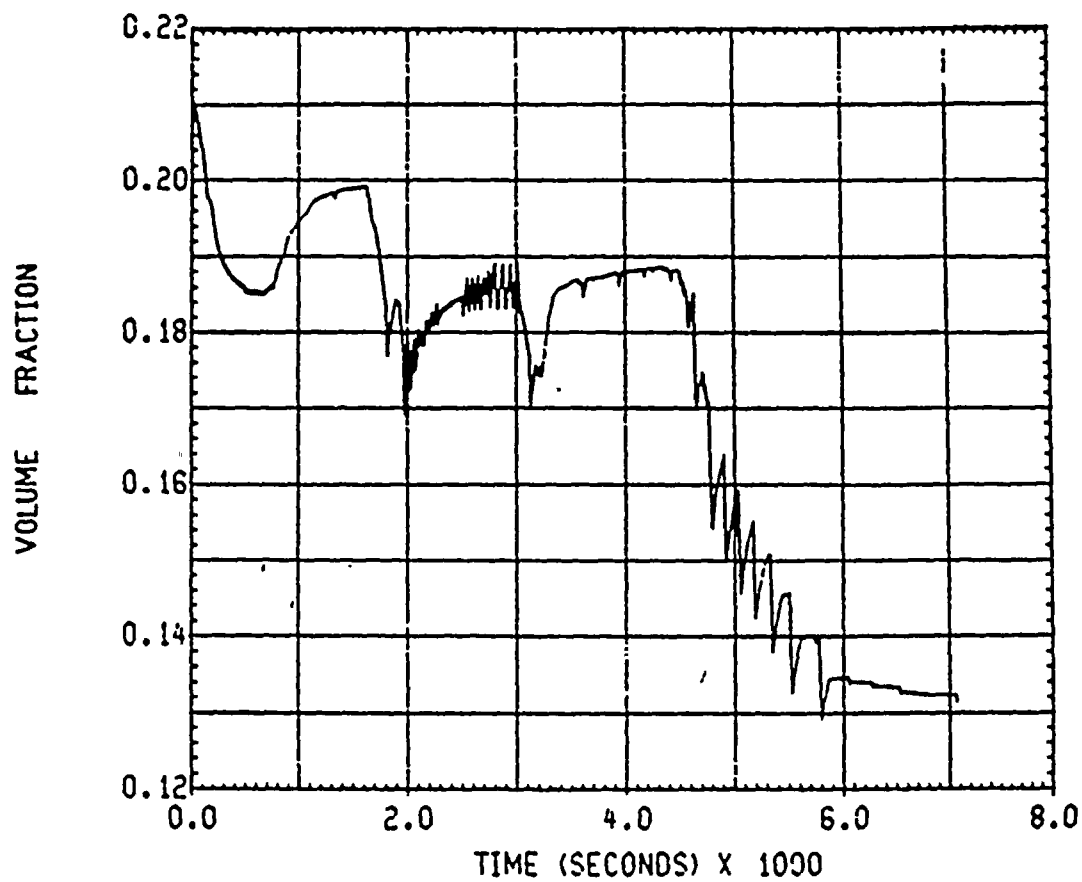
AEP D.C. COOK S2D BASE CASE
UCHIDA HTC 6328 GPM SPR 2FAN 85PCT 8V/O
UPPER PLN 02 GAS CONCENTRATION

Figure 1-16



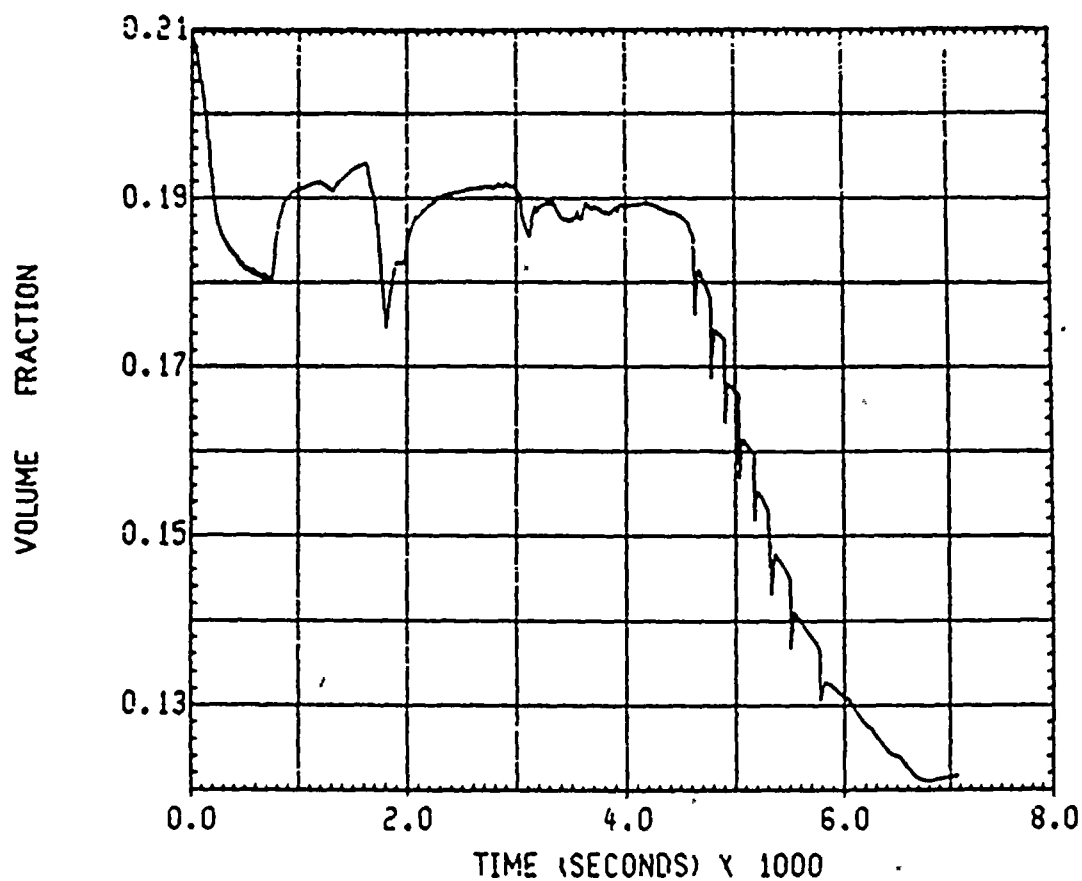
AEP D.C. COOK S2D BASE CASE
UCHIDA HTC 6328 GPM SPR 2FAN 85PCT 8V/O
UPPER COM O2 GAS CONCENTRATION

Figure 1-17



AEP D.C. COOK S20 BASE CASE
UCHIDA HTC 6328 GPM SPR 2FAN 85PCT 8V/O
DEAD-END O2 GAS CONCENTRATION

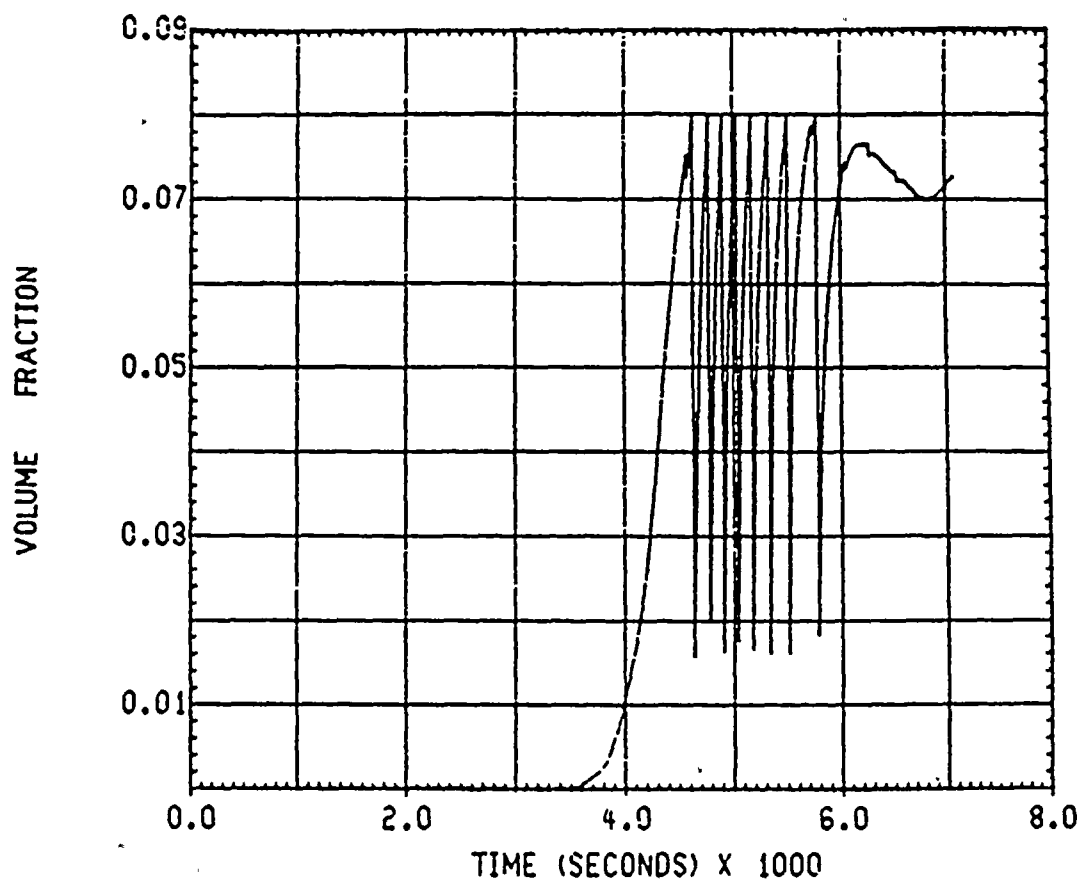
Figure 1-19



AEP D.C. COOK S2D BASE CASE
UCHIDA HTC 6328 GPM SPR 2FAN 85PCT 8V/O
FAN/AC RM O2 GAS CONCENTRATION

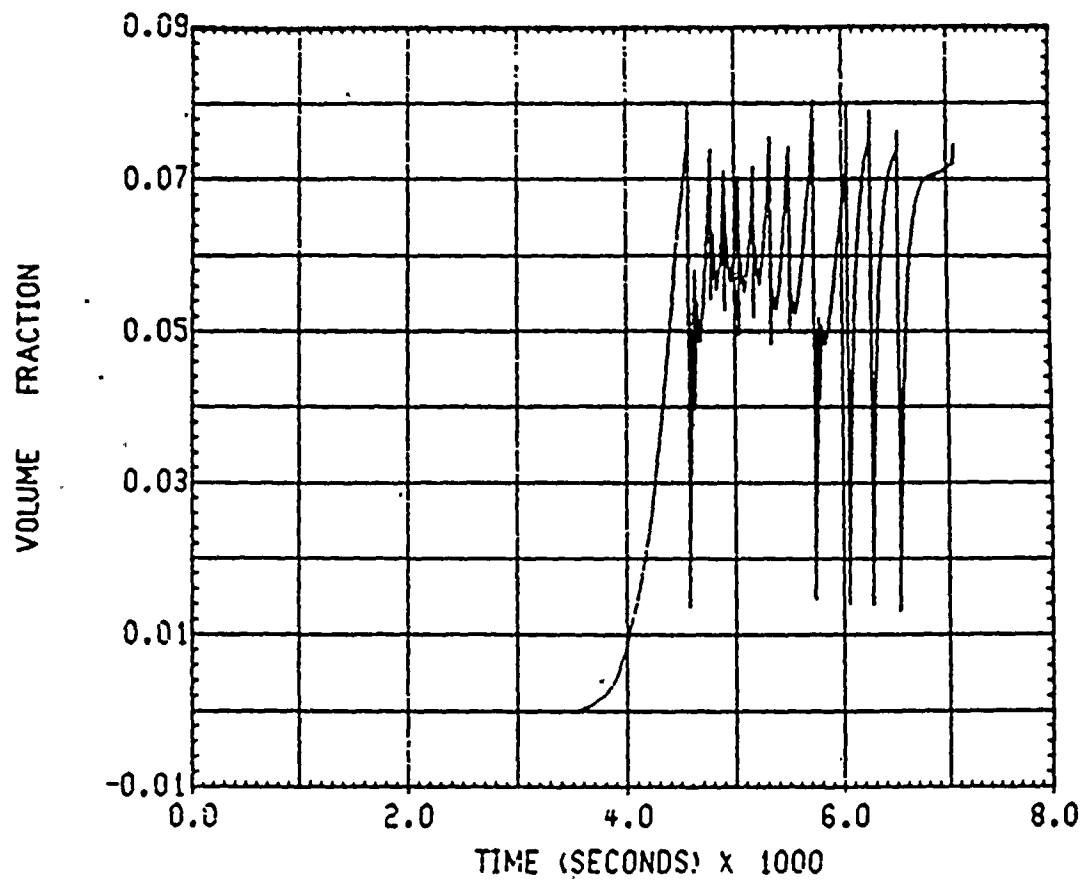
Figure 1-19





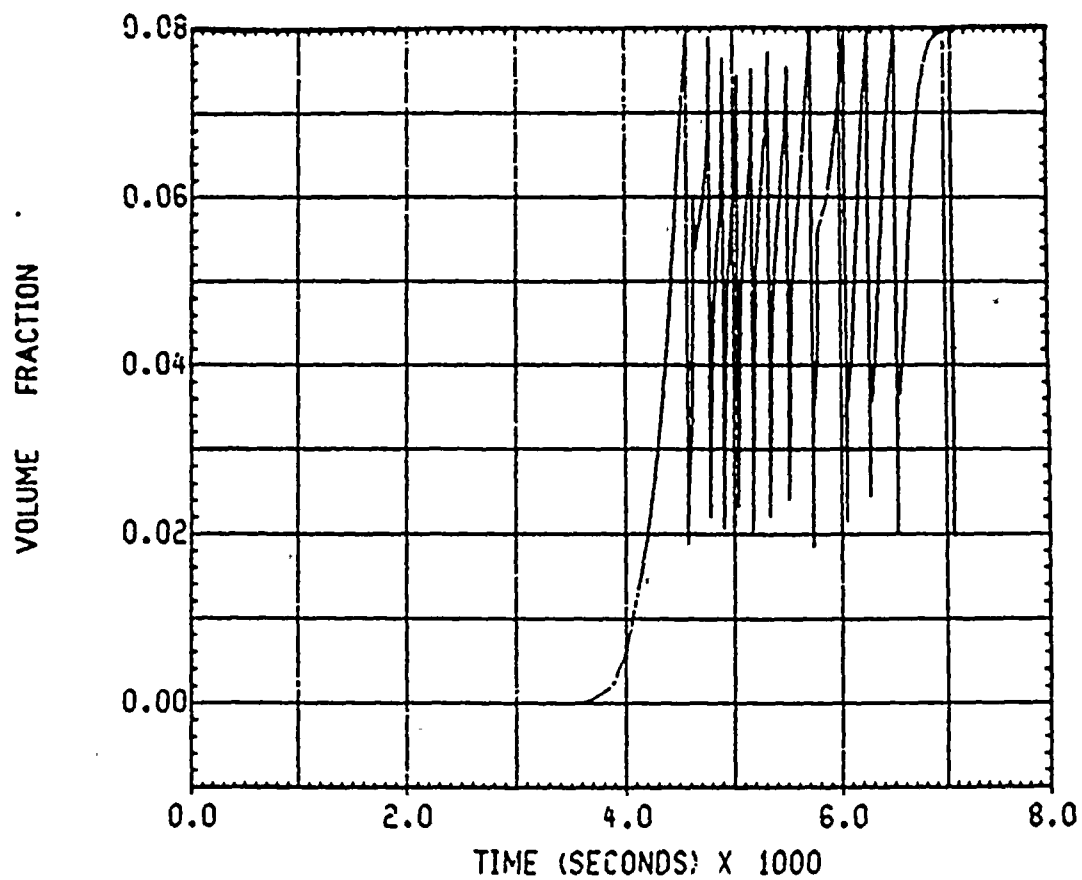
AEP D.C. COOK S2D BASE CASE
UCHIDA HTC 6328 GPM SPR 2FAN 85PCT 8V/O
LOWER COM H2 GAS CONCENTRATION

Figure 1-20



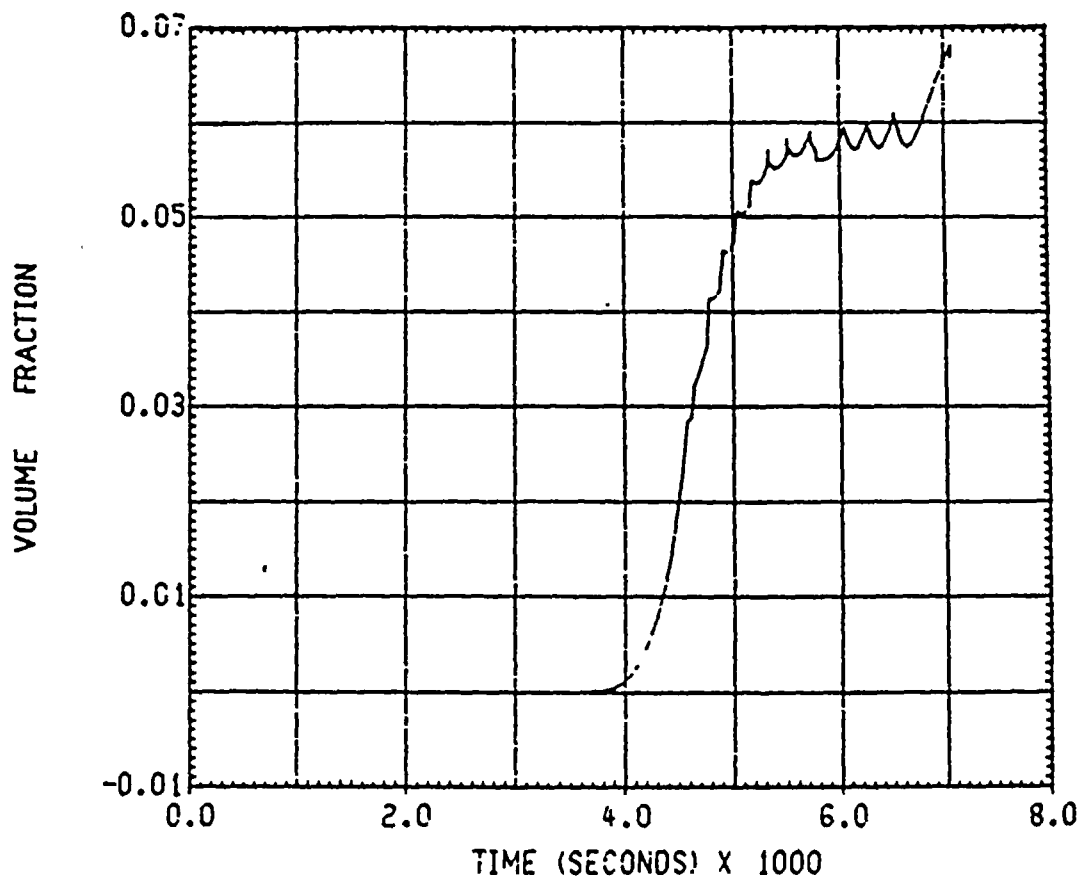
AEP D.C. COOK S2D BASE CASE
UCHIDA HTC 6328 GPM SPR 2FAN 85PCT 8V/O
LOWER PLN H2 GAS CONCENTRATION

Figure 1-21



AEP D.C. COOK S2D BASE CASE
UCHIDA HTC 6328 GPM SPR 2FAN 85PCT 8V/O
UPPER PLN H2 GAS CONCENTRATION

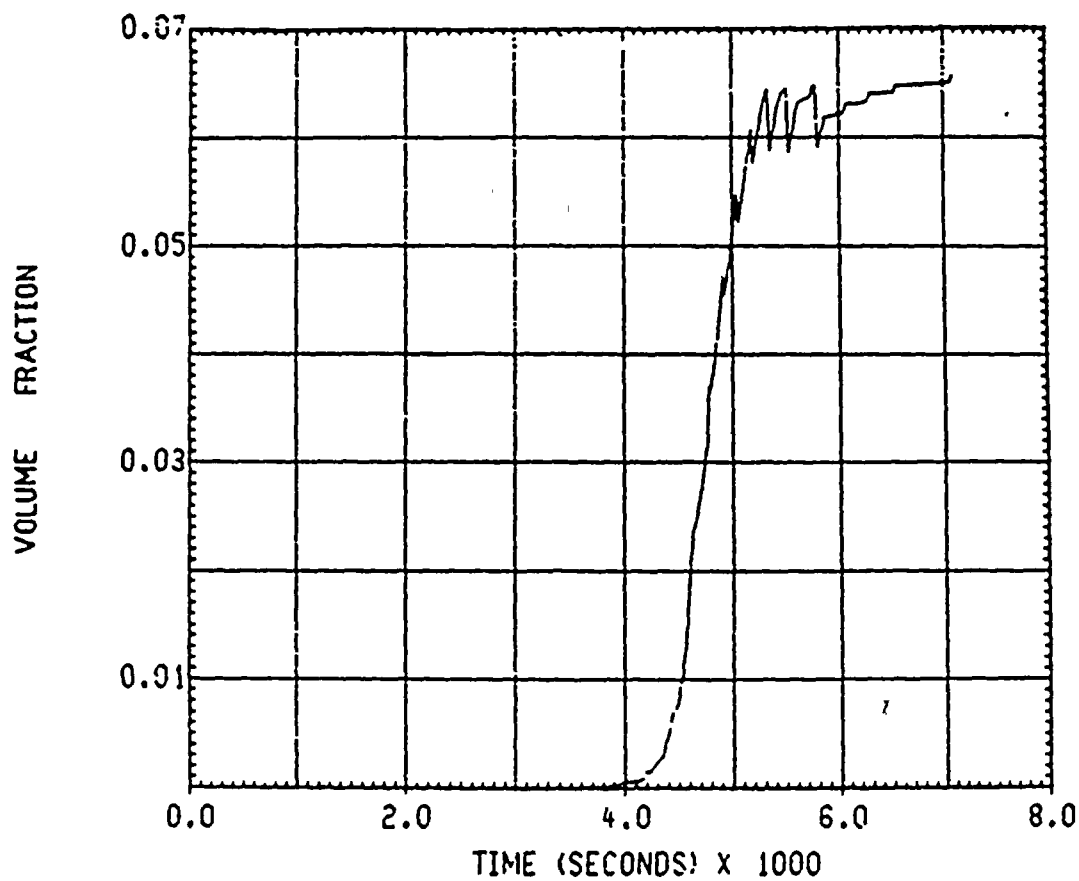
Figure 1-22



AEP D.C. COOK S2D BASE CASE
UCHIDA HTC 6328 GPM SPR 2FAN 85PCT 8V/O
UPPER COM H2 GAS CONCENTRATION

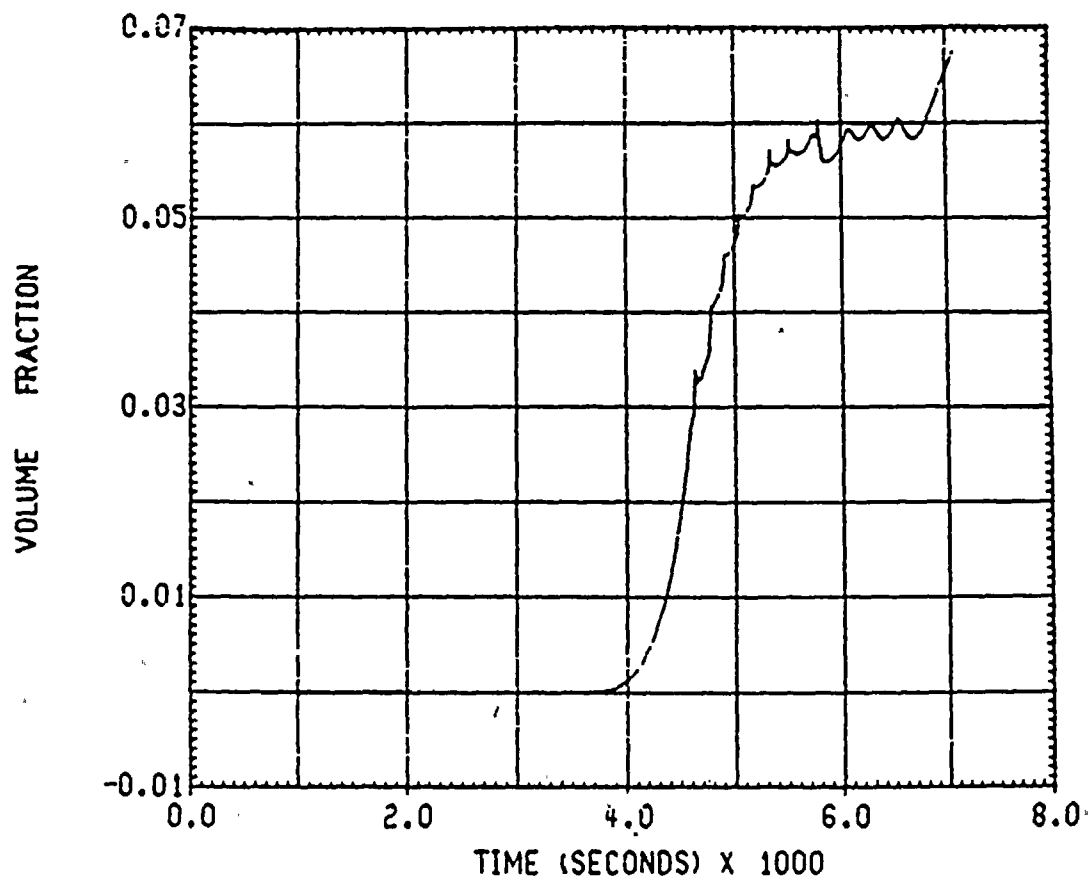
Figure 1-23





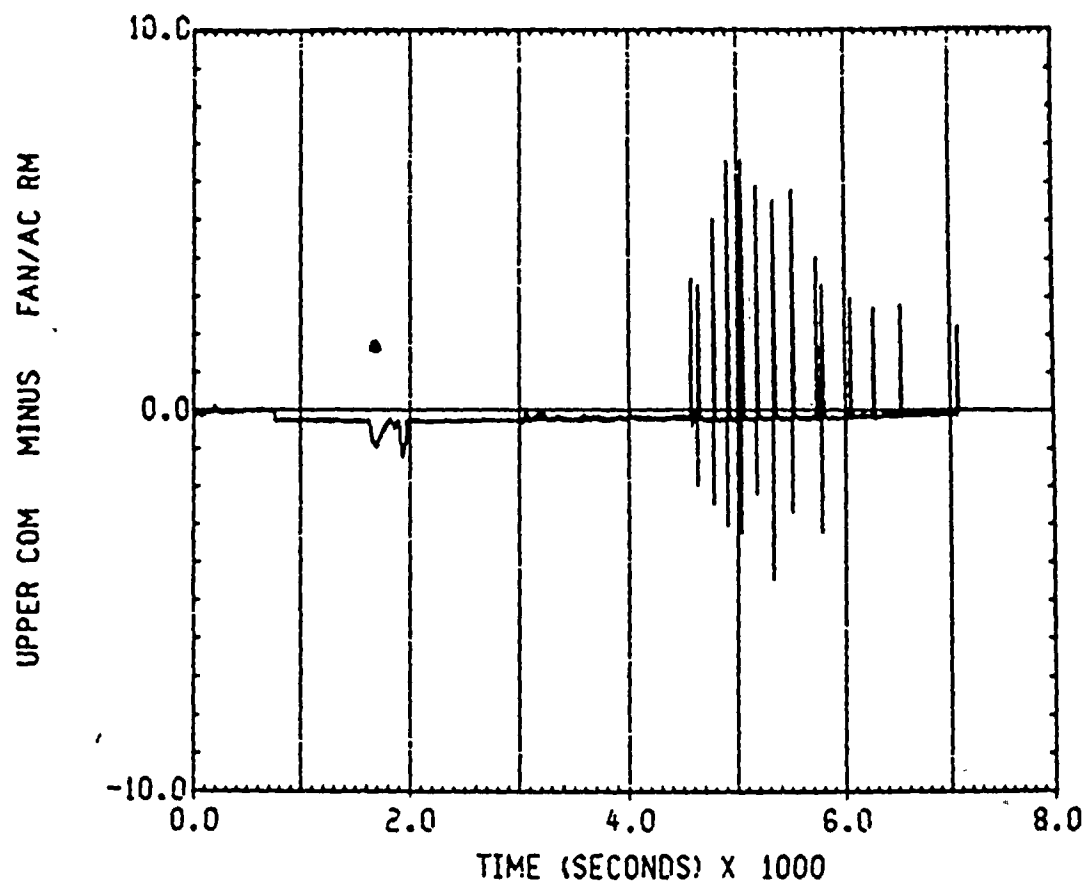
AEP D.C. COOK S2D BASE CASE
UCHIDA HTC 6328 GPM SPR 2FAN 85PCT 8V/O
DEAD-END H2 GAS CONCENTRATION

Figure 1-24



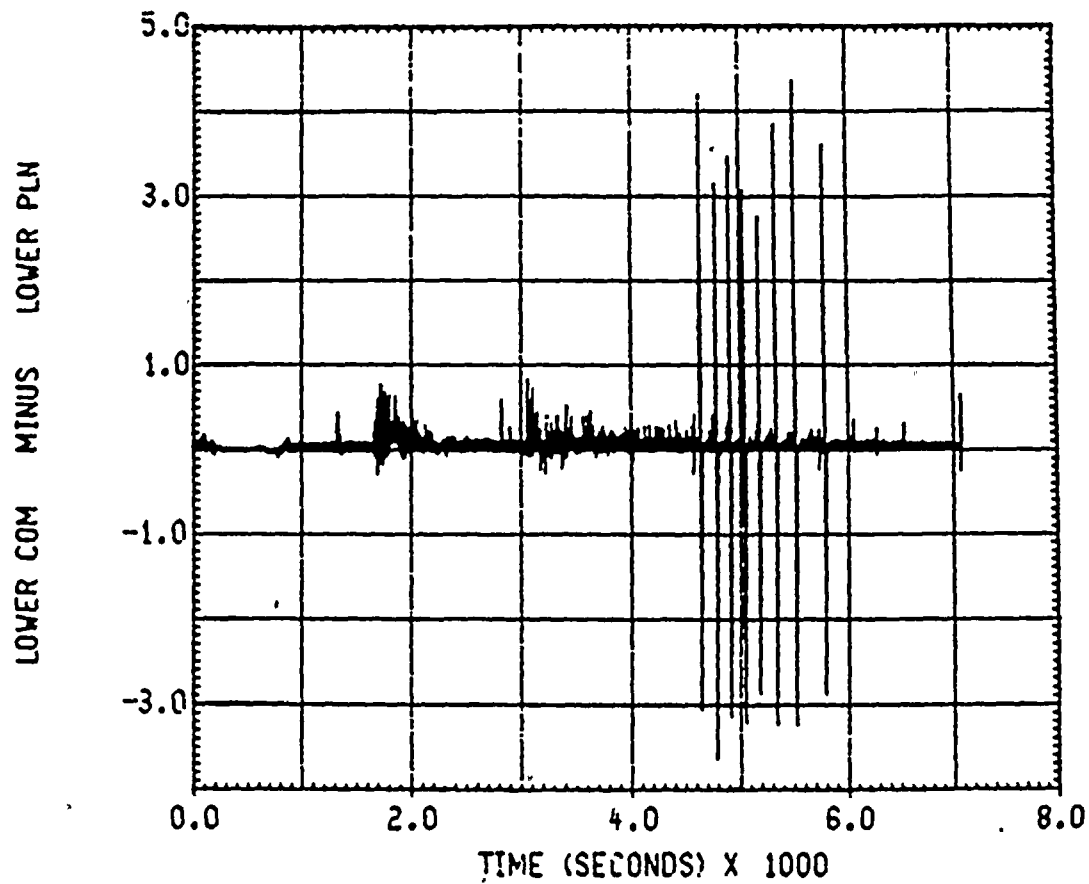
AEP D.C. COOK S2D BASE CASE
UCHIDA HTC 6328 GPM SPR 2FAN 85PCT 8V/O
FAN/AC RM H2 GAS CONCENTRATION

Figure 1-25



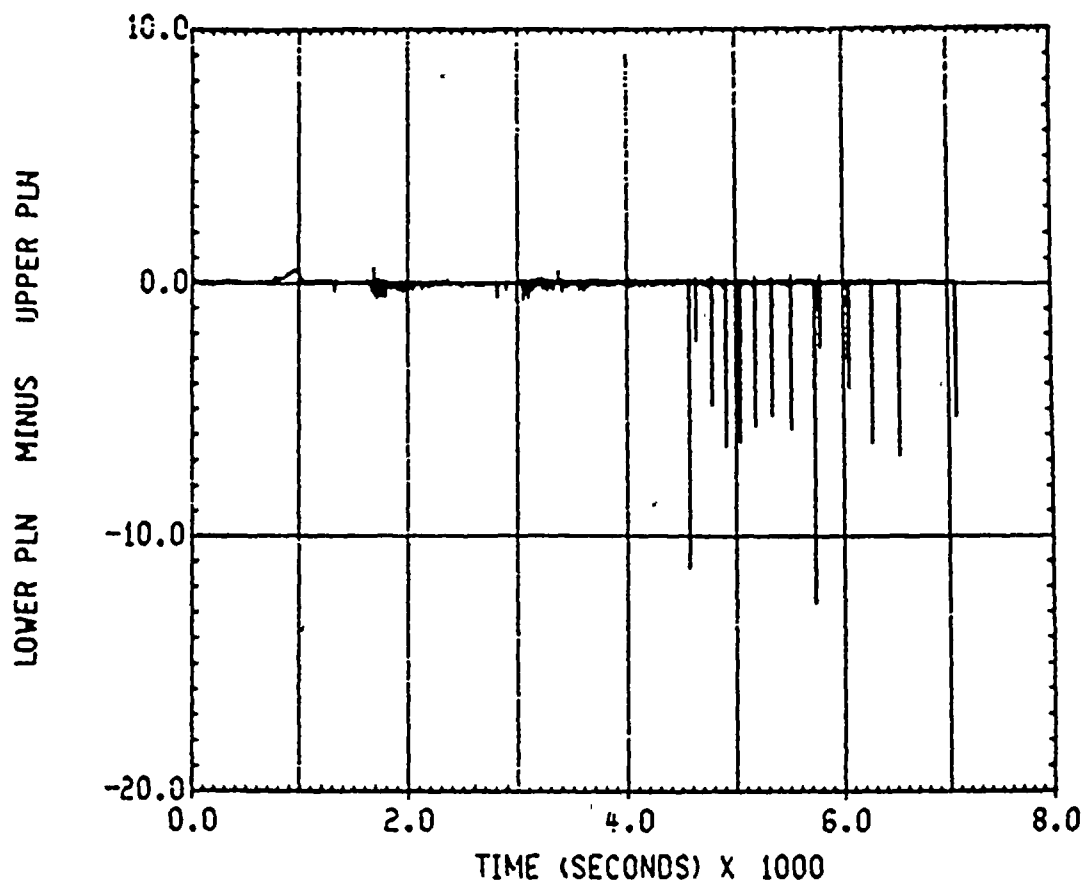
AEP D.C. COOK S2D BASE CASE
UCHIDA HTC 6328 GPM SPR 2FAN 85PCT 8V/0
DIFFERENTIAL PRESSURE

Figure 1-26



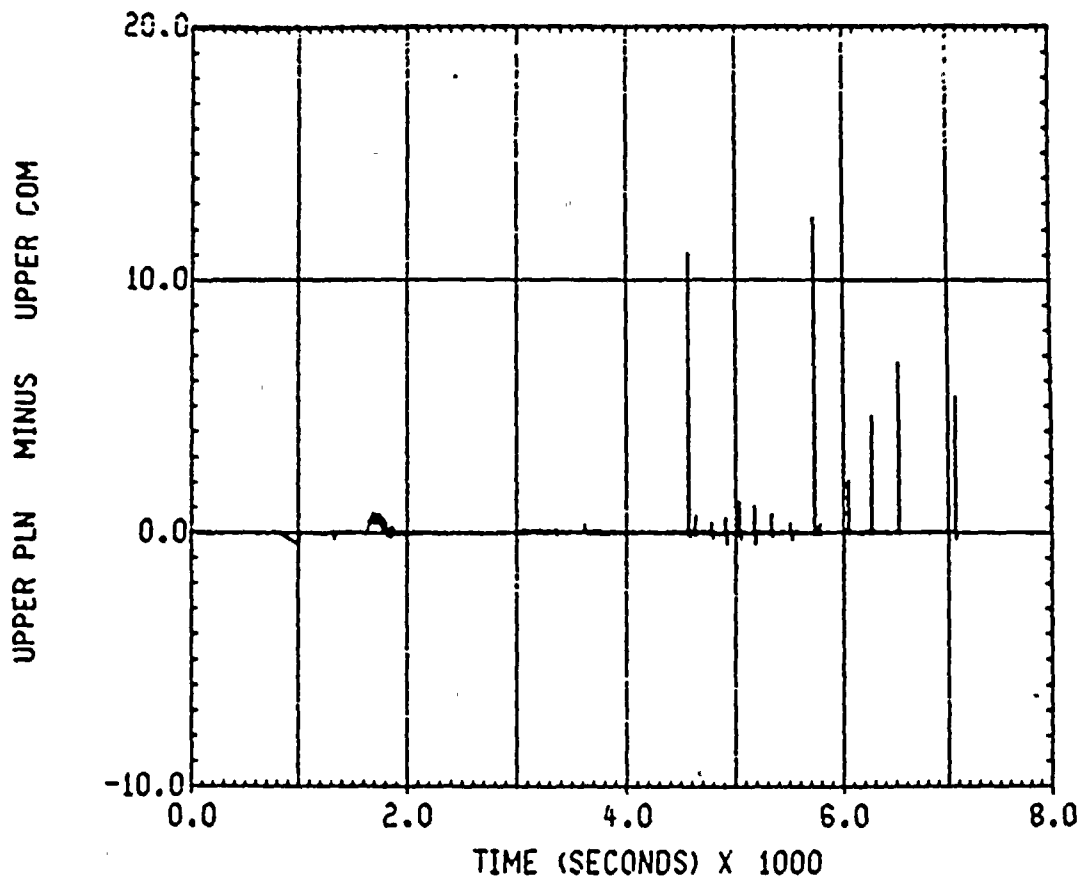
AEP D.C. COOK S2D BASE CASE
UCHIDA HTC 6328 GPM SPR 2FAN 85PCT 8V/0
DIFFERENTIAL PRESSURE

Figure 1-27



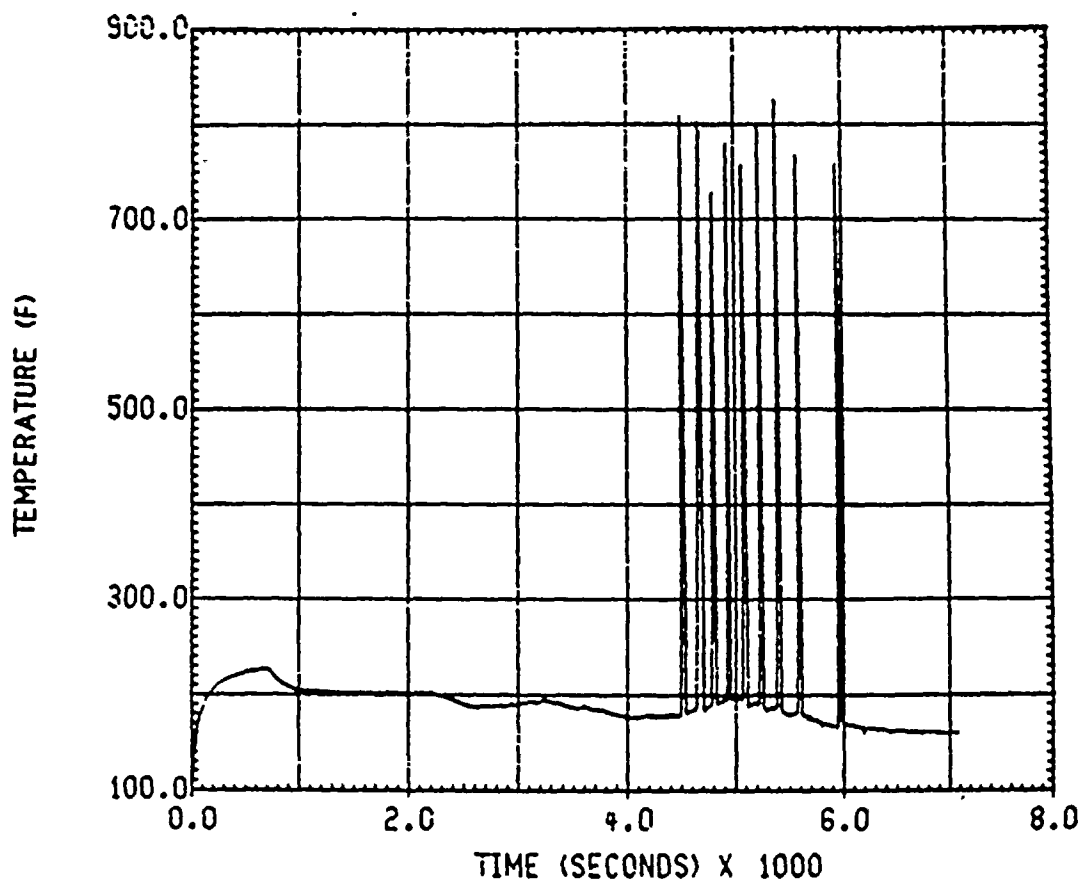
AEP D.C. COOK S2D BASE CASE
UCHIDA HTC 6328 GPM SPR 2FAN 85PCT 8V/0
DIFFERENTIAL PRESSURE

Figure 1-28



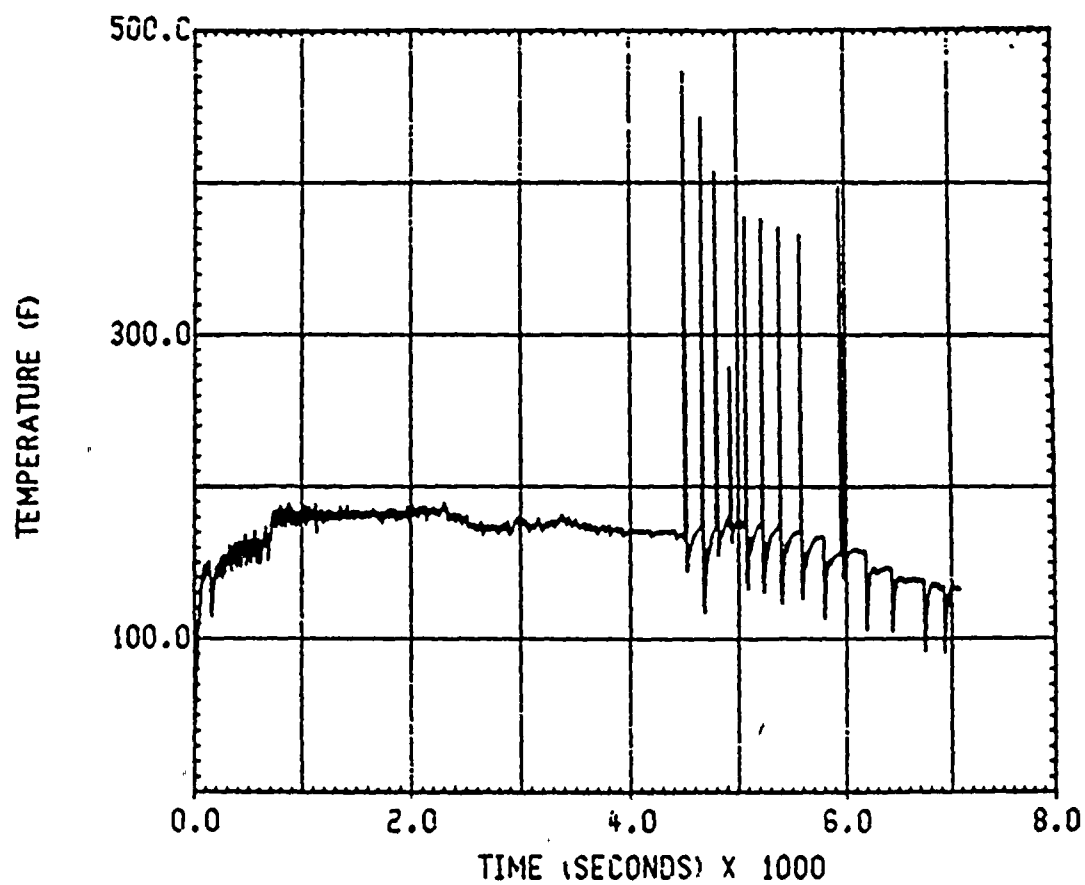
AEP D.C. COOK S2D BASE CASE
UCHIDA HTC 6328 GPM SPR 2FAN 85PCT 8V/O
DIFFERENTIAL PRESSURE

Figure 1-29



AEP D.C. COOK S20 TAGAMI CASE
TAGAMI HTC 6328 GPM SPR 2FAN 85PCT 8V/O
LOWER COM TEMPERATURE

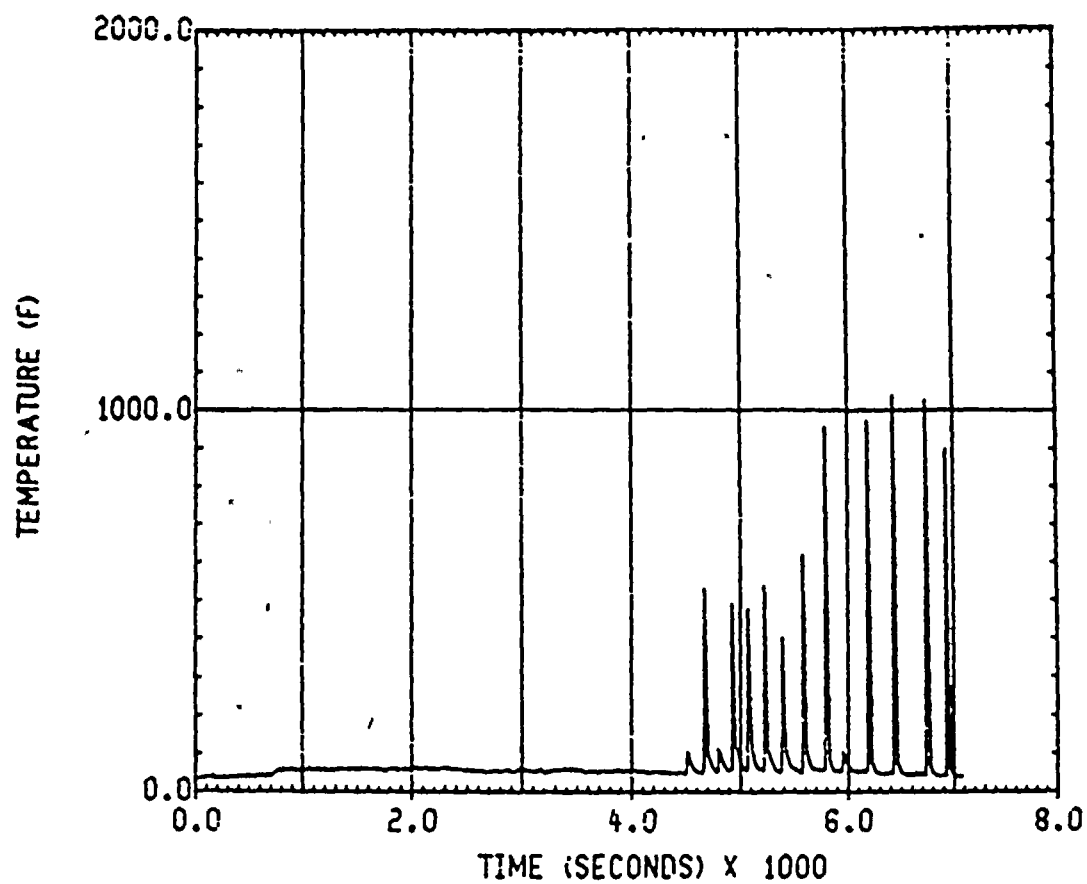
Figure 1-30



AEP D.C. COOK S2D TAGAMI CASE
TAGAMI HTC 6328 GPM SPR 2FAN 85PCT 8V/0
LOWER PLN TEMPERATURE

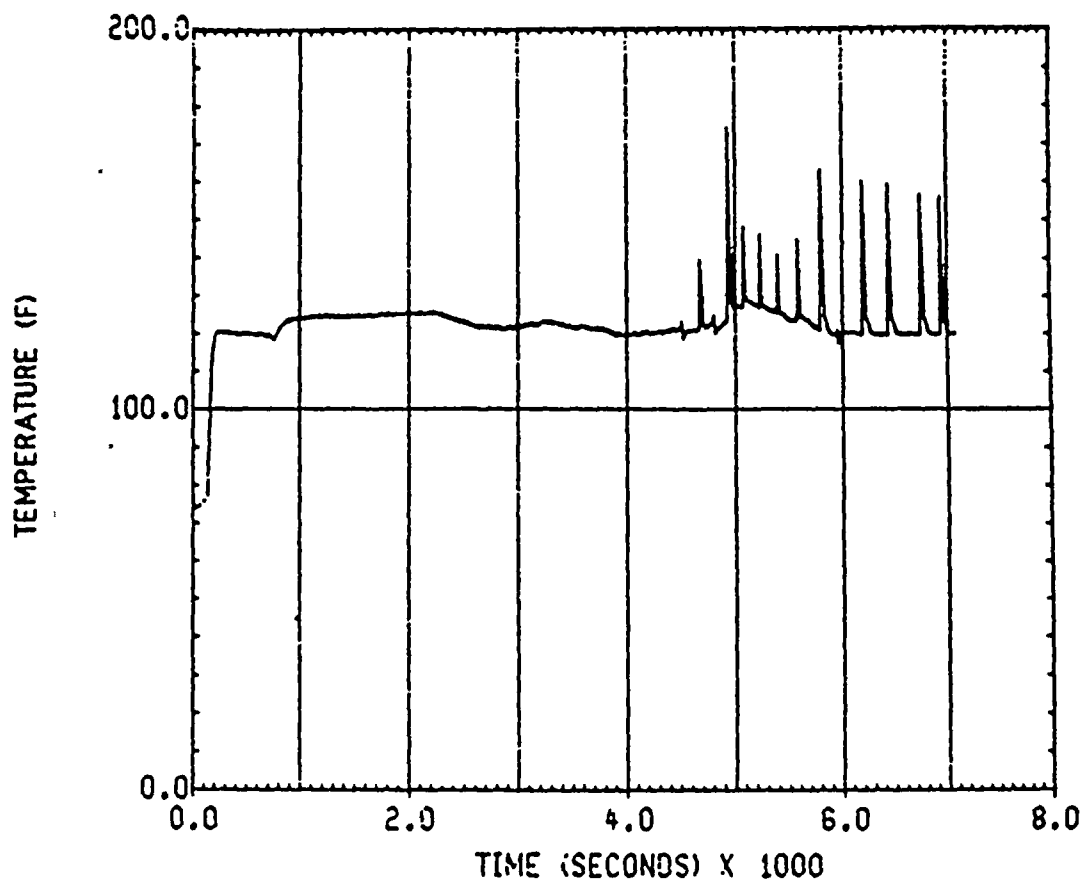
Figure 1-31





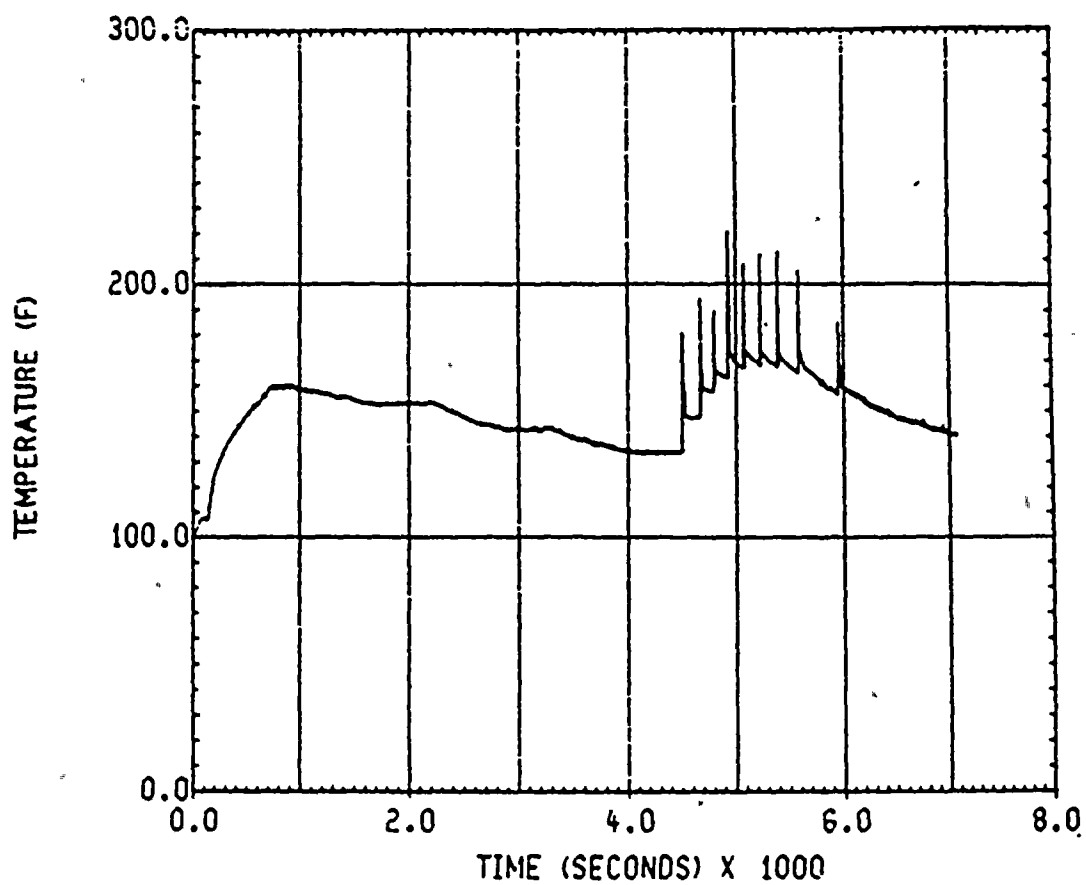
AEP D.C. COOK S2D TAGAMI CASE
TAGAMI HTC 6328 GPM SPR 2FAN 85PCT 8V/O
UPPER PLN TEMPERATURE

Figure 1-32



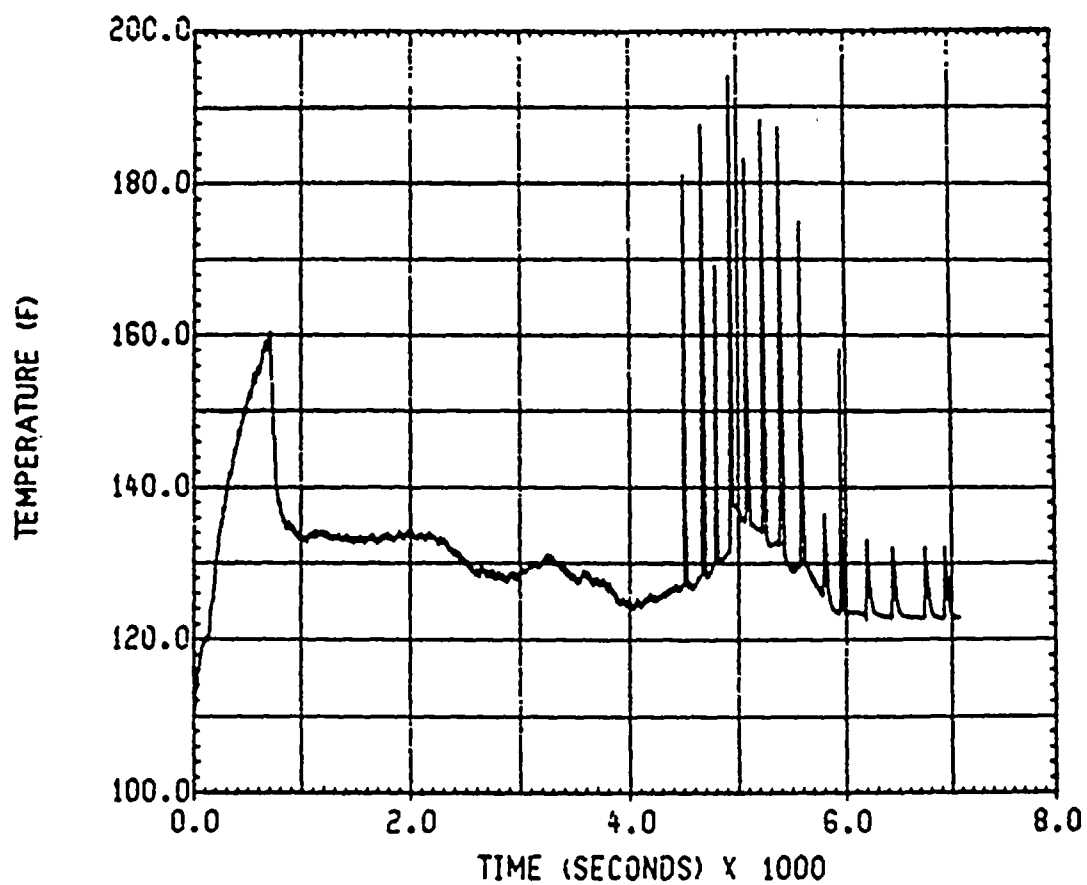
AEP D.C. COOK S2D TAGAMI CASE
TAGAMI HTC 6328 GPM SPR 2FAN 85PCT 8V/0
UPPER COM TEMPERATURE

Figure 1-33



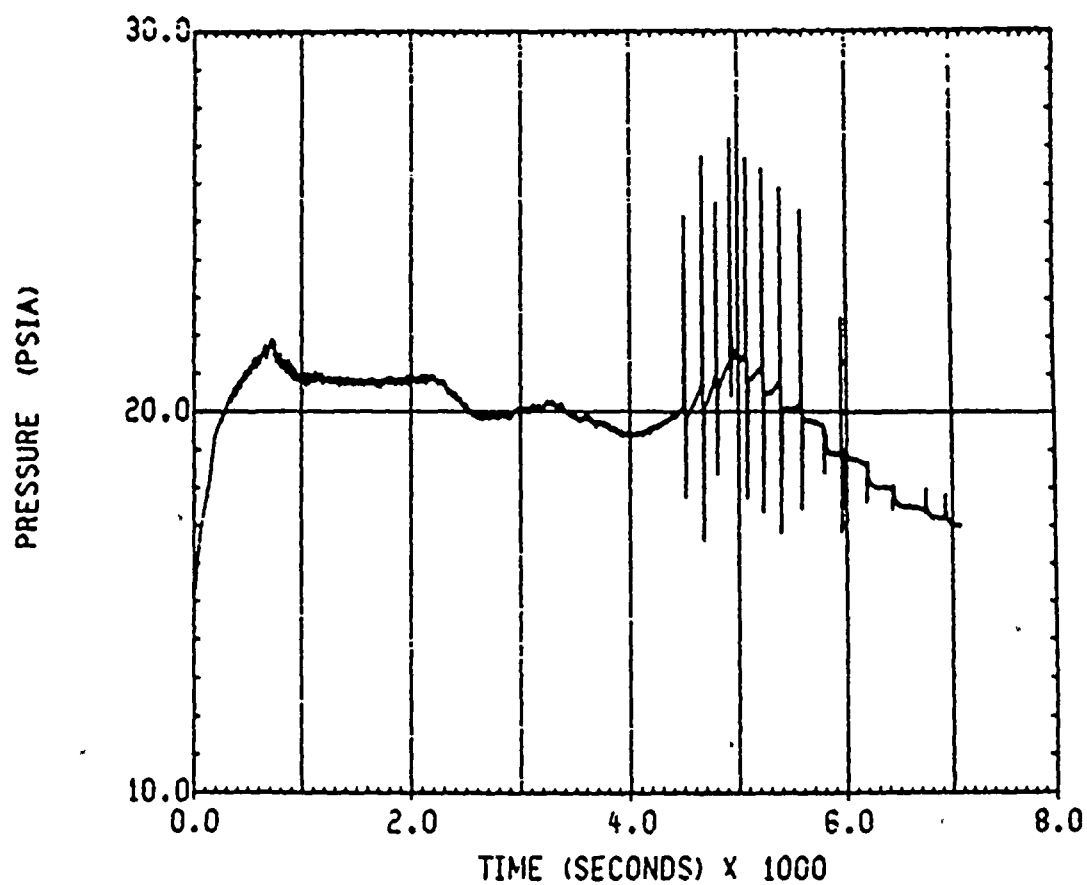
AEP D.C. COOK S2D TAGAMI CASE
TAGAMI HTC 6328 GPM SPR 2FAN 85PCT 8V/0
DEAD-END TEMPERATURE

Figure 1-34



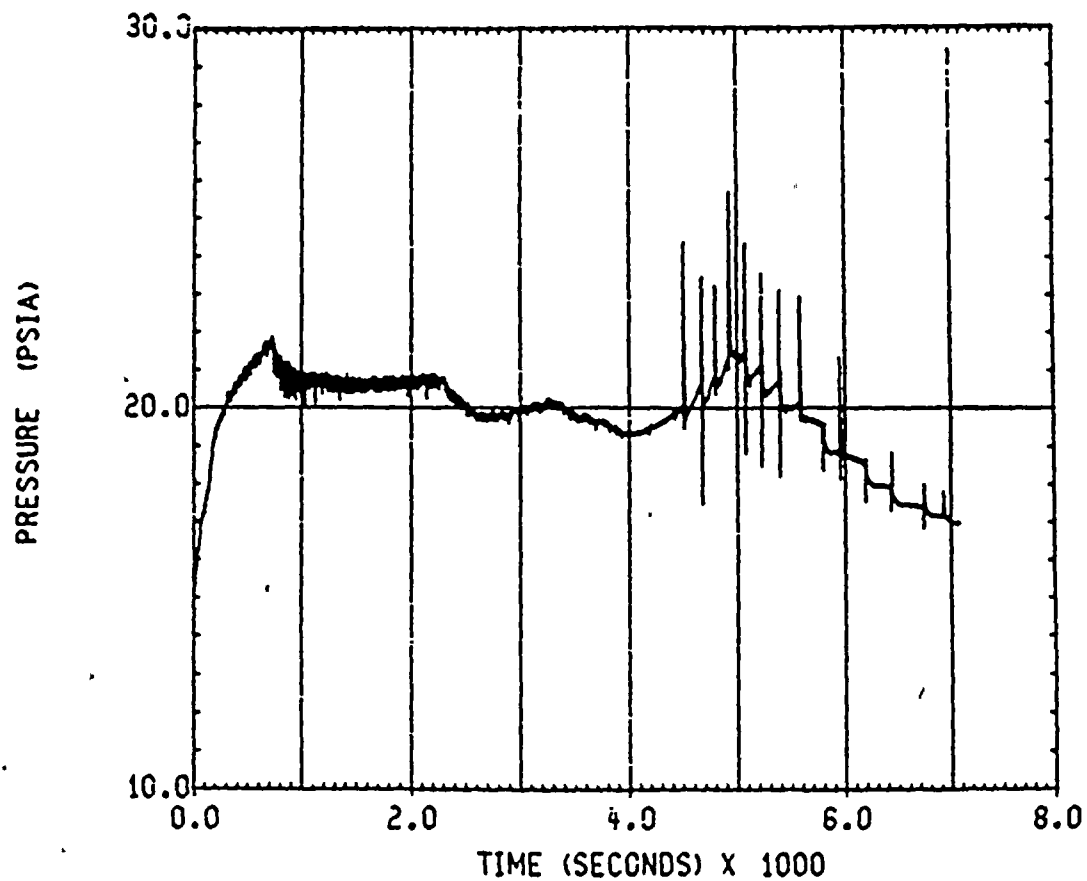
AEF D.C. COOK S2D TAGAMI CASE
TAGAMI HTC 6328 GPM SPR 2FAN 85PCT 8V/O
FAN/AC RM TEMPERATURE

Figure 1-35



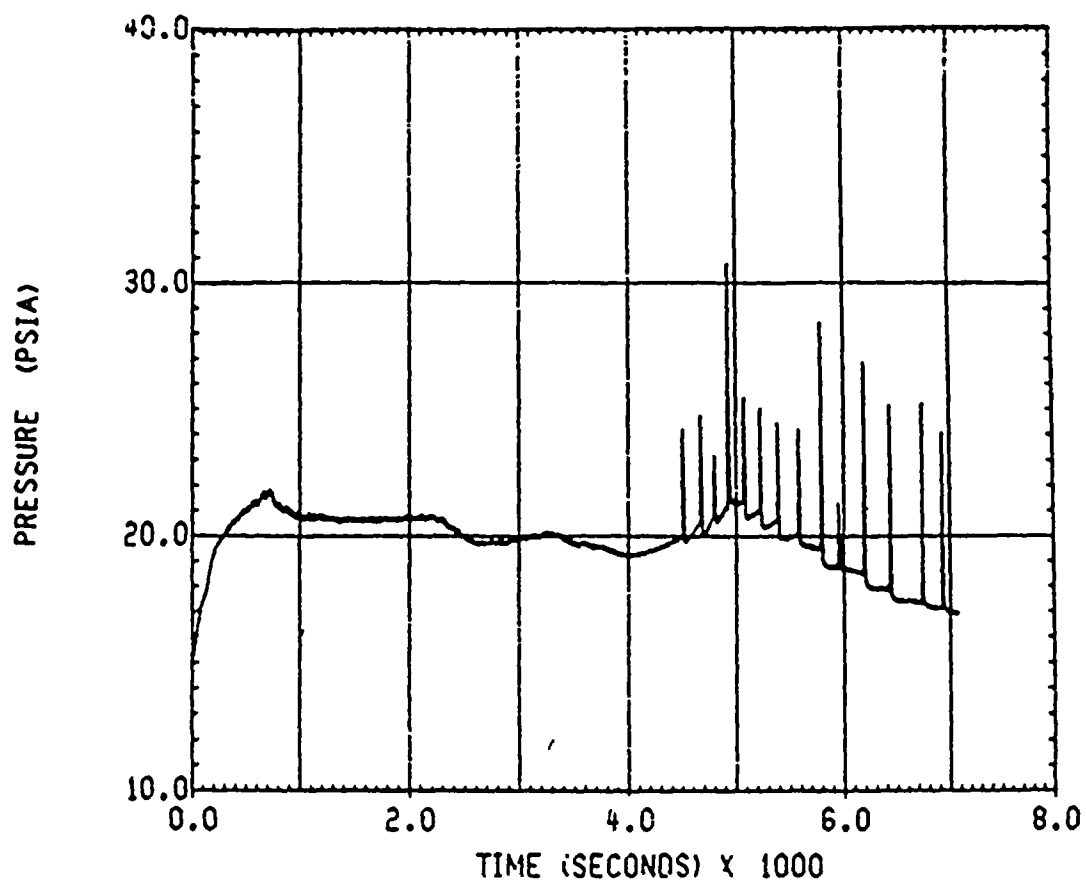
AEP D.C. COOK S2D TAGAMI CASE
TAGAMI HTC 6328 GPM SPR 2FAN 85PCT 8V/O
LOWER COM PRESSURE

Figure 1-36



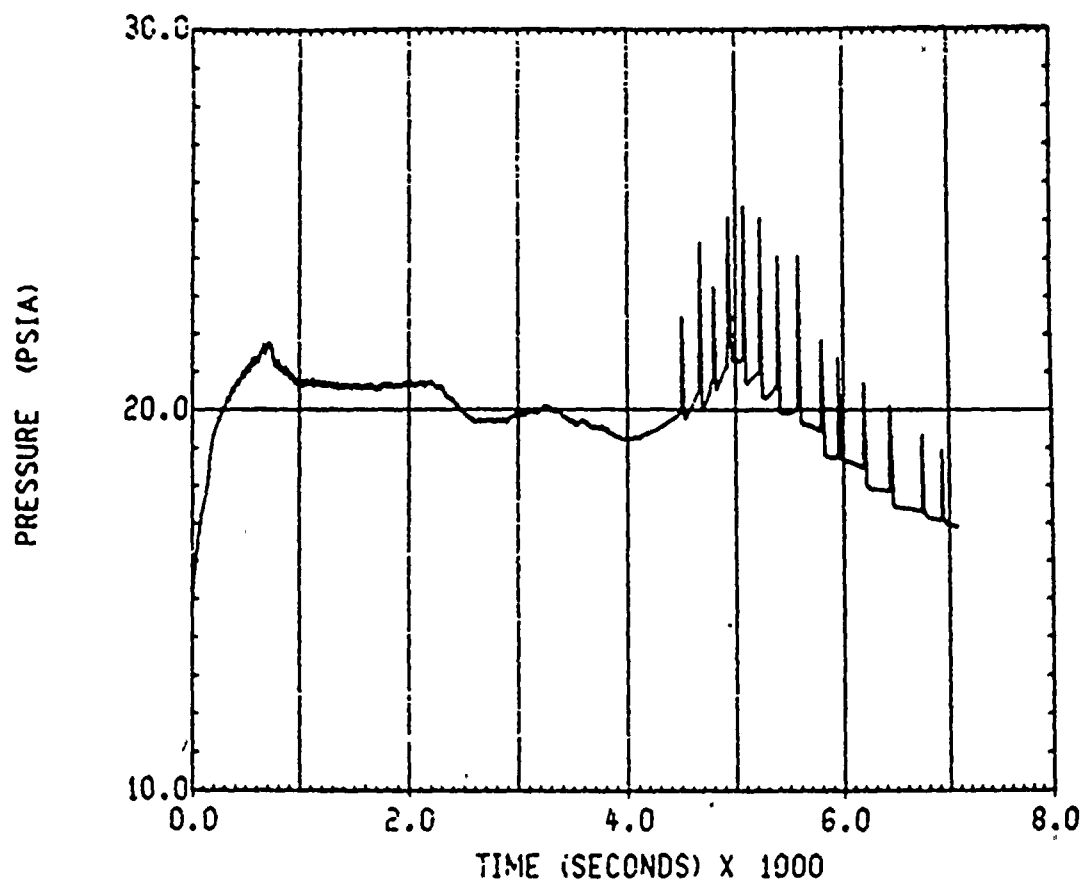
AEP D.C. COOK S20 TAGAMI CASE
TAGAMI HTC 6328 GPM SPR 2FAN 85PCT 8V/0
LOWER PLN PRESSURE

Figure 1-37



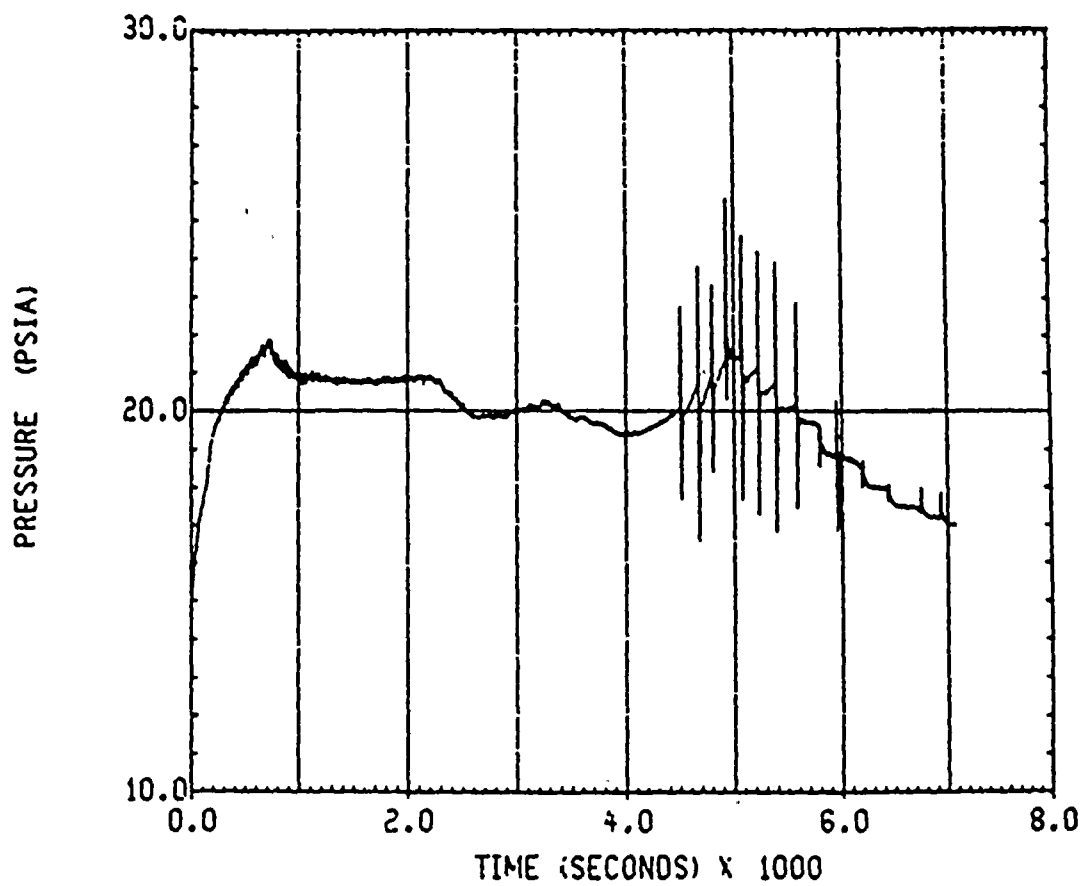
AEP D.C. COOK S2D TAGAMI CASE
TAGAMI HTC 6328 GPM SPR 2FAN 85PCT 8V/O
UPPER PLN PRESSURE

Figure 1-38



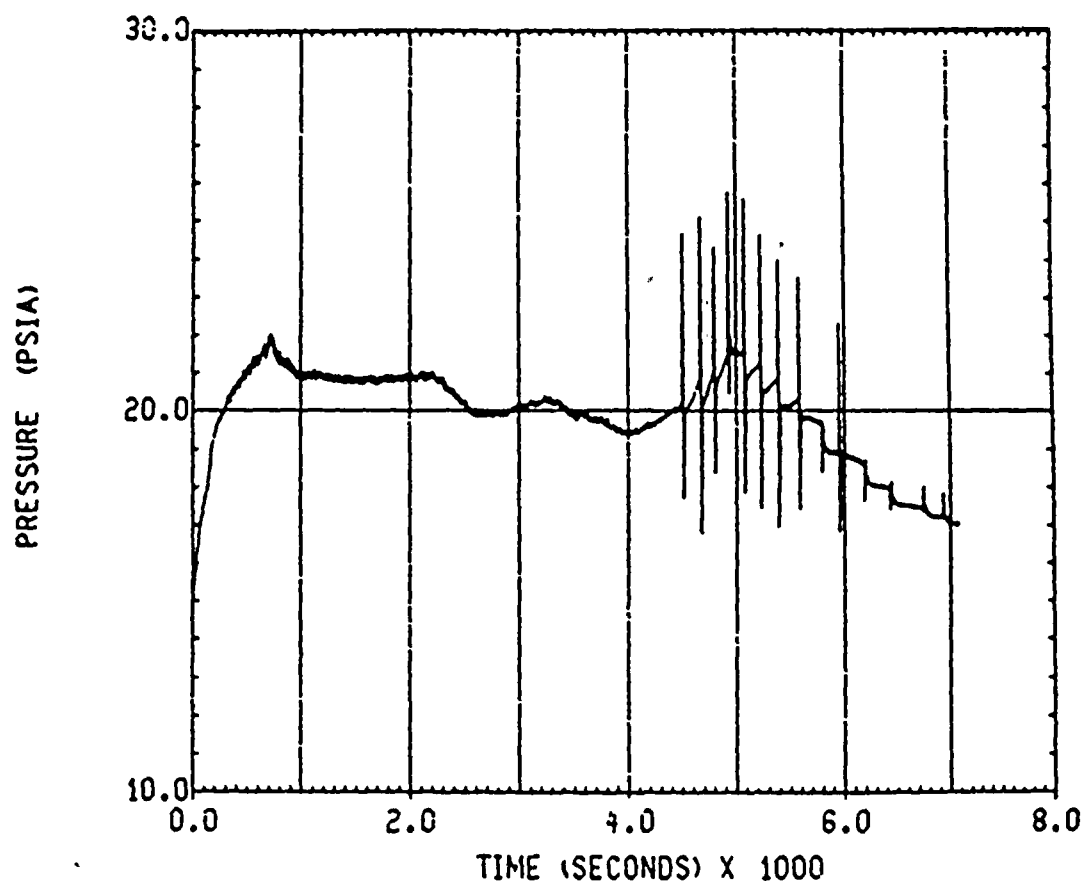
AEP D.C. COOK S2D TAGAMI CASE
TAGAMI HTC 6328 GPM SPR 2FAN 85PCT 8V/O
UPPER COM PRESSURE

Figure 1-39



AEP D.C. COOK S2D TAGAMI CASE
TAGAMI HTC 6328 GPM SPR 2FAN 85PCT 8V/O
DEAD-END PRESSURE

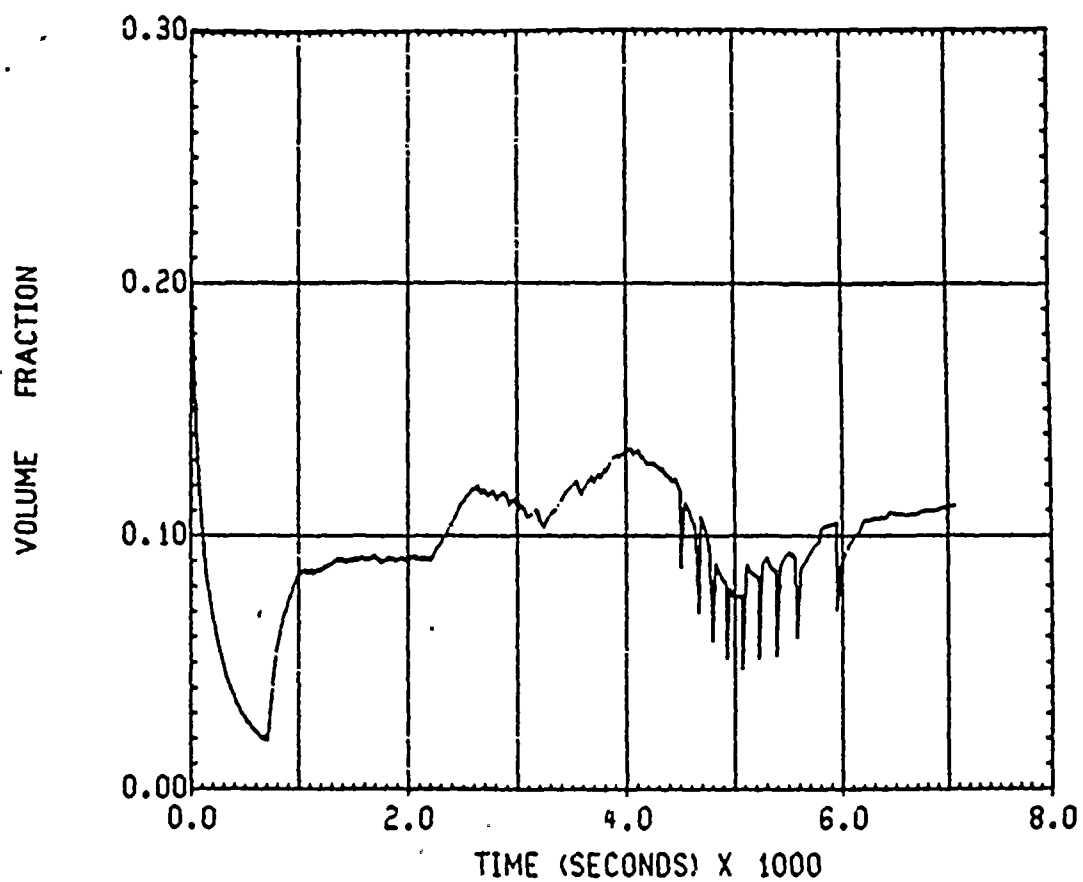
Figure 1-40



AEP D.C. COOK S20 TAGAMI CASE
TAGAMI HTC 6328 GPM SPR 2FAN 85PCT 8V/O
FAN/AC RM PRESSURE

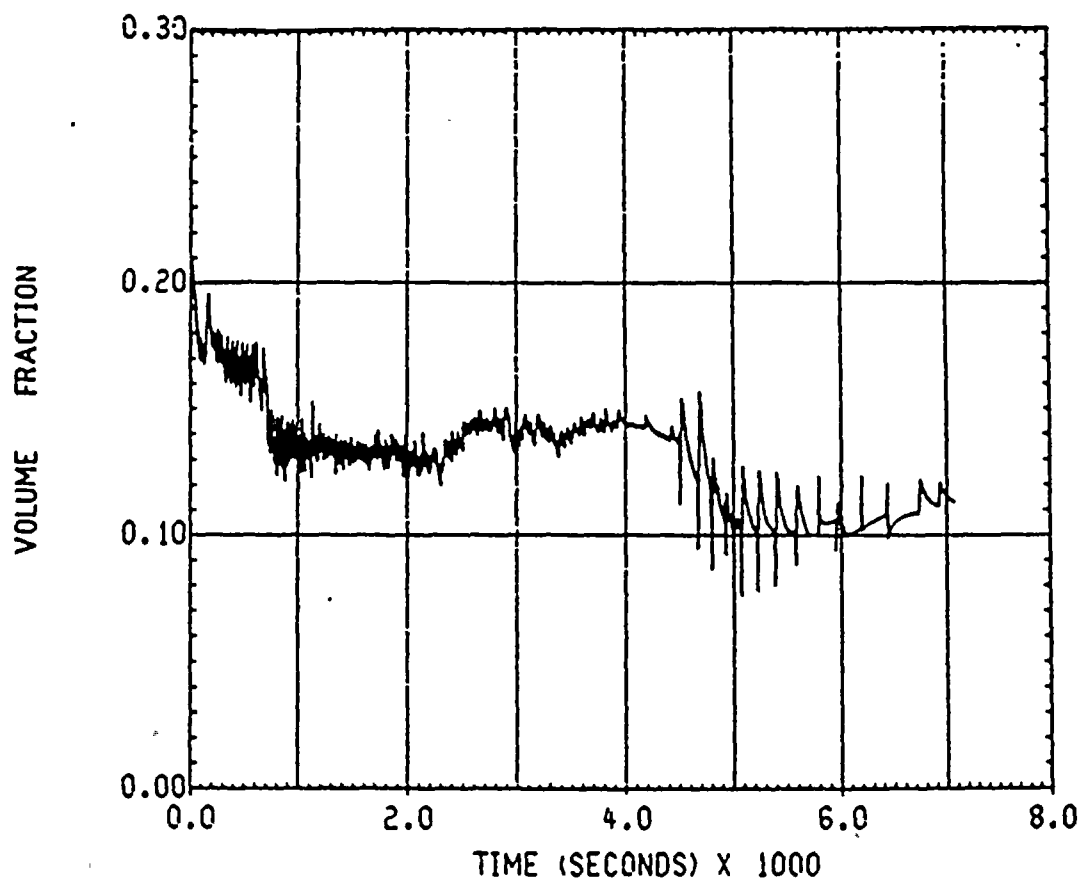
Figure 1-41





AEP D.C. COOK S2D TAGAMI CASE
TAGAMI HTC 6328 GPM SPR 2FAN 85PCT 8V/O
LOWER COM 02 GAS CONCENTRATION

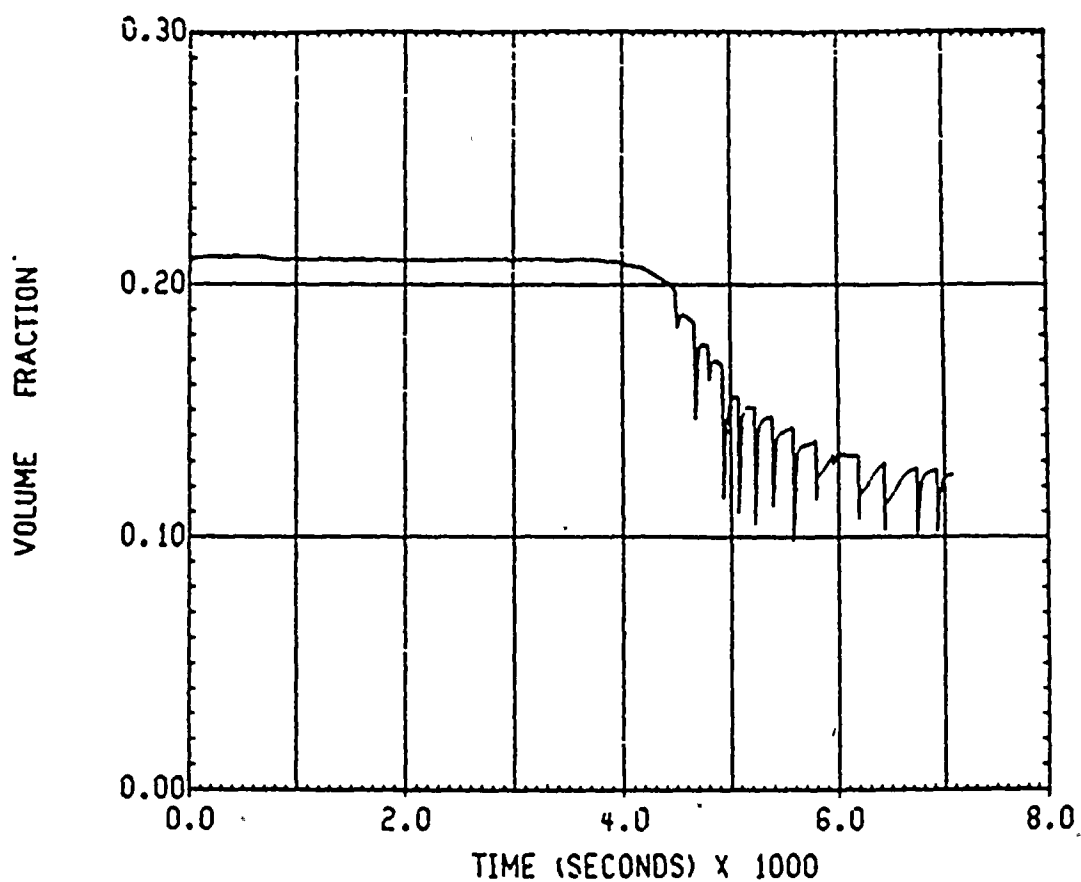
Figure 1-42



AEP D.C. COOK S20 TAGAMI CASE
TAGAMI HTC 6328 GPM SPR 2FAN 85PCT 8V/O
LOWER PLN 02 GAS CONCENTRATION

Figure 1-43

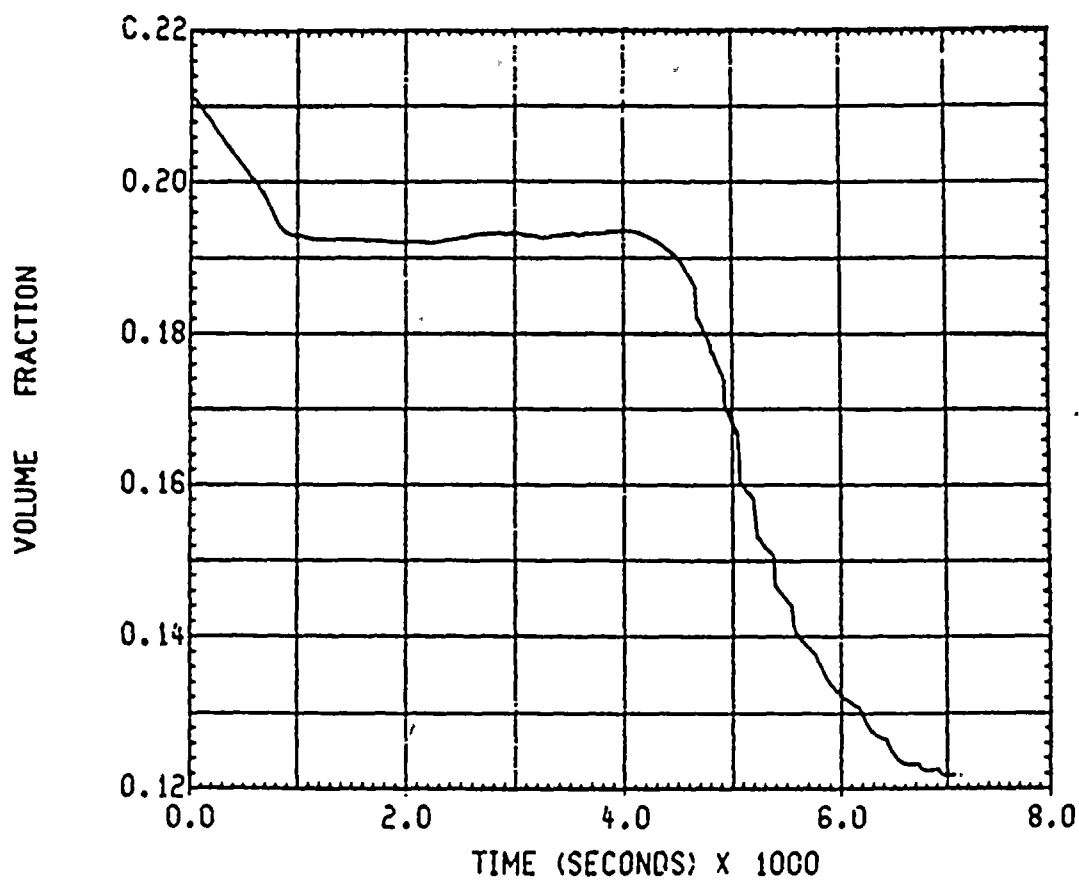




AEP D.C. COOK S2D TAGAMI CASE
TAGAMI HTC 6328 GPM SPR 2FAN 85PCT 8V/O
UPPER PLN .02 GAS CONCENTRATION

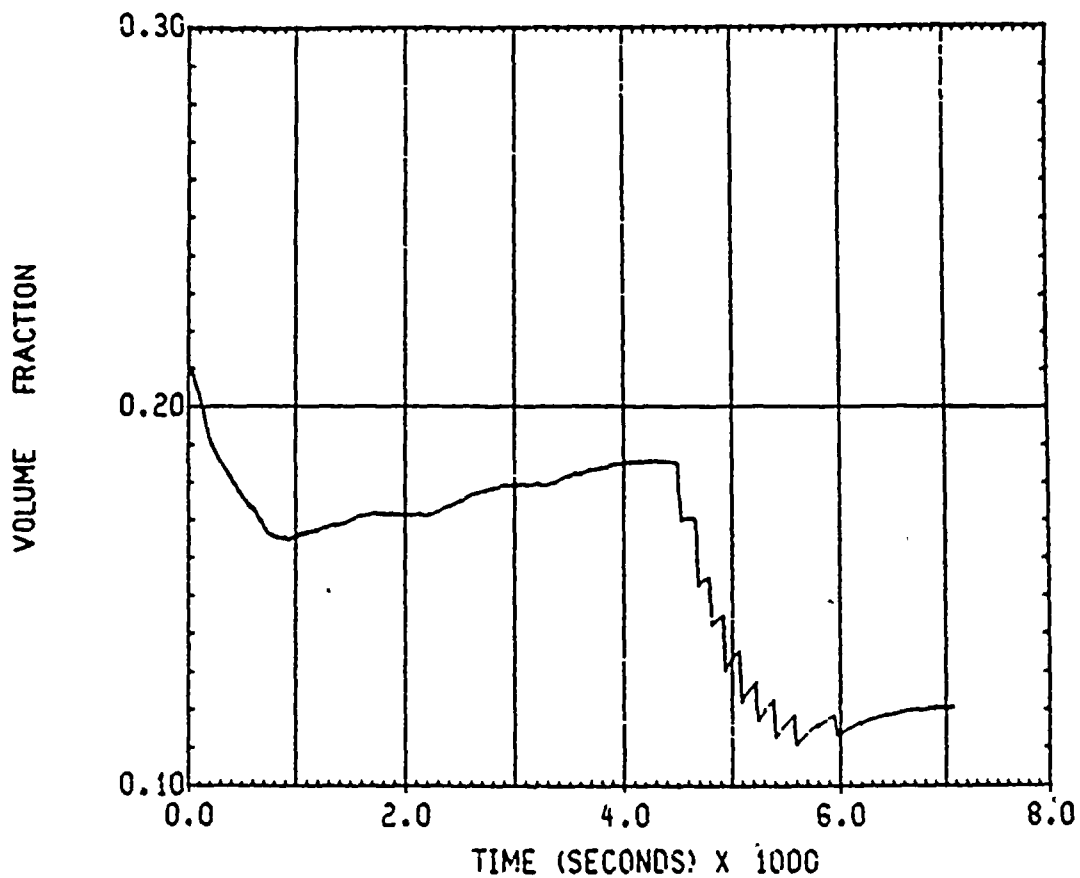
Figure 1-44





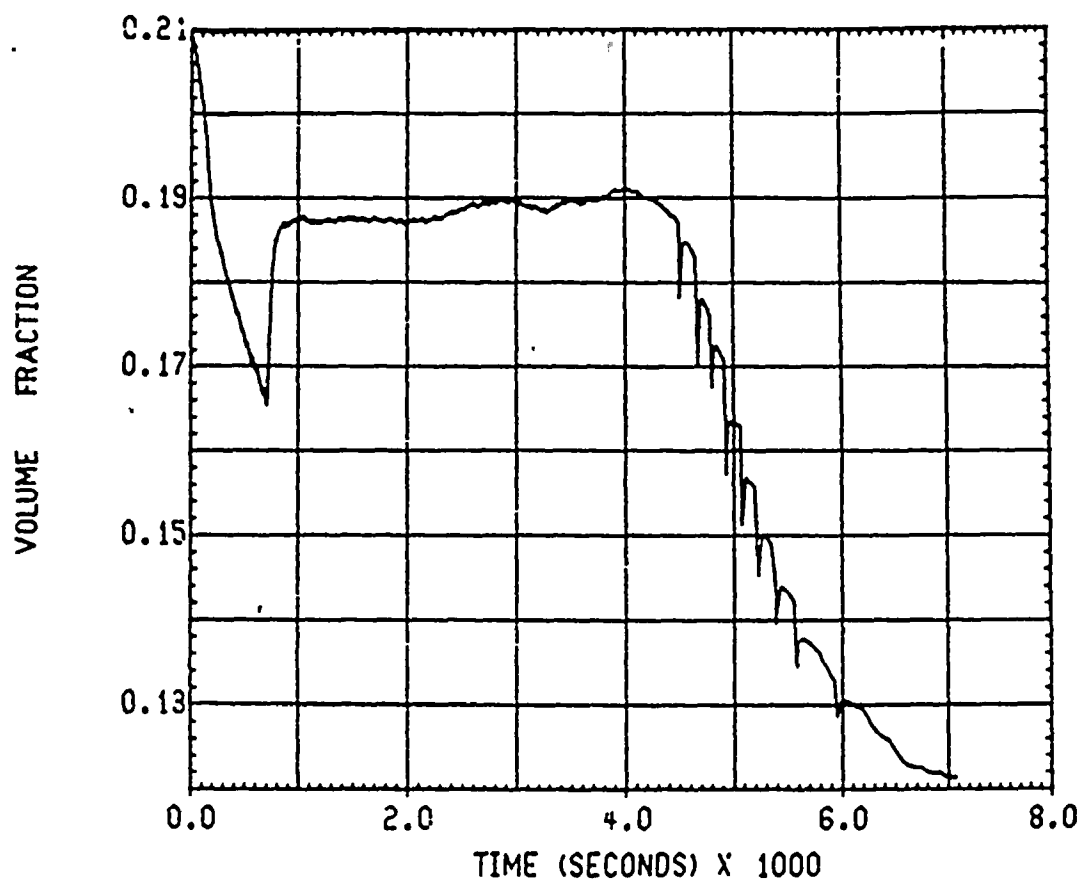
AEP D.C. COOK S2D TAGAMI CASE
TAGAMI HTC 6328 GPM SPR 2FAN 85PCT 8V/O
UPPER COM 02 GAS CONCENTRATION

Figure 1-45



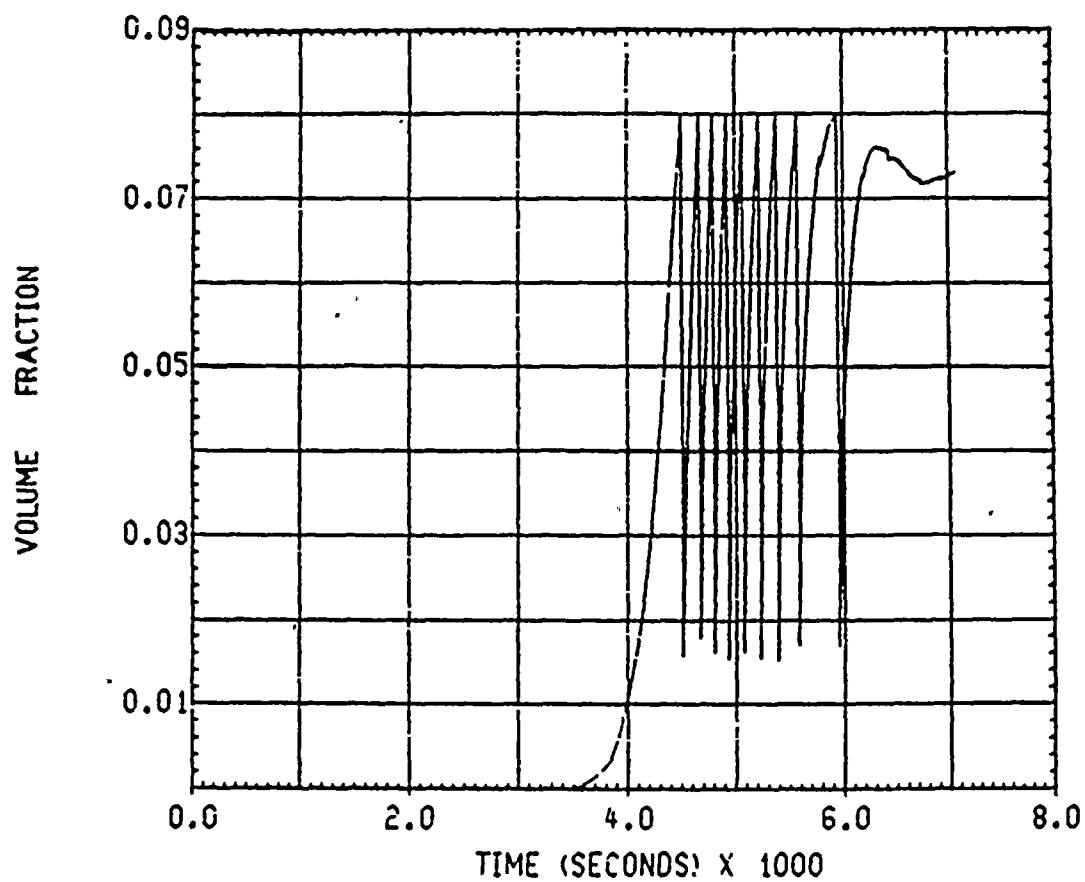
AEP D.C. COOK S2D TAGAMI CASE
TAGAMI HTC 6328 GPM SPR 2FAN 85PCT 8V/O
DEAD-END O2 GAS CONCENTRATION

Figure 1-46



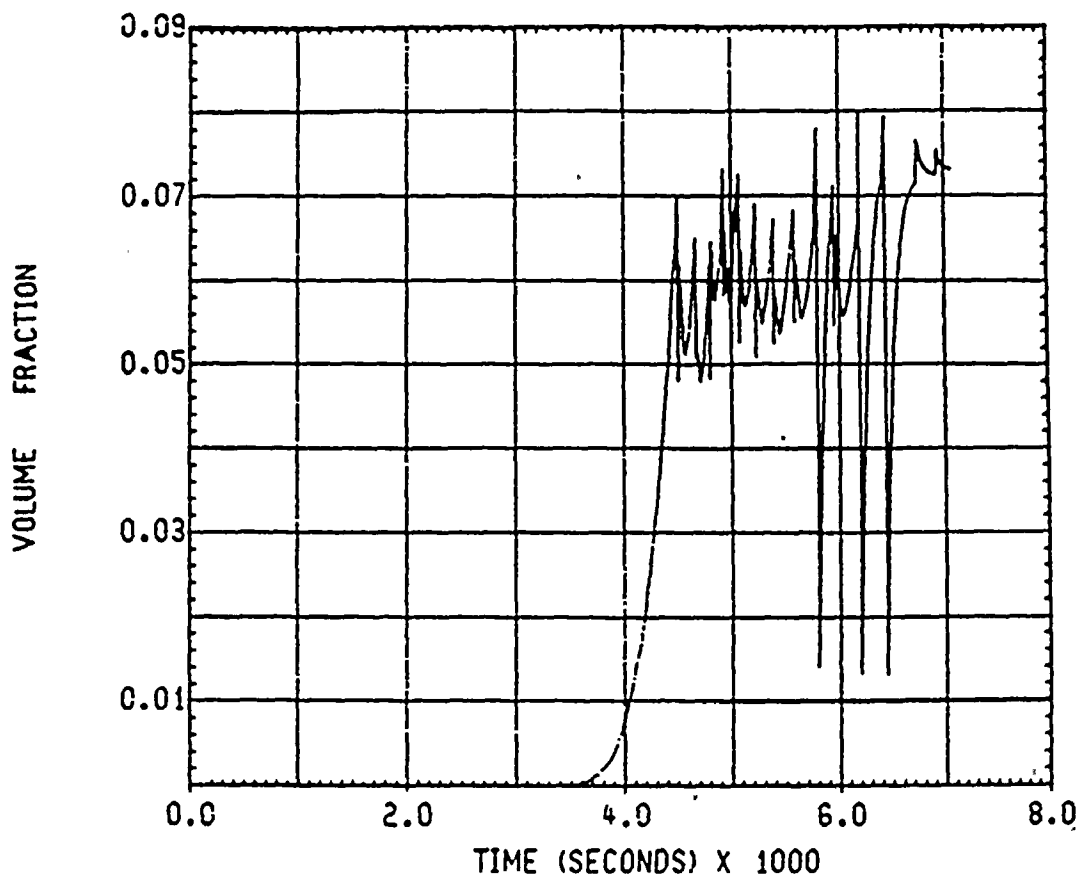
AEP D.C. COOK S2D TAGAMI CASE
TAGAMI HTC 6328 GPM SPR 2FAN 85PCT 8V/O
FAN/AC RM 02 GAS CONCENTRATION

Figure 1-47



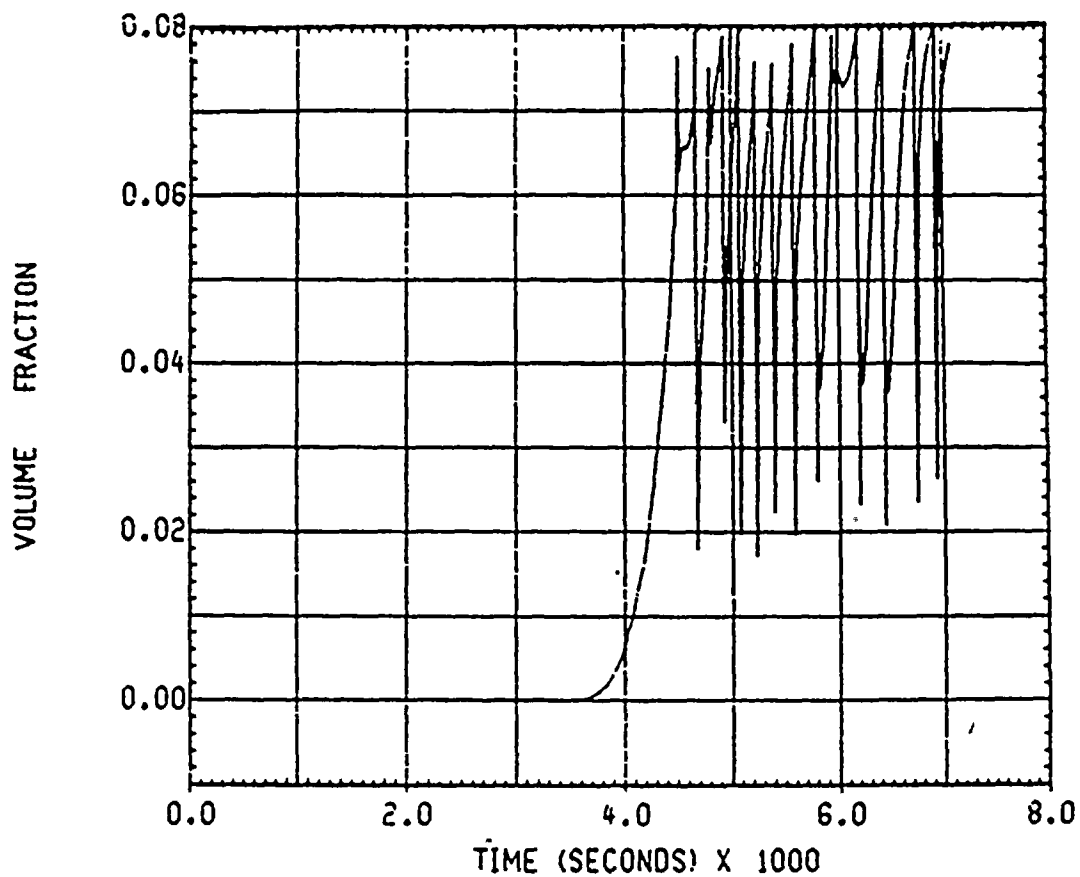
AEP D.C. COOK S20 TAGAMI CASE
TAGAMI HTC 6328 GPM SPR 2FAN 85PCT 8V/0
LOWER COM H2 GAS CONCENTRATION

Figure 1-48



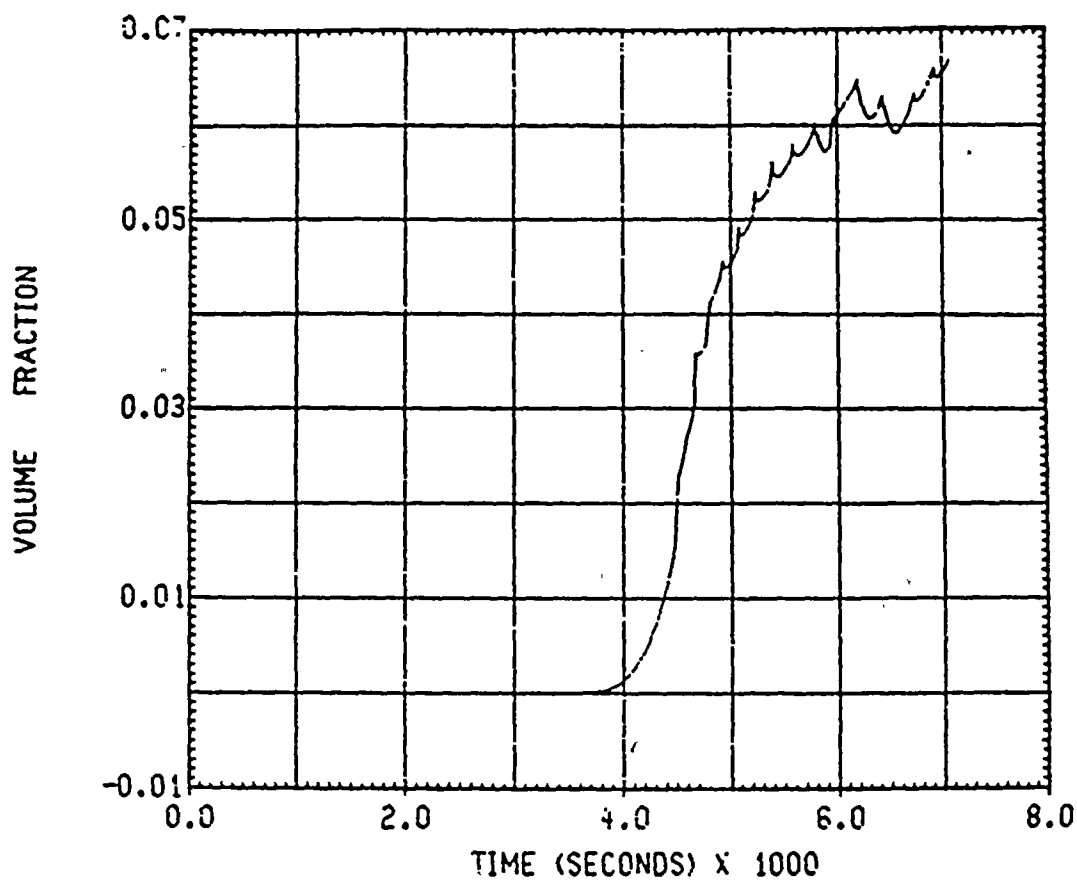
AEP D.C. COOK S2D TAGAMI CASE
TAGAMI HTC 6328 GPM SPR 2FAN 85PCT 8V/O
LOWER PLN H2 GAS CONCENTRATION

Figure 1-49



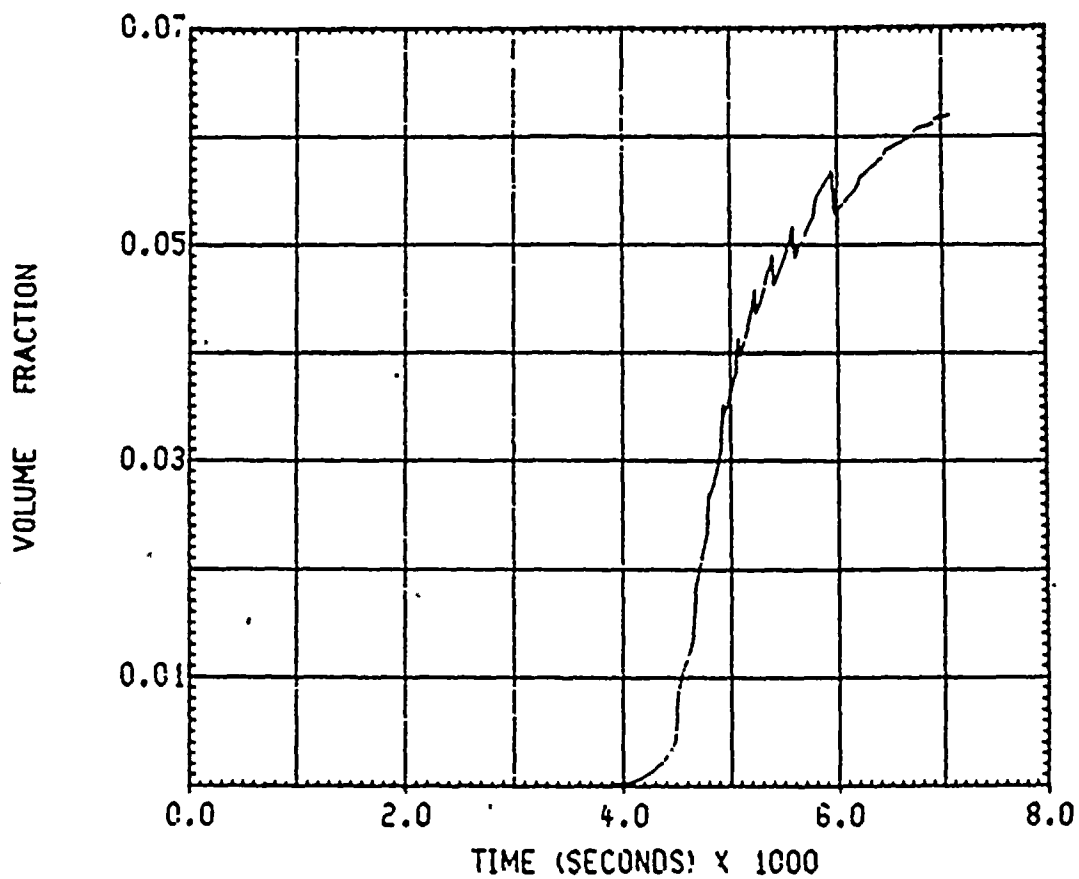
AEP D.C. COOK S2D TAGAMI CASE
TAGAMI HTC 6328 GPM SPR 2FAN 85PCT 8V/0
UPPER PLN H2 GAS CONCENTRATION

Figure 1-50



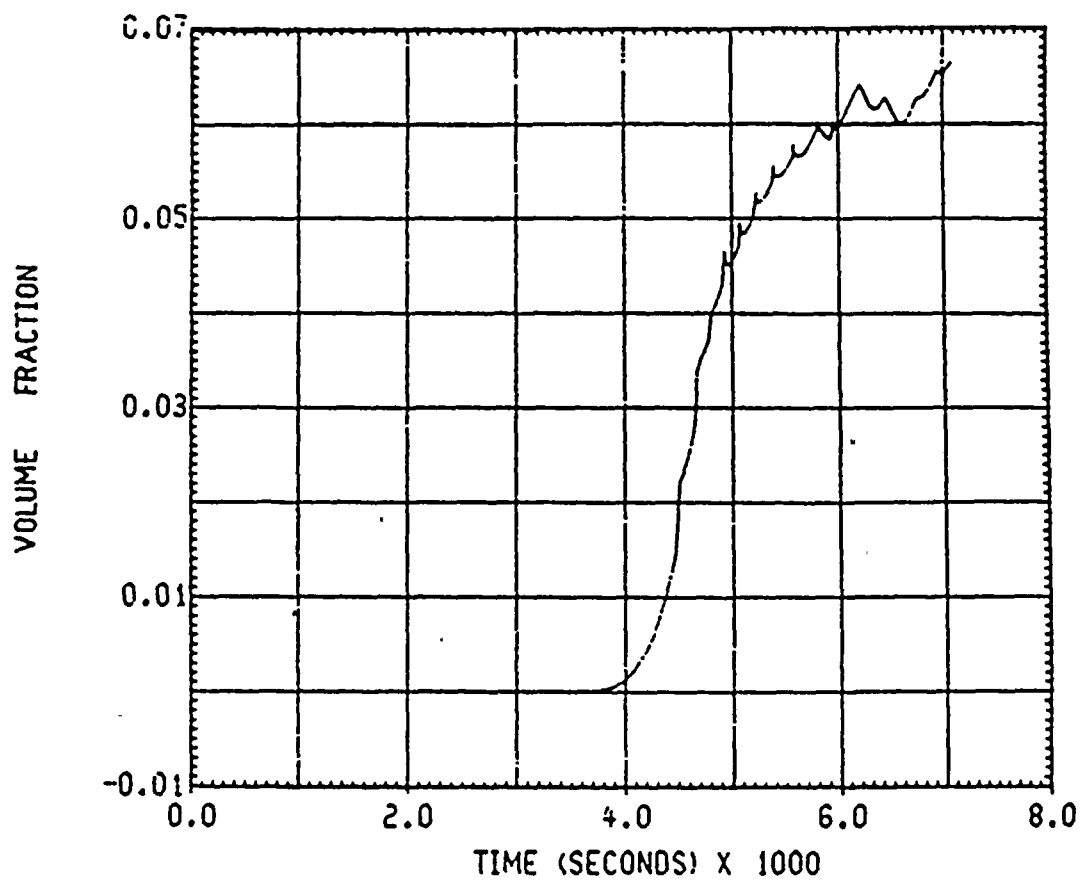
AEP D.C. COOK S2D TAGAMI CASE
TAGAMI HTC 6328 GPM SPR 2FAN 85PCT 8V/O
UPPER COM H2 GAS CONCENTRATION

Figure 1-51



AEP D.C. COOK S2D TAGAMI CASE
TAGAMI HTC 6328 GPM SPR 2FAN 85PCT 8V/O
DEAD-END H2 GAS CONCENTRATION

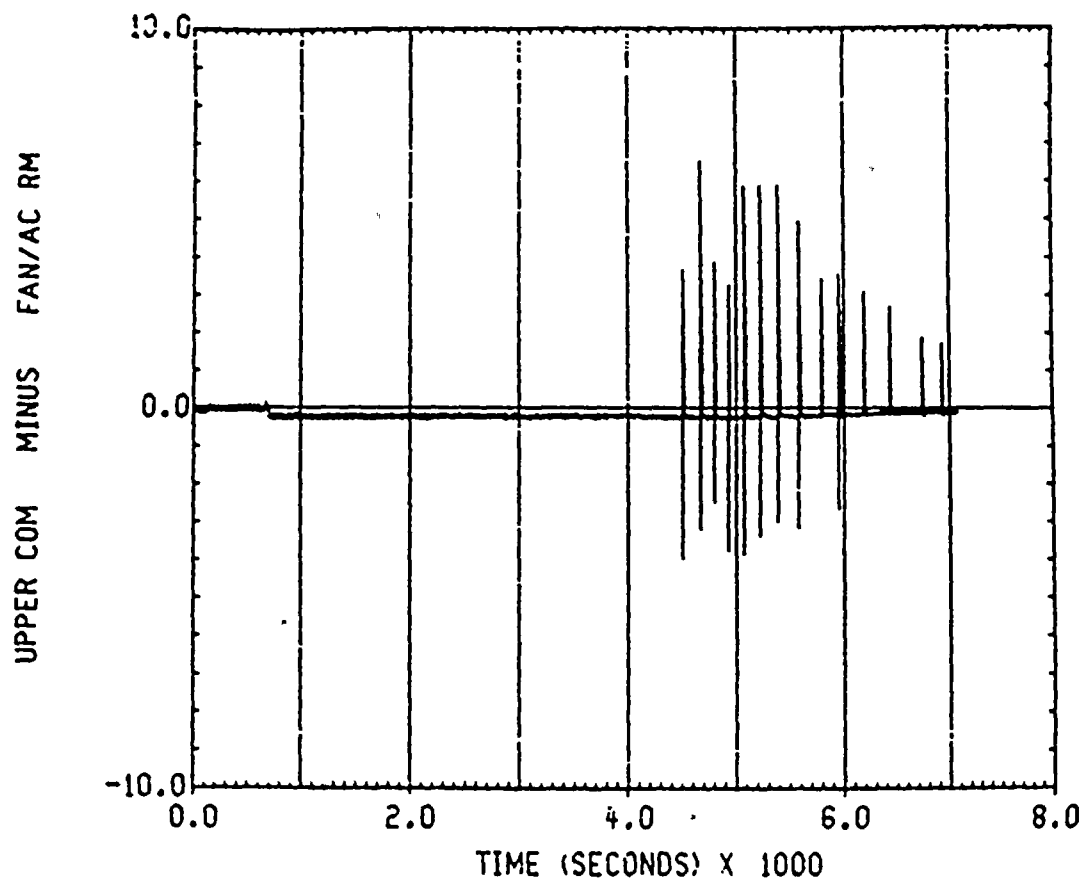
Figure 1-52



AEP D.C. COOK S2D TAGAMI CASE
TAGAMI HTC 6326 GPM SPR 2FAN 85PCT 8V/O
FAN/AC RM: H2 GAS CONCENTRATION

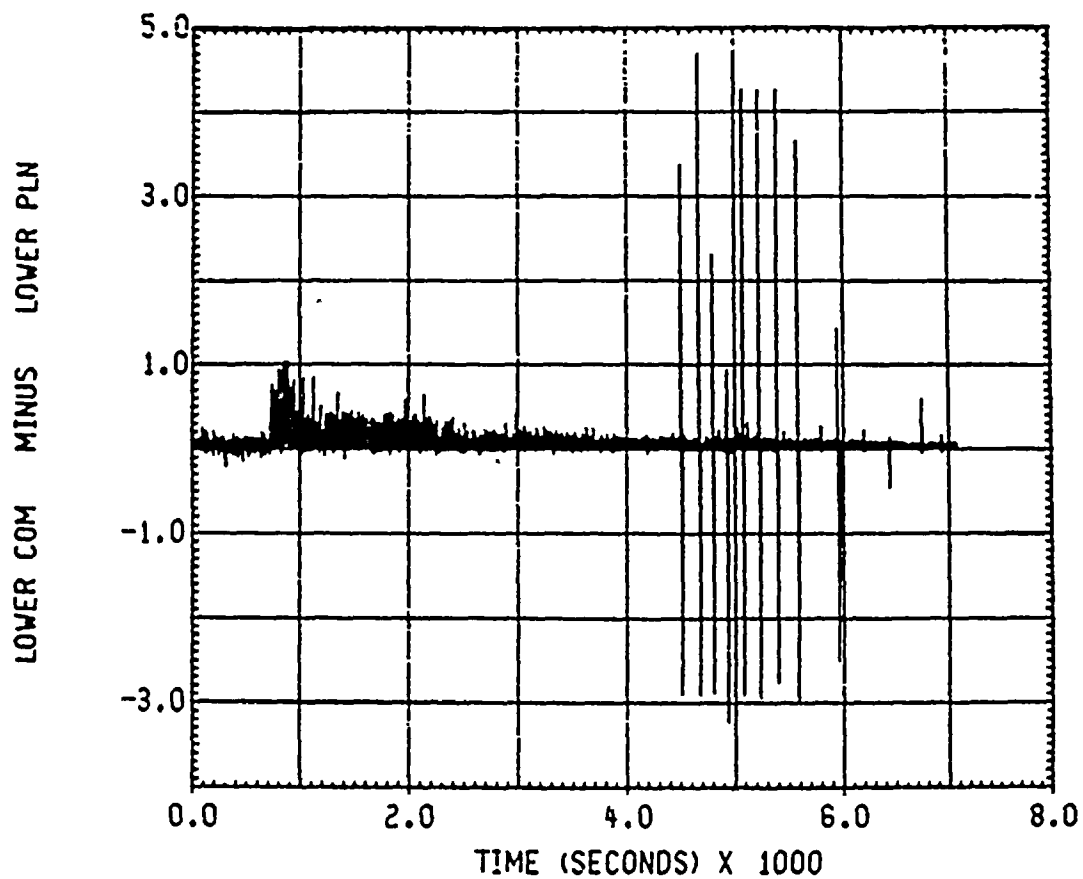
Figure 1-53





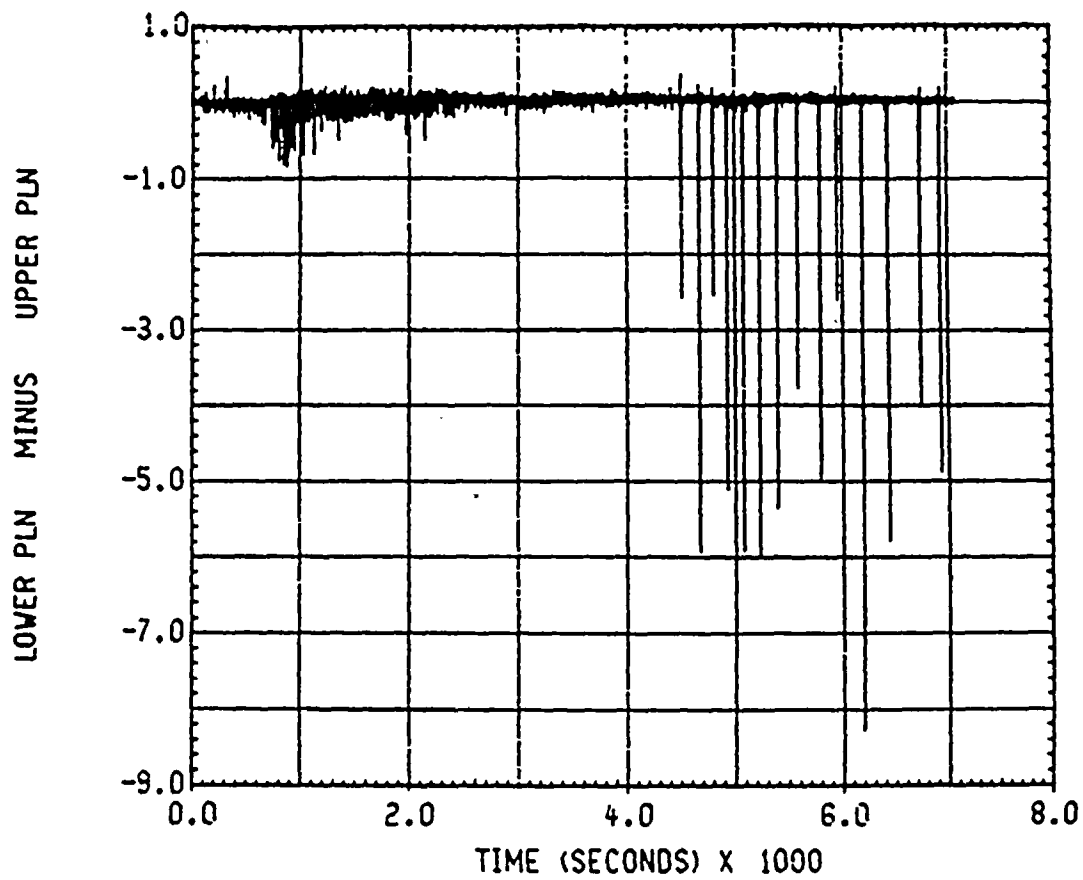
AEP D.C. COOK S2D TAGAMI CASE
TAGAMI HTC 6328 GPM SPR 2FAN 85PCT 8V/0
DIFFERENTIAL PRESSURE

Figure 1-54



AEP D.C. COOK S2D TAGAMI CASE
TAGAMI HTC 6328 GPM SPR 2FAN 85PCT 8V/0
DIFFERENTIAL PRESSURE

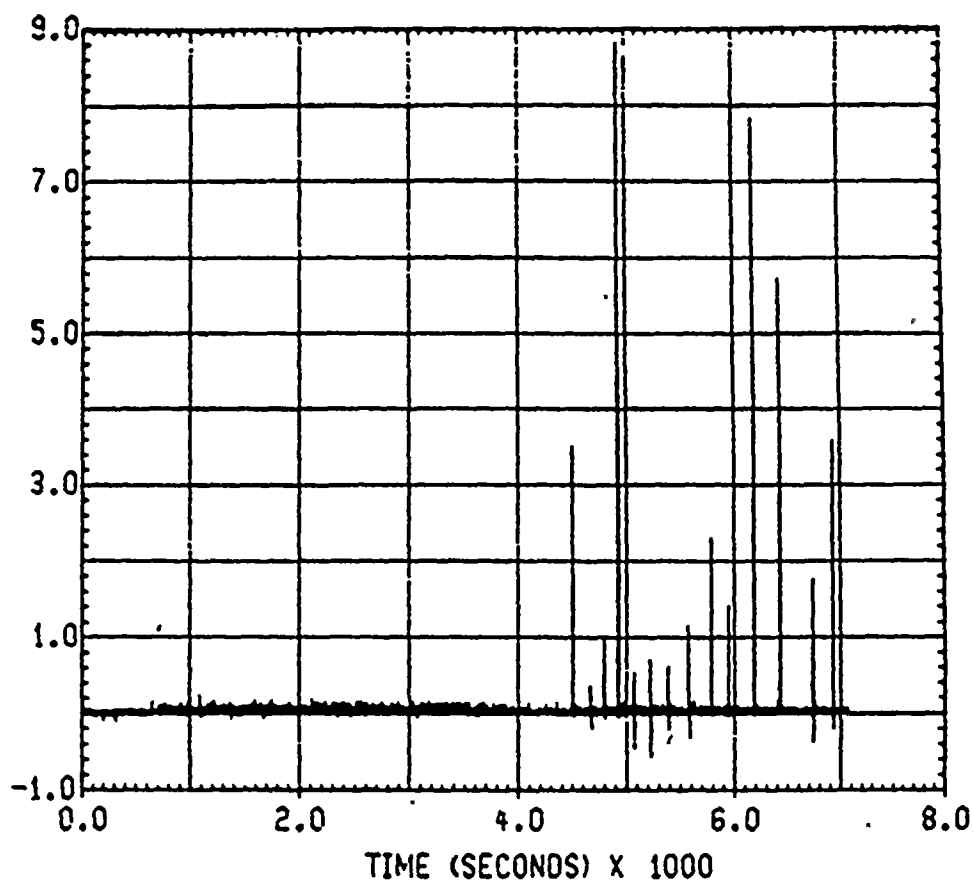
Figure 1-55



AEP D.C. COOK S2D TAGAMI CASE
TAGAMI HTC 6328 GPM SPR 2FAN 85PCT 8V/O
DIFFERENTIAL PRESSURE

Figure 1-56

UPPER PLN MINUS UPPER COM



AEP D.C. COOK S2D TAGAMI CASE
TAGAMI HTC 6328 GPM SPR 2FAN 85PCT 8V/O
DIFFERENTIAL PRESSURE

Figure 1-57

ATTACHMENT 2 TO AEP:NRC:0500M
RESPONSES TO QUESTIONS ON HYDROGEN CONTROL
CONTAINED IN MR. S. A. VARGA'S LETTER DATED SEPTEMBER 16, 1982
DONALD C. COOK NUCLEAR PLANT UNIT NOS. 1 AND 2

Question 6:

The analysis provided to date concerning the survivability of air return fans and hydrogen skimmer fans neglects any fan overspeed or motoring which occurs as a result of postulated hydrogen combustion in the upper plenum and upper compartment. Describe how the fans will react to the differential pressure associated with hydrogen combustion, and justify the assumptions concerning fan overspeed. Describe the effects of combustion in the lower compartment, e.g., fan stalling.

Response to Question 6:

Combustion in the lower compartment is sufficiently slow that the backdraft damper will close in time to protect the fan from damage due to a reverse flow.

For a discussion of fan overspeed, see our response to Questions 2(a) through 2(d) of Mr. S. A. Varga's letter dated August 10, 1983, contained in Attachment 1 to this letter.

Question 7:

With regard to the equipment survivability analysis, the level of conservatism implicit in the temperature forcing functions developed for the lower containment and the upper plenum is not apparent and quantifiable. Additional analyses should be conducted to provide a baseline or "best estimate" of equipment response, and to ensure that temperature curves assumed in the analyses embody all uncertainties in the accident sequence and combustion parameters. Accordingly, provide analyses of equipment temperature response to:

- a) the base case transient assumed in the containment analyses;
- b) the containment transients resulting from a spectrum of accident scenarios; and
- c) the containment transients resulting under different assumed values for flame speed and ignition criteria for the worst case accident sequence.

The range of these combustion parameters assumed for the equipment survivability analyses should include but not necessarily be limited to the values assumed in the containment sensitivity studies, i.e., 1 - 12 ft/sec flame speed and 6 - 10% hydrogen for ignition.

Response to Question 7:

The issue of equipment survivability for the Donald C. Cook Nuclear Plant is presently under review by our consultant, Westinghouse Electric Corporation/Offshore Power Systems. It is presently anticipated that a response to this question will be transmitted to NRC on or before April 30, 1984.

Question 8:

For the survivability analysis, it is our understanding that the current thermal model assumes radiation from the flame to the object only during a burn, with convection occurring at all times outside the burn period. In an actual burn, radiation from the cloud of hot gases following the flame front can account for a substantial portion of the total heat transfer to the object. An additional heat flux term or a combined radiation-convection heat transfer coefficient should be used to account for this radiant heat source. In this regard, clarify the treatment of heat transfer following the burn and justify the approach taken.

Response to Question 8:

The issue of equipment survivability for the Donald C. Cook Nuclear Plant is presently under review by our consultant, Westinghouse Electric Corporation/Offshore Power Systems. It is presently anticipated that a response to this question will be transmitted to NRC on or before April 30, 1984.

Question 12:

In the CLASIX spray model it is not clear whether the mass of spray treated in a time increment is assumed to be only that amount of spray mass which is introduced in a single time step, or the mass of droplet accumulated in the atmosphere over the fall time period. Clarify the spray mass accounting used in CLASIX and the mass of spray treated in a single time step. Discuss the significance of any errors introduced by the apparent assumption that only one time increment of spray mass is exposed to the containment atmosphere during a single time step.

Response to Question 12:

The mass of spray treated in a time increment by the CLASIX spray model is the amount of spray introduced in a single time step and not the accumulated mass of spray in the compartment atmosphere. The CLASIX spray model operates in a different time domain from that of the compartment atmosphere. The compartment conditions are frozen while a mass of spray is introduced into the compartment atmosphere and completes its fall while interacting with the compartment atmosphere. The compartment mass and energy balance is then updated to reflect the effects of the spray. The spray interaction is determined by a classical transient technique which is fully described in our responses to specific questions contained in Mr. S. A. Varga's letter dated July 30, 1982 (in particular, see our responses to Questions 11(a) and 11(b) of the referenced request for information, contained in Attachment 3 to this letter; additionally, see our responses to Questions 10(c) and 10(d) of the referenced request for information, transmitted via letter No. AEP:NRC:0500J, dated October 15, 1982, Mr. R. S. Hunter (IMECo) to Mr. H. R. Denton (NRC)).

Based on these discussions, it is concluded that the CLASIX spray model provides an appropriate treatment of spray and containment atmospheric behavior for hydrogen burn transients.

Question 13:

CLASIX spray model analyses provided to date have been limited to the comparison of pressure, temperature, and integrated heat removal for the purpose of evaluating the effect of the spray operating in a separate time domain. Additional information is needed, however, to confirm the adequacy of the heat and mass transfer relationships and assumptions implicit in the CLASIX spray model, especially in treating a compartment in which hydrogen combustion is taking place. In this regard:

- (a) Provide a quantitative description of the spray heat and mass transfer under containment conditions typical of a hydrogen burn. Include in your response plots of containment temperature, spray heat transfer, spray mass evaporation, and suspended water mass as a function of time for both the CLASIX spray model and a model in which the spray mass is tracked throughout the fall (and allowed to accumulate in the containment atmosphere).
- (b) Provide analyses of spray mass evaporation and pressure suppression effects for an upper compartment burn.
- (c) Justify the drop film coefficient value used in the spray model analyses ($20 \text{ Btu/hr-ft}^2\text{-}^\circ\text{F}$) and discuss the effect of using a constant value throughout a burn transient.

Response to Question 13:

The surface heat transfer coefficient for a single spray droplet may be determined from the rigid droplet model proposed by Ranz and Marshall (Reference (2-1)). This model has been shown to compare favorably with the spray efficiency model of the CONTEMPT computer code (Reference (2-2)), and is utilized in the MARCH computer code (Reference (2-3)). According to Ranz and Marshall, the droplet film coefficient is given by the following:

$$\text{Nu} = 2.0 + 0.6(\text{Re}^{1/2})(\text{Pr}^{1/3}) \quad (2-1)$$

where: Nu = Nusselt number

Re = Reynolds number

Pr = Prandtl number

Equation (2-1) may also be expressed as follows:

$$h = (k_f/D) (2.0 + 0.6(V_o D \rho_f)^{1/2} (c_{p_f}/k_f)^{1/3} (1/\mu)^{1/6}) \quad (2-2)$$

where: h = droplet film coefficient (Btu/hr-ft²-°F)

k = thermal conductivity (Btu/hr-ft-°F)

D = droplet diameter (ft)

V_o = velocity of droplet relative to ambient gases (ft/hr)

ρ = density (lbm/ft³)

c_p = specific heat (Btu/lbm-°F)

μ = dynamic viscosity (lbm/hr-ft)

f = subscript denoting conditions of ambient gases (i.e., air-steam mixture) through which droplet is moving

Equation (2-2) predicts that the magnitude of the droplet film coefficient is directly proportional to V_o , ρ , c_p , and k , and inversely proportional to D and μ . Furthermore, Equation (2-2) indicates that these physical property effects are effectively superimposed upon the heat conduction condition for a sphere in an infinite stagnant medium, $Nu = 2.0$ (see References (2-1) and (2-4)).

A conservative lower limit for heat transfer to falling spray droplets may now be determined. To do so, we need only determine the conservative bounding values of the six variables in Equation (2-2), where the conservative bounding values are defined as minimum values for V_o , ρ , c_p , and k , and maximum values for D and μ . For present purposes, these values may be chosen at one atmosphere pressure and in the temperature range of interest (i.e., 0 - 2000°F). Additionally, it is assumed here that the value of a physical property (e.g., density, viscosity, etc.) for an air-steam mixture will lie between the two separate values for the air and the steam components. This allows for the use of single-component (i.e., either air or steam) property tables in the determination of the bounding values.

In order to compute a conservatively low value for the heat transfer coefficient predicted by Equation (2-2), a conservatively low value for the density of the ambient gases was selected (i.e., a value of $\rho_f = 0.0100$ lbm/ft³ was chosen for this analysis). Additionally, the bounding values for the other physical property parameters were chosen as follows: $c_p = 0.239$ Btu/lbm-°F; $k_f = 0.013$ Btu/hr-ft-°F; and $\mu_f = 0.109$ lbm/hr-ft.

It was also assumed for the purpose of this analysis that the minimum value for V_o is 25,000 ft/hr (6.94 ft/sec). This value is less than the spray droplet velocities given in Reference (2-5) for the Donald C. Cook Nuclear Plant upper compartment, lower compartment, and fan/accumulator room sprays. The droplet diameter, D , was chosen to be the Donald C. Cook Nuclear Plant spray droplet mean diameter of 700

microns (0.0023 ft) (Reference (2-5)); this is the same value used in CLASIX computer code analyses of hydrogen combustion events.

Substituting these bounding values into Equation (2-2) yields:

$$h = (0.026/D) + (0.471/D)^{1/2} \quad (2-3)$$

or:
$$h = 21.125 \text{ Btu/hr-ft}^2\text{-}^\circ\text{F (when } D = 0.0023 \text{ ft)}$$

Therefore, for the case of spray droplet heating at a constant spray droplet diameter of 0.0023 ft, the CLASIX spray heat transfer model should remove less energy from a compartment atmosphere than a more mechanistic spray heat transfer model. This effect, which would tend to result in CLASIX overpredictions of containment temperature and pressure, directly follows from the fact that the CLASIX droplet surface coefficient of $20 \text{ Btu/hr-ft}^2\text{-}^\circ\text{F}$ should always be less than the surface coefficient predicted by a more mechanistic model, even when very conservative values for physical properties are used in the mechanistic model.

Equation (2-3) also indicates that a more mechanistic heat transfer model has a dependence upon spray droplet diameter. Thus, as the spray droplet diameter decreases due to vaporization, the film coefficient predicted by the more mechanistic model will increase, whereas the $20 \text{ Btu/hr-ft}^2\text{-}^\circ\text{F}$ value used in the CLASIX computer code analyses will not. Although the factor of interest for this case of decreasing droplet diameter is really the surface film coefficient multiplied by the surface area of the spray droplet, the increase in the film coefficient for the more mechanistic model should still ensure a higher heat transfer rate to the spray droplets. As an example, it is noted that the CLASIX model predicts a heat transfer rate of $8.31 \times 10^{-5} \text{ Btu/hr-}^\circ\text{F}$ for a single spray droplet with a diameter of 0.00115 ft; using the more mechanistic model with bounding physical properties (i.e., using Equation (2-3)) for the same droplet diameter predicts a value of $1.52 \times 10^{-4} \text{ Btu/hr-}^\circ\text{F}$, or about an 80% higher heat transfer rate than the CLASIX model for the same temperature gradient and droplet diameter.

Based on the above, it is concluded that during the early portion of a hydrogen burn transient, CLASIX spray droplets would take longer to rise in temperature to the saturation point than spray droplets modeled in a more mechanistic fashion. Thus, CLASIX would tend to remove less heat from the containment atmosphere, and higher temperatures and pressures in containment would result. Additionally, the spray droplets modeled in a more mechanistic manner would flash sooner in the transient, thereby decreasing their surface areas and raising the heat transfer rate even more. Thus, the spray droplets modeled in a more mechanistic fashion should vaporize more completely during a hydrogen burn than the spray droplets modeled as in the CLASIX computer code, and thus the CLASIX computed peak temperatures and pressures should be higher.

Obviously, this would appear to create a feedback effect, with higher temperature gradients existing between containment temperatures and CLASIX spray droplets, and thus possibly higher heat transfer rates to the CLASIX spray droplets. This, however, should not be a concern as long as the computational mesh is fine enough to ensure solution stability (for example, see Appendix D to Reference (2-6) for a comparison of the CLASIX spray model to a finite difference spray model which assumed constant heat transfer coefficient). The discussion above justifies the use of the CLASIX spray droplet heat transfer coefficient of $20 \text{ Btu/hr-ft}^2 \text{ } ^\circ\text{F}$ for calculational convenience.

With regard to spray mass vaporization during hydrogen combustion events, a hand calculation utilizing the CLASIX spray heat transfer model has been performed for an upper compartment burn previously reported to the NRC via Reference (2-7). In particular, the percentage of spray mass vaporized from a spray droplet completing its fall through a compartment is as follows:

$$M_{\% \text{vap}} = (1 - (D_{\text{fall}}/D_o)^3) \times 100\% \quad (2-4)$$

where: $M_{\% \text{vap}}$ = percentage of spray mass vaporized
 D_o = spray droplet diameter at start of fall (ft)
 D_{fall} = spray droplet diameter at end of fall (ft)

The droplet diameter at the end of fall, D_{fall} , is given by Equation (E-21) of Reference (2-6) as:

$$D_{\text{fall}} = D_o - (2h(T_c - T_{\text{sat}})/\rho h_{\text{fg}})(t_{\text{fall}} - t_{\text{sat}}) \quad (2-5)$$

where: T_c = compartment temperature ($^\circ\text{F}$)
 T_{sat} = saturation temperature corresponding to compartment total pressure ($^\circ\text{F}$)
 h_{fg} = droplet heat of vaporization (Btu/lbm)
 t_{fall} = fall time of droplets in compartment (sec)
 t_{sat} = time interval required to raise droplet temperature to T_{sat} after start of droplet fall (sec)

From Equations (E-14) and (E-16) of Reference (2-6), however, we know that:

$$t_{\text{sat}} = (\rho_c D_o / 6h) \ln ((T_c - T_{\text{sp}})/(T_c - T_{\text{sat}})) \quad (2-6)$$

where: T_{sp} = spray droplet temperature at start of fall ($^{\circ}\text{F}$)

Combining Equations (2-4), (2-5), and (2-6) yields:

$$M_{\%vap} = 100(1 - (1 - (2h(T_c - T_{sat})/\rho D_o h_{fg})(t_{fall} - (\rho c_p D_o / 6h) \ln((T_c - T_{sp})/(T_c - T_{sat}))))^3) \quad (2-7)$$

Equation (2-7) is the equation to be used in determining the spray mass vaporization rate during a compartment burn. As an example, a calculation for a single upper compartment burn is presented below. The chosen burn is the second upper compartment burn in our CLASIX Case E, reported via Reference (2-7). This burn is initiated at 6 volume percent hydrogen, and burns to 60% completeness in less than 10 seconds. CLASIX output for this analysis indicates that 129.262 lbm of hydrogen was consumed during this burn.

Basic data which was used in the vaporization evaluation was as follows:

$$\begin{aligned} h &= 20 \text{ Btu/hr-ft}^2\text{-}^{\circ}\text{F} = 0.005556 \text{ Btu/sec-ft}^2\text{-}^{\circ}\text{F} \\ \rho &= 62.4 \text{ lbm/ft}^3 \\ D_o &= 0.0023 \text{ ft} \\ t_{fall} &= 10.66 \text{ sec} \\ c_p &= 1.0 \text{ Btu/lbm-}^{\circ}\text{F} \\ T_{sp} &= 125 \text{ }^{\circ}\text{F} \end{aligned}$$

The above data are consistent with CLASIX input parameters for the Donald C. Cook Nuclear Plant. Upper compartment total pressures and temperatures at 1 second time intervals over the accident time range of interest (i.e., 6107 - 6129 seconds) are presented in Table 2-1. These values were obtained from CLASIX "short form" output. Also shown in Table 2-1 are the corresponding saturation temperatures (to the nearest $^{\circ}\text{F}$) and heats of vaporization for each data point (i.e., each 1 second time interval). Substituting these values into Equation (2-7) thus yields the percentage of spray mass vaporized at each data point.

Based on a total spray mass flow rate of 556 lbm/sec for the Donald C. Cook Nuclear Plant upper compartment, the rate of spray mass vaporization has thus been calculated for this case. The values obtained from this analysis are presented in the last column of Table 2-1, and are plotted in Figure 2-1. The results indicate that a peak spray mass vaporization rate of 330 lbm/sec will be reached at the time of peak compartment temperature and pressure.

Furthermore, Table 2-1 lists spray mass vaporization percentages of 32.78% and 23.45% at 6110 and 6120 seconds, respectively. CLASIX "long form" output lists the net drain rates from the upper compartment at these times, from which it is indicated that the corresponding CLASIX calculated vaporization percentages at these times are 31.32% and 23.34%, respectively. Since the differences in the hand calculated and CLASIX calculated vaporization rates is small, it is concluded that the simple calculational model described above yields an adequate representation of CLASIX spray mass vaporization.

Also of interest is the pressure suppression effects which the sprays may induce. The data in Table 2-1 has been analyzed with the use of Simpson's approximation in order to determine the total spray mass vaporized during the transient. These results indicate that 1300.52 lbm of spray mass vaporized between the burn ignition time and the time of peak pressure and temperature. During the subsequent cool down period, another 1756.25 lbm of spray mass vaporized in the hot upper compartment gases. Thus, the total spray mass vaporized during and after this upper compartment burn transient accounted for approximately 37% of the total high heat of combustion released by the burning hydrogen. Indeed, this signifies a major impact of upper compartment sprays upon reducing temperatures and pressures during a hydrogen burn in that region.

Question 14(d):

Concerning the CLASIX containment response analyses, provide the results of CLASIX analyses for flame speeds of 10 and 100 times the present value.

Response to Question 14(d):

It is believed that additional flame speed sensitivity studies are not warranted at this time. The Tennessee Valley Authority has previously provided the results of CLASIX analyses which envelope an order of magnitude shift in flame speed. A two order of magnitude shift in flame speed for the Donald C. Cook Nuclear Plant CLASIX base case (i.e., raising the flame speed to approximately 600 ft/sec) is not considered realistic. Although our response to Question 2 of Mr. S. A. Varga's July 30, 1982, request for information (see Attachment 3 to this letter) indicates that high velocity flows may occur within containment as a result of hydrogen deflagration, such high velocity flows are expected to be limited to the vicinity of a flow junction. Additionally, the duration of any high velocity flow is expected to be short, and the flow is expected to be extremely lean in hydrogen (since the flow should occur at the end of a burn when the pressure differential between compartments is greatest). Application of the two order of magnitude shift in flame speed to conditions other than transient gas flow through a junction at the end of a burn is therefore unrealistic.

Question 14(e):

To assess the effect of igniter system failure or ineffectiveness, provide the results of sensitivity studies in which the lower and dead-ended compartments are effectively inerted, and the upper plenum igniters burn with low efficiency or not at all. Assume combustion in the upper compartment at 9 - 10% hydrogen.

Response to Question 14(e):

Reference (2-8) provides the results of an analysis essentially equivalent to the postulated case of upper plenum igniter failure, coincident with inerting in all other ice condenser compartments except for the upper compartment region. This analysis, which was performed with an early version of the CLASIX computer code, is designated as Tennessee Valley Authority sensitivity study "JV903". The JV903 sensitivity study assumed that ignition would occur at a hydrogen concentration of 10 volume percent, and burn to 100% completion with a flame speed of 6 ft/sec. Ignition in and propagation to any compartment with less than 5 volume percent oxygen were suppressed. Additionally, the Tennessee Valley Authority case assumed that there was no fan forced flow within containment.

In this case, steam and hydrogen exiting the break pushed oxygen out of the lower compartment, thereby reducing the oxygen inventory in that region below the 5 volume percent required for burn initiation. As the accident progressed hydrogen accumulated in the upper compartment and eventually ignited. This burn then propagated into the ice condenser, with the burn combination effectively resulting in a redistribution of the atmospheric constituents within containment. Indeed, oxygen was introduced into the lower compartment region, while hydrogen was introduced into the upper compartment area. With the addition of hydrogen to the lower compartment, a burn was initiated in that region. This burn also propagated into the ice condenser, forcing more hydrogen into the still burning upper compartment.

As a result, approximately 1200 lbm of hydrogen was burned in the JV903 sensitivity study, with about 860 lbm out of the 1200 lbm of hydrogen being burned in the upper compartment. The resultant peak pressure and temperature for this Tennessee Valley Authority sensitivity case were 92.4 psia and 2583° F, respectively, with the peak pressure occurring in the upper compartment and the peak temperature occurring in the ice condenser. (The peak pressure in the ice condenser was 86.4 psia, whereas the peak temperature in the upper compartment was 1088° F. Likewise, the peak pressure and temperature in the lower compartment was 46.4 psia and 2370° F, respectively.)

Additional studies which have been performed by the Duke Power Company with regard to inerting are documented in Section 4.0 of Reference (2-9). In particular, Section 4.6.6 of the referenced Duke Power Company report discusses a CLASIX analysis in which the lower compartment is effectively inerted, but in which ignition is allowed to occur in the upper plenum of the ice condenser and in the dead ended

regions within containment. Section 4.6.7 of the referenced report describes a similar CLASIX analysis; however, in this case the upper plenum is effectively inerted and ignition is allowed to occur in the lower compartment.

In the first of the two Duke Power Company sensitivity studies cited above, hydrogen was consumed by a series of fifteen burns in the ice condenser upper plenum and two burns in the dead ended region. In the second of the two cases, hydrogen was consumed by eight burns in the lower compartment and one burn in the upper compartment. All burns were assumed to be initiated at a hydrogen concentration of 8.5 volume percent, and burn to 100% completeness at a flame speed of 2 ft/sec. The peak pressures produced in any containment compartment for these two Duke Power Company sensitivity studies were approximately 26 and 29 psia, respectively, for the inerted lower compartment and inerted ice condenser upper plenum analyses.

Review of the Tennessee Valley Authority and Duke Power Company analyses cited above indicates that the Duke Power Company analyses are, in general, applicable to the Donald C. Cook Nuclear Plant. The Tennessee Valley Authority CLASIX analysis discussed above is considered to be too conservative for application to the Donald C. Cook Nuclear Plant because of the following:

- (a) The cited analysis was performed with an earlier version of the CLASIX computer code; this version varies from the latest version of the code in many important aspects. Indeed, the earlier version does not contain certain models relating to radiant heat transfer, passive heat sinks, heat transfer correlations, and ice condenser nodalization. Incorporation of these models into the CLASIX computer code has resulted in the prediction of containment peak pressures considerably lower than those previously predicted with the earlier version of the CLASIX computer code.
- (b) The primary reason for conducting the JV903 sensitivity study was to assess the effect of fan forced flow on CLASIX analyses. Indeed, this case indicates that fan forced flow is desired throughout a degraded core accident to ensure mixing of the containment atmosphere.

Due to similarities in the design of the McGuire Nuclear Plant and Donald C. Cook Nuclear Plant containments, it is therefore reasonable to conclude from the Duke Power Company sensitivity studies that a hydrogen burn which is initiated at 8.5 volume percent, and burns at 2 ft/sec to 100% completeness, could result in a pressure peak on the order of 30 psia for the Donald C. Cook Nuclear Plant. This pressure peak is of the same order as that reported in our CLASIX Case "E" of Reference (2-7) for an upper compartment burn which ignited at 6 volume percent hydrogen and burned to 60% completion at a conservative flame speed of 6 ft/sec.

Additionally, it is noted that the scenario described herein is dependent on the assumption of postulated igniter system failure or ineffectiveness. Postulated igniter system failure or ineffectiveness during degraded core accidents has already been studied for the Donald C. Cook Nuclear Plant. Igniter ineffectiveness has been studied during the research and development programs co-funded by American Electric Power Service Corporation, Tennessee Valley Authority, Duke Power Company, and the Electric Power Research Institute. The results of these studies have previously been transmitted to the NRC via Reference (2-10). Igniter failure has been addressed by providing redundant trains of igniters with Class IE emergency power supplies. In summary, it is believed that the basis for this question does not reflect current Distributed Ignition System design and, even if igniter failure is postulated, best estimate peak pressures would be of the same order as present CLASIX analyses predict. Therefore, no additional work needs to be performed on this topic.

References, Attachment 2

- (2-1) Ranz, W. E., and W. R. Marshall, Jr., "Evaporation From Drops: Part I," Chem. Eng. Progress, 48, No. 3, pp. 141-146 (1952).
- (2-2) Minner, G. L., "Reactor Containment Spray Calculation Model," Proceedings of Topical Meeting on Thermal Reactor Safety, Sun Valley, Idaho, Volume I, pp. 569-582 (July 31 - August 4, 1977).
- (2-3) Wooton, R. O., and H. I. Avci, "MARCH (Meltdown Accident Response CHaracteristics) Code Description and User's Manual," NUREG/CR-1711, BMI-2064, R-3, dated October 1980.
- (2-4) Rohsenow, W. M., and H. Y. Choi, Heat, Mass, and Momentum Transfer, Prentice-Hall, Inc., 1961.
- (2-5) Milioti, S. J., et. al., "Analytical Studies of Elemental Iodine Removal By Sprays In The Donald C. Cook Nuclear Plant," Nuc. Tech., 16, pg. 497 (1972).
- (2-6) Westinghouse Electric Corporation/Offshore Power Systems Report No. OPS-07A35, "The CLASIX Computer Program For The Analysis Of Reactor Plant Containment Response To Hydrogen Release And Deflagration," Westinghouse Proprietary Class 2, Revision 1, dated January 1982.
- (2-7) Letter No. AEP:NRC:0500H, dated September 30, 1982, Mr. R. S. Hunter (IMECo) to Mr. H. R. Denton (NRC).
- (2-8) "Tennessee Valley Authority Sequoyah Nuclear Plant Core Degradation Program: Volume 2; Report on the Safety Evaluation of the Interim Distributed Ignition System," Appendix U, dated December 15, 1980.
- (2-9) "An Analysis of Hydrogen Control Measures at McGuire Nuclear Station," Revision 9, updated via letter dated October 20, 1983, Mr. H. B. Tucker (Duke Power Company) to Mr. H. R. Denton (NRC).
- (2-10) Letter No. AEP:NRC:0500I, dated March 1, 1984, Mr. M. P. Alexich (IMECo) to Mr. H. R. Denton (NRC).

TABLE 2-1

SPRAY VAPORIZATION
DURING AN UPPER COMPARTMENT BURN*

<u>Time</u> <u>(sec)</u>	<u>Total</u> <u>Pressure</u> <u>(psia)</u>	<u>T_c</u> <u>(°F)</u>	<u>T_{sat}</u> <u>(°F)</u>	<u>h_{fg}</u> <u>(Btu/lbm)</u>	<u>M_{%vap}</u>	<u>Mass</u> <u>Vaporiza-</u> <u>tion Rate</u> <u>(lbm/sec)</u>
6107	21.3	233.5	232	957.4	0.00	0.00
6108	22.9	300.8	235	955.5	9.93	55.21
6109	24.2	362.2	238	953.5	21.98	122.21
6110	25.4	417.8	239	952.8	32.78	182.26
6111	26.3	467.7	243	950.2	41.13	228.68
6112	27.2	512.1	245	948.8	48.32	268.66
6113	27.9	552.1	246	948.1	54.45	302.74
6114	28.6	587.8	248	946.8	59.35	329.99
6115	27.2	540.2	245	948.8	52.80	293.57
6116	26.2	496.1	243	950.8	46.04	255.98
6117	25.3	457.2	239	952.8	40.07	222.79
6118	24.6	423.1	239	952.8	33.79	187.87
6119	23.9	393.3	238	953.5	28.24	157.01
6120	23.4	367.3	236	954.8	23.45	130.38
6121	23.1	343.8	236	954.8	18.66	103.75
6122	22.8	323.2	235	955.5	14.61	81.23
6123	22.5	305.4	234	956.1	11.13	61.88
6124	22.3	289.7	234	956.1	7.89	43.87
6125	22.1	275.6	233	956.8	5.30	29.47
6126	21.8	263.2	232	957.4	3.18	17.68
6127	21.6	252.3	232	957.4	1.35	7.51
6128	21.4	242.2	231	958.1	0.15	0.83
6129	21.3	233.9	231	958.1	0.00	0.00

*Note: Analyzed upper compartment burn is the second upper compartment burn occurring in the Donald C. Cook Nuclear Plant CLASIX Case "E" (see Reference (2-7)).

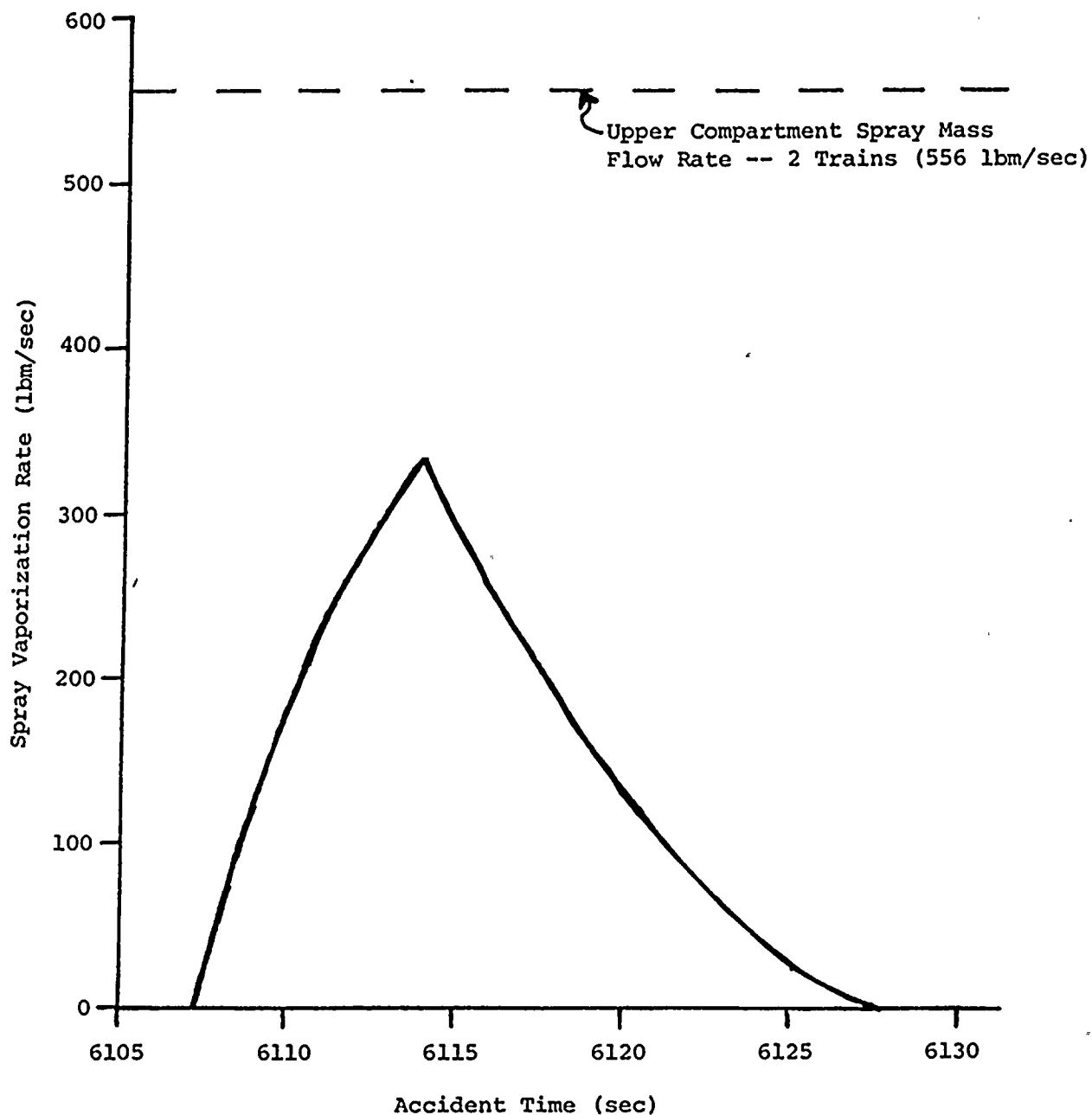


Figure 2-1. Spray mass vaporization during a CLASIX upper compartment burn.

ATTACHMENT 3 TO AEP:NRC:0500M
RESPONSES TO QUESTIONS ON HYDROGEN CONTROL
CONTAINED IN MR. S. A. VARGA'S LETTER DATED JULY 30, 1982
DONALD C. COOK NUCLEAR PLANT UNIT NOS. 1 AND 2

Question 2:

With regard to the CLASIX flow equations (A-4, A-8) provide the following information:

- (a) Equation (A-4) is used until a Mach number of one is reached without adjusting the loss coefficient for the variation of compressibility over this range of Mach number. Please justify the assumption of a constant loss coefficient.
- (b) The use of steady-flow equations assumes that the effects of transient phenomena, such as inertia, are not important. However, inertia would increase the pressure rise associated with a burn because pressure relief by outflow is reduced. Please describe the junction flow transients and transitions to sonic flow which occur at each of the flow junctions during blowdown and hydrogen burns, and justify that the steady-flow equations are valid for hydrogen burn transients.
- (c) The flow equations require a density and velocity. These should be the density and the velocity at the vena contracta (minimum flow area). However, the density defined by Equation (A-7) provides a density that is the average of the source and the sink volumes, which will not be the vena contracta density. In addition, the velocity used in Equation (A-4) is not defined. Please explain and justify the bases for the density and velocity used in the flow equations.
- (d) Two-phase flow conditions might result from (1) the breakflow or (2) a condensation fog from the ice condenser. As a result, the effects of mechanical (slip), thermal, and chemical (vapor diffusion) nonequilibria may become important. Justify the use of Equations (A-4) and (A-8) to estimate the transient flow of a two-phase fluid.

Response to Question 2(a):

The CLASIX computer code computes the transition to sonic flow when the pressure ratio between two compartments connected by a flow path is less than a preselected single value which is intended to represent a reasonable approximation of the critical pressure ratio. When this test is met, CLASIX computes the flow between the compartments as a function of only upstream pressure and a sonic flow constant, as described in Section V.A.2 of Reference (3-1).

This is a simplification which appears to have been made for calculational convenience. We do not believe that this simplification has a significant effect on the CLASIX analyses which were transmitted in Attachment 1 to Reference (3-2). This conclusion follows, in part, from a comparison of the CLASIX flow equations with a more realistic compressible flow model for gaseous flow driven by a high differential pressure through the refueling canal drains (i.e., the 2.2 ft² operating deck bypass area assumed in CLASIX). This examination indicates that:

- (a) At the peak differential pressure predicted by CLASIX for this flow path, the CLASIX flow model may overpredict the gaseous mass flow rate by about 70% when compared with a compressible flow model; and,
- (b) Even if this apparent overprediction was conservatively assumed to exist throughout the identified upper compartment burn transient, rather than just at the end of the burn, the total upper compartment mass would change by only 1 or 2% from the CLASIX predicted values.

Additionally, a case involving a relatively large differential pressure for a high flow area (i.e., the upper plenum to upper compartment junction, with a flow area of 2040 ft²) has been examined. Evaluation of CLASIX output for this case indicates that, at the beginning of a hydrogen deflagration in the upper plenum, differential pressures are typically low enough to ensure that the pressure driven gaseous flow will have a low flow velocity. Near the end of the burn the differential pressure across the junction may increase into the range where CLASIX computed flows are high enough to indicate the need for a compressible flow model. CLASIX output, however, indicates that this high velocity flow may last for only a few hundredths of a second. Indeed, the pressure relief afforded by the large flow area appears to limit the amount of time a high differential pressure (and thus high flow velocity) can exist across this junction. Therefore, use of a compressible flow model instead of the CLASIX flow model is not expected to result in significant changes in the containment analysis predictions performed to date.

Response to Question 2(b):

For inertia to be considered as an important effect, the ratio of volume length to junction flow area must be significant. As Duke Power Company explained in their response to this question (see Reference (3-3)), typical values of this ratio for ice condenser containment compartments are usually not considered significant enough. Indeed, the most likely location within containment where inertia effects may become important appears to be the bypass area between the upper and lower compartments (the drain holes in the refueling cavity are essentially embedded pipes with large length-to-area ratios). This bypass area has, however, been considered in the response to Question 2(a) above, and has been determined to be responsible for only a small fraction of volumetric flow within containment. Additionally, the refueling cavity should contain some water post-accident, thereby interfering with flow through the bypass area. It is thus concluded that inertia effects may be disregarded in CLASIX containment response calculations.

Response to Question 2(c):

The CLASIX flow equations appear to be derived from the general equation for pressure drop phenomena known as Darcy's formula. With suitable restrictions, Darcy's formula may be used when compressible flow of fluids, such as air, steam, etc., is considered.

As explained in Reference (3-4), if the calculated pressure drop between two points on a flow path is greater than about 10%, but less than about 40%, of the inlet (i.e., higher) pressure, then the Darcy formula may be used with reasonable accuracy if an average density based on upstream and downstream conditions is utilized in the computation. Since the pressure drop for even the high differential pressure case identified above for the refueling cavity drains was only about 32%, it is concluded that an average density would have to be used in the CLASIX computations to be consistent with Darcy formula utilization practices.

Response to Question 2(d):

The CLASIX flow model was developed for single phase homogeneous flow with the assumption that the effects of two phase flow would be negligible. Furthermore, it is noted that during the period of fan operation, flow rates and direction would be dictated primarily by the fan, except for brief periods during and after hydrogen combustion. Fan forced flow induces an atmospheric turnover rate that is sufficiently high to ensure quick dilution of suspended matter, especially for a small break LOCA scenario. Therefore, nonequilibrium effects should be considered inconsequential in CLASIX containment response analyses, as they are in other containment response codes such as CONTEMPT.

Question 4(f):

It is our understanding that the hydrogen burn rate, \dot{M}_B , is determined upon ignition by Equation (D-2) and held constant for the duration of each burn, while the mass of hydrogen to be burned is updated each interval by Equation (G-20). Intuitively the burn rate should also be updated to reflect the mass of hydrogen present, which may be greater or lesser than that at the onset of burning depending on the hydrogen injection rate. Please justify the use of a constant burn rate in view of the changing hydrogen concentration during a burn.

Response to Question 4(f):

As noted in Section 7.0 of Reference (3-3), it is not believed that the use of a constant burn rate significantly affects the results of CLASIX analyses. More specifically, the maximum hydrogen injection rate utilized in CLASIX input is 1.07 lbm/sec. At this peak injection rate, the amount of hydrogen that could be added to the lower compartment during a burn in that region would be limited. The effect of this added hydrogen would be to lower the burn time; however, this effect is bounded by CLASIX sensitivity studies performed by the ice condenser owners in which the burn time was lowered by raising the flame speed.

Question 5:

Provide the following information regarding the calculation of heat and mass transfer to passive heat sinks:

- (a) Equation (B-1) provides for the use of either the Tagami or Uchida correlation to determine the heat and mass transfer to passive heat sinks. The Tagami correlation is for conditions very different from those expected for the application of CLASIX, that is, small-break containment analyses. The Uchida correlation is for natural convection heat transfer, including condensation, in the presence of a noncondensable gas. Clarify how Equation (B-1) is used and justify the use of the Tagami correlation.
- (b) The natural convection heat transfer correlation for $Gr < 10^9$ that is used in the Tagami/Natural convection heat transfer correlation Equation (B-6), yields heat transfer rates lower than other text book correlations by a factor of three. Please discuss this discrepancy.
- (c) Describe and justify the passive heat sink heat transfer assumptions regarding (i) the temperature difference used with the film coefficients; (ii) the model used to account for the removal of mass that is condensed on the heat sink surfaces; and (iii) the energy removal associated with the condensed mass.

Response to Question 5:

As noted in Section 7.0 of Reference (3-3), the Tagami/natural convection heat transfer correlation presented in Reference (3-1) was in error, due to a misplaced exponent. Application of the erroneous correlation was, however, considered conservative because it resulted in a lower heat transfer rate from the containment atmosphere.

A new CLASIX analysis has been performed for the Donald C. Cook Nuclear Plant. This new analysis utilizes an optional passive heat sink heat transfer correlation based on the Uchida correlation. The results of this analysis are presented in Attachment 1 to this letter.

Question 8:

Regarding the analysis of heat transfer in the ice bed:

- (a) The assumption that no condensation occurs in the ice bed if the water vapor is superheated, and that condensation only occurs when the vapor is saturated does not seem realistic because (a) both heat and mass transfer can occur simultaneously if there is both a temperature and a concentration gradient; and (b) the vapor concentration gradient can extend into the superheated region. Provide justification for this assumption, perhaps via an analysis of



the mass transport occurring in the superheated and in the saturated sections of the ice bed.

- (b) The possibility exists to produce a condensate fog in the ice bed capable of being convected along with the flowing gas instead of collecting on the surface of the ice bed. Provide analyses or cite relevant studies which would justify the assumption that no condensate fog leaves the ice condenser.
- (c) Provide additional details of the CLASIX ice bed heat transfer solution process, specifically, the procedure by which the ice condenser is subdivided into incremental lengths, and the superheat and saturated heat transfer correlations are applied.
- (d) In the condensing region of the ice bed, Equation (C-26) is applied until the flow temperature is equal to the outlet plenum temperature. Explain why the outlet plenum temperature is used as a cutoff point for the saturated heat transfer correlation rather than some fixed temperature.
- (e) The film coefficient correlation for heat transfer to the ice, Equation (C-1), was developed based on ice bed inlet conditions typical of design basis accidents, i.e., relatively low flow velocities and saturated to slightly superheated vapor qualities. Inlet velocities and degree of superheat resulting from a postulated lower compartment burn will be significantly higher than for the design basis accidents. Justify the use of the correlation under hydrogen burn conditions.
- (f) Specify the parameter dimensions, condensate length, and flow area assumed in Equation (C-1). Also provide some typical calculated values for the film coefficient in the superheated and condensing regions.
- (g) Discuss the basic differences between the CLASIX treatment of the ice bed heat transfer and the treatments used in other ice condenser codes such as LOTIC and TMD. Describe the method of handling the heat and mass transport under superheated and saturated conditions in each code.

Response to Question 8:

The CLASIX ice condenser heat transfer model is based on the heat transfer correlation presented in Reference (3-5). This correlation is based on extensive testing performed relative to licensing activities for the ice condenser containment. The ice condenser model in CLASIX is the same as that used in TMD and LOTIC.

Question 10(a):

With regard to the CLASIX spray model, the mass, momentum, and energy transfer accounting seems to be incomplete. For example, the equations should account for the simultaneous occurrence of either vaporization or condensation with or without a change in the spray drop temperature. Please verify the CLASIX spray model by comparison with a spray model that includes a more thorough accounting for the mass, energy, and momentum transfers, such as the model developed by G. Minner (Reference (3-6)).

Response to Question 10(a):

The spray model developed by G. Minner provides a strict accounting of spray mass, energy, and momentum transfer. This is expected since the Minner model is a finite difference approximation to the transient equations which describe these phenomena. The CLASIX spray model explicitly models spray mass and heat transfer by assuming that the compartment conditions are frozen during the time step.

Minner performed parametric studies to include the effects of droplet size, initial speed, flow rate, temperature, and fall distance. Minner found that calculations using a large drop size are conservative. The CLASIX analyses used a droplet diameter approximately 2.5 times larger than the manufacturer's published average value. Minner found that any parameter which increased the residence time in the compartment atmosphere increased the effect of the spray on the atmosphere. The fall time in CLASIX conservatively limits (shortens) the residence time and, thereby, according to Minner's studies, decreases heat transfer. The Minner parametric studies demonstrate that the CLASIX spray model predicts conservatively low heat removal rates.

CLASIX updates the mass and energy transfer to the atmosphere in a procedure similar to that used by Minner for each sub-region. The mass and energy of the spray water is correctly removed from the compartment atmosphere. In earlier versions of CLASIX, the mass and energy transferred to the sump were ignored; however, the latest version appropriately maintains an inventory of sump parameters.

Question 11:

In the evaluation of the effect of a separate spray time domain, it is stated that: 1) the CLASIX spray model always predicts conservatively high containment pressure and temperature responses; and 2) the difference in the heat removal calculated using the CLASIX spray subroutine and the finite difference subroutine approaches zero as the transient progresses. In light of this,

- a) Discuss why the CLASIX spray model underpredicts heat removal as the first statement implies. Holding compartment ambient conditions constant on an increasing temperature ramp would seem to support this. However, if ambient temperature would expose droplets to higher temperatures on the average,

resulting in greater CLASIX spray heat removal (sic). Provide additional comparisons of the rates of heat removal for the two models assuming increasing containment ambient conditions, decreasing ambient conditions, and postulated hydrogen burn conditions; i.e., a rapid ambient temperature increase followed by a gradual temperature decrease.

- b) With regard to the second statement, describe the effect that non-linearities in heat transfer/thermodynamic processes have on the agreement between the two models.

Response to Question 11(a):

The statement that the CLASIX spray model underpredicts heat removal is based upon results of comparison with the transient response of a more detailed finite difference model (see Appendix D to Reference (3-1)). The finite difference procedure is a widely accepted method of obtaining accurate transient solutions of complex heat transfer problems. This finite difference algorithm determines the interaction of a spray droplet from the time of introduction into the compartment until it completes its fall or is vaporized. The heat transfer rate computed by the algorithm includes the effects of changing ambient conditions within the compartment. The finite difference spray model yields an accurate approximation of the heat removal rate. The CLASIX spray model assumes that ambient conditions encountered by each spray droplet of a given time step are constant during the fall time. Ambient conditions are updated for each succeeding time step. The accuracy of the heat transfer rates calculated by the CLASIX spray model will therefore depend on the specific transient.

The compartment transient considered in the comparison analysis was an increasing ambient temperature and pressure followed by a decrease to the initial conditions. Since the CLASIX spray model uses a constant ambient condition for the total spray released during a time step, the CLASIX heat removal rate will lag behind the transient. For the test transient, CLASIX underpredicts the rate of heat removal during the period of rising temperature and results in a conservatively high compartment temperature and pressure. During the period of falling temperature, CLASIX overpredicts the rate of heat removal so that over the cycle, the correct amount of heat is removed. Thus, the CLASIX spray model predicts conservatively high temperatures.

Response to Question 11(b):

The CLASIX spray subroutine is a classical transient solution of the governing mass and energy equations. The finite difference solution is expected to approach the classical transient solution (due to the decreasing rate of change in compartment conditions) as the transient progresses. Although the finite difference model yields a better estimate of nonlinearities in the heat transfer process, most of the difference between the two models is due to the method of handling the changes in compartment conditions with time rather than heat transfer nonlinearities.

References, Attachment 3

- (3-1) Westinghouse Electric Corporation/Offshore Power Systems Report No. OPS-07A35, "The CLASIX Computer Program For The Analysis Of Reactor Plant Containment Response To Hydrogen Release And Deflagration," Westinghouse Proprietary Class 2, Revision 1, dated January 1982.
- (3-2) Letter No. AEP:NRC:0500H, R. S. Hunter (IMECo) to H. R. Denton (NRC), dated September 30, 1982.
- (3-3) "An Analysis of Hydrogen Control Measures at McGuire Nuclear Station," (McGuire Red Books), Revision 9, updated via letter dated October 20, 1983, Mr. H. B. Tucker (Duke Power Company) to Mr. H. R. Denton (NRC).
- (3-4) "Flow of Fluids Through Valves, Fittings, and Pipe," Crane Technical Paper No. 410, Seventeenth Printing, 1978.
- (3-5) "Ice Condenser Containment Pressure Transient Analysis Methods," WCAP-8077 (Proprietary Class 2), March 1973, WCAP-8078 (Proprietary Class 3), March 1973.
- (3-6) Minner, G. L., "Reactor Containment Spray Calculation," Thermal Reactor Safety CONF-770708 (July 1977), Vol. I, pp. 569-582.

